

GEOLOGICA ULTRAIECTINA

Mededelingen van het
Instituut voor Aardwetenschappen der
Rijksuniversiteit te Utrecht

No. 33

GEOCHEMISTRY
OF THE PANASQUEIRA
TUNGSTEN-TIN DEPOSIT,
PORTUGAL

RUDOLF W. BUSSINK

STELLINGEN

1

'Greisenisatie', zoals goed gedefinieerd door Shcherba (1970), dient met meer zorgvuldigheid gebruikt te worden.

Shcherba, G.N. (1970): Greisens. Int. Geol. Rev., 12, 114-151, 239-254.

2

'Fission tracks' in apatiet worden bij ongeveer 105°C uitgewist in plaats van 150°C (Kelly & Wagner, 1977). Deze temperatuur kan in Panasqueira bereikt zijn door uitwisseling met warme fluids uit de latere "Alpiene" breuken.

Kelly, W.C. & Wagner, G.A. (1977): Paleothermometry by combined application of fluid inclusion and fission track methods.

N. Jahrb. Min. Monatsh., 1, 1-15.

Gleadow, A.J.W. & Duddy, I.R. (1981): A natural long-term track annealing experiment for apatite. Nucl. Tracks, 5, 169-174.

3

'Wolfram granieten' kunnen naar analogie van 'tin granieten' alleen gekarakteriseerd worden indien betere wolfram bepalingen beschikbaar zijn.

4

Het is sterk aan te bevelen voor water en gesteente analyses aparte ion-selectieve fluor elektroden te gebruiken.

5

Gezien het rijgedrag van de 'Eend' zou deze van verenstaal gemaakt kunnen zijn.

6

Het aanleggen van rijkswegen voor recreatieve doeleinden (zoals bijvoorbeeld rijksweg 28) dient sterk te worden aanbevolen.

7

Het ontbreken van titels in literatuurlijsten veroorzaakt een aanzienlijke toename van het aantal gemaakte nutteloze fotocopien.

8

Erts exploratie in Middeneuropese middelgebergten werd in de Middeleeuwen vergemakkelijkt door de afwezigheid van bossen.

9

Bij het werken met geautomatiseerde analytische systemen besteedt de analist meer tijd aan de analyse van het systeem dan aan het analytische probleem.

10

De geur van de bloeiende Betuwe wordt op doordeweekse dagen ten onrechte toegeschreven aan de bloesem maar blijkt het industriële parfum van bestrijdingsmiddelen te zijn.

11

De ware tekstverwerker bent U, geïnteresseerde lezer.

Utrecht, 4 juni 1984

R.W. Bussink

Stellingen behorende bij het proefschrift: Geochemistry of the Panasqueira tungsten-tin deposit, Portugal.

GEOLOGICA ULTRAIECTINA

Mededelingen van het
Instituut voor Aardwetenschappen der
Rijksuniversiteit te Utrecht

No. 33

GEOCHEMISTRY OF THE PANASQUEIRA TUNGSTEN-TIN DEPOSIT, PORTUGAL

X. VII. 12

GEOCHEMISTRY
OF THE PANASQUEIRA
TUNGSTEN-TIN DEPOSIT,
PORTUGAL

GEOCHEMIE
VAN DE PANASQUEIRA
WOLFRAAM-TIN AFZETTING,
PORTUGAL

(met een samenvatting in het nederlands)

PROEFSCHRIFT

TER VERKRIJGING VAN DE GRAAD VAN DOCTOR IN
DE WISKUNDE EN NATUURWETENSCHAPPEN AAN
DE RIJKSUNIVERSITEIT TE UTRECHT, OP GEZAG VAN
DE RECTOR MAGNIFICUS PROF. DR. O. J. DE JONG,
VOLGENS BESLUIT VAN HET COLLEGE VAN DECANEN
IN HET OPENBAAR TE VERDEDIGEN OP MAANDAG
4 JUNI 1984 DES NAMIDDAGS TE 2.30 UUR

DOOR

RUDOLF WILLEM BUSSINK

GEBOREN OP 13 SEPTEMBER 1951 TE EINDHOVEN

PROMOTOR: PROF. DR. R.D. SCHUILING
CO-PROMOTORES: DR. M. G. OOSTEROM
DR. R. KREULEN

Aan mijn Ouders

Voorwoord

Bij het tot stand komen van dit proefschrift wil ik in het bijzonder bedanken:

Mijn promotor, Prof.Dr. R.D. Schuiling, voor zijn kritische aantekeningen bij de tekst.

Dr. M.G. Oosterom, voor zijn begeleiding tijdens het veldwerk, zijn introductie in de tin-wolfraam afzettingen van Portugal, de daarmee gerelateerde gespecialiseerde granieten en hun kenmerken, de mijnbouwkundige aspecten, de geochemische exploratie, het ter beschikking stellen van diverse Portugese en Spaanse granieten en zijn kritische aantekeningen bij de tekst.

Dr. Rob Kreulen, voor zijn begeleiding tijdens het vloeistof insluitel, gas analyse en stabiele isotopen onderzoek en suggesties betreffende de tekst.

Drs. Simon Vriend, voor zijn begeleiding bij de statistische data verwerking, het ter beschikking stellen van data van Regoufe en zijn kritische aantekeningen bij de tekst.

Dr. Ben Jansen, voor zijn hulp bij het slijpplaten onderzoek.

Dr. Arie de Jong, voor het bepalen van de $\delta^{18}\text{O}$ waarden van mineralen en suggesties wat betreft de vloeistof insluitels en het stabiele isotopen gedeelte.

Drs. Mario Moura, voor het verrichten van diverse gesteente analyses.

Drs. Jaap Kocken, voor zijn assistentie bij de ICP analyses.

Jan Meesterburrie en Anita van Leeuwen voor het meten van de $\delta^{13}\text{C}$ en $\delta^{18}\text{O}$ van CO_2 en carbonaten.

Paul Anten, Leo Belle, Jan van der Wal en Vian Govers voor de hulp tijdens de AAS, ISE en XRF analyses.

K.M. Stephan, Giel Eussen, Theo van Zessen en Ir. Bertha Djie-Kwee voor de hoofd element bepalingen en neutronen activerings analyses te Delft.

Drs. Bas van Eeckhout, voor het meten van de $\delta^{15}\text{N}$ en $\delta^{13}\text{C}$ van totaal koolstof in de vloeistof insluitels.

Alle mensen van de slijpkamer die er steeds weer in slaagden om dubbel gepolijste doorsneden van vaak kleine mineralen te maken.

Verder iedereen van de tekenkamer en foto afdeling die steeds bereid waren er nog even iets tussen door te doen.

Drs. Cees Walen, Drs. Jan Brill, Drs. Steven Luitjens en Drs. Cees Dekker, voor het ter beschikking stellen van gesteente monsters en/of analyses van Fundao, Belmonte, Capinha, Bruco, Fonte Santa en Panasqueira.

I would like to thank the Beralt Tin and Wolfram Portugal, S.A.R.L. for their underground permission and hospitality, especially Dr. R. de Barros, J. Pinto Jr. and G. Duarte for their underground assistance.

Dit proefschrift kwam tot stand met financiële steun van de Nederlandse Organisatie voor Zuiver-Wetenschappelijk Onderzoek (Z.W.O.) door middel van A.W.O.N. subsidie 18.23.002.

ABSTRACT

Major tin-tungsten deposits in Portugal are related to intrusions of the Younger Series (300-280 Ma) of Hercynian granitoids. Mineralized granites are 'specialized' by a specific increase or decrease of major, minor and trace element contents in comparison with non-mineralized occurrences. Component analysis is used to make distinctions between the various geochemical types of barren and mineralized granites (Chapter 2). A one-component model is characterized by positive loadings for Rb, Sn, Cs, Li, Nb, F, Ta, Zn, W and P₂O₅ and negative loadings for Zr, Ba, TiO₂ and Sr. In this one-component model the component scores increase from barren to highly specialized granites.

In a two-component model component 1 (F, Li, Cs, Rb, Zn, Sn, P₂O₅, Nb and W) expresses a hydrothermal influence upon the granites, whereas component 2 (TiO₂, Ba, Zr, Sr, -Ta, -Nb, -Rb and -Sn) possibly represents the magmatic differentiation trend. In this model the composition of the individual granites concentrate in one of several fields according to their loadings by the element parameters. Muscovite granites, albitized and greisenized granites deviate clearly in composition from the more common granites.

The geochemical variability of granites, greisens and schists of the Panasqueira tungsten-tin deposit is investigated in great detail (Chapter 3). The trace element contents of the Panasqueira cupola are compared with those of other granite occurrences in the surroundings. Only ore-bearing granites show a geochemical differentiation concurrent with mineralization. The major elements illustrate the general chemical evolution from muscovite-albite granite to greisenized granite; trace elements, however, show in addition distinct groups of granitoids. The general trend in the granitoids of Panasqueira is an increase in Rb, Li, F, Sn, Cs, W, Fe₂O₃, P₂O₅, Zn, As, Nb, Ta and Cu contents while Na₂O, CaO, MgO, Sr, Zr, Ba and TiO₂ contents decrease. Rare earths are strongly depleted in the greisen. This alteration in composition is the result of metasomatic and hydrothermal processes;

closed in an early stage but thereafter opened due to the development of sub-horizontal joints.

The schist along the hydrothermal ore veins at Panasqueira is affected as well by the mineralizing fluids in the veins; tourmaline and sericite alteration zones contain elevated amounts of the ore-related elements Rb, Li, Cs, Sn, W and Na₂O and K₂O. Schist samples were also taken at the surface and used for litho-geochemical exploration purposes. The same elements, when plotted in contour maps, outline the outcropping ore zones very well and can be used as a tool in geochemical exploration (Chapter 4).

A major part of this investigation is dedicated to the physical conditions under which the mineralization of Panasqueira was formed (Chapter 5). Homogenization temperatures of fluid inclusions in the minerals of Panasqueira point to an interval between 325 and 250°C for the early stages; salinities are between 5 and 10 wt% NaCl. In the final hydrothermal stage homogenization temperatures dropped to about 100°C; the salinity is also lower, down to 3 wt% or less. Due to trapping of CO₂-rich fluids against an impermeable granite-schist contact, fluid pressures point to an 'overpressure' of about 1 kbar before opening of the joint system. Opening of this joint system caused vigorous boiling of the fluids in the ore veins at a depth of about 1800 m.

Gas chromatographic analyses show next to CO₂ the presence of CH₄ and N₂. The presence of CH₄ suggests a reducing environment during ore deposition. The origin of the CH₄ and N₂ is possibly found by assimilation of schist containing organic matter.

Stable isotopes of carbon, oxygen and nitrogen indicate a homogeneous isotopic source for the early fluids. High overpressures in the earliest stage and about constant oxygen, carbon and nitrogen isotopes strongly favour a 'magmatic' origin for the initial mineralizing fluids. Oxygen and carbon isotopes of the fluids differ strongly in the latest stage and point to a large influx of meteoric water.

SAMENVATTING

Belangrijke tin-wolfraam afzettingen in Portugal zijn gebonden aan de 'Younger Series' (280-300 Ma) van Hercynische granitoiden. Gemineraliseerde granieten worden gekenmerkt door specifieke veranderingen in gehalten aan hoofd-, neven- en sporen-elementen ten opzichte van niet gemineraliseerde granieten. Component analyse werd toegepast om onderscheid te maken tussen steriele en gemineraliseerde granieten (Hoofdstuk 2). Het één-component model wordt gekarakteriseerd door positieve 'loadings' voor Rb, Sn, Cs, Li, Nb, F, Ta, Zn, W en P_2O_5 , verder door negatieve 'loadings' voor Zr, Ba, TiO_2 en Sr. Door toepassing van het één-component model kunnen granieten geklassificeerd worden als steriel, gespecialiseerd en zeer gespecialiseerd.

In het twee-componenten model brengt component 1 (F, Li, Cs, Rb, Zn, Sn, P_2O_5 , Nb en W) de hydrothermale beïnvloeding tot uitdrukking; component 2 (TiO_2 , Ba, Zr, Sr, -Ta, -Nb, -Rb en -Sn) geeft mogelijk de magmatische differentiatie trend aan. De granieten vallen in afzonderlijke velden uiteen volgens de 'loadings' van hun sporenelement parameters. Muscoviet granieten, gealbitiseerde en gegreiseniseerde granieten wijken in samenstelling sterk af van meer gewone granieten.

De geochemische variatie van de granieten, greisen en schisten uit het Panasqueira wolfraam-tin gebied is op zeer gedetailleerde manier onderzocht (Hoofdstuk 3). Sporen-elementen in gesteenten uit de Panasqueira cupola zijn vergeleken met die van andere granieten in de omgeving. De hoofd-elementen geven een chemische evolutie aan van muscoviet-albiet graniet naar de gegreiseniseerde componenten. Sporenelement verdelingen geven verschillende groepen binnen de granieten van de Panasqueira cupola. De volgende verdeling tendenzen kunnen onderscheiden worden: verhoogde gehalten aan Rb, Li, W, Fe_2O_3 , Sn, Nb, Ta, P_2O_5 , Zn, As, F, Cs en Cu terwijl de gehalten aan Na_2O , CaO, MgO, Sr, Zr, en TiO_2 afnemen. Zeldzame aarden verdwijnen bijna totaal in de greisen.

De oorsprong van deze trend dient gezocht te worden in de aard van het

hydrothermale systeem, namelijk gesloten in het begin maar geopend in latere stadia.

Ook de schisten langs de hydrothermale ertsaders tonen de invloed van de hydrothermale werking; toermalijn en sericiet omzetting zones bevatten verschillende gehalten aan Rb, Li, Cs, Sn, W, Na₂O en K₂O. Schist monsters werden aan het oppervlak verzameld en geanalyseerd als test voor hun bruikbaarheid als litho-geochemische prospectie methode. Geplot in 'contour maps' duiden deze elementen de dagzomende ertszones zeer goed aan en kunnen voor praktische exploratie gebruikt worden.

Een belangrijke sectie van dit onderzoek is gewijd aan de fysische condities van ertsvorming in de aders van Panasqueira (Hoofdstuk 5). Homogenisatie temperaturen van vloeistof insluitels in mineralen van Panasqueira zijn van 325 tot 250°C voor de vroege stadia; de saliniteit ligt tussen de 5 tot 10 gew.% NaCl. In het eindstadium dalen de homogenisatie temperaturen tot ongeveer 100°C; de saliniteiten zijn ook lager, namelijk 3 gew.% of minder. CO₂-rijke oplossingen in de allereerste fase geven een vloeistof 'overdruk' van ongeveer 1 kbar wat veroorzaakt wordt door een ondoorlatend graniet-schist contact. Het openen van het sub-horizontale diaklaassysteem veroorzaakt een heftig koken in de ertsaders op een diepte van ongeveer 1800 m.

Gas chromatografie geeft behalve CO₂ ook de aanwezigheid van CH₄ en N₂ aan. Uit de aanwezigheid van CH₄ blijkt een reducerend milieu ten tijde van de erts afzetting. De herkomst van de CH₄ en N₂ dient gezocht te worden in de assimilatie van organisch materiaal uit schisten.

Stabiele isotopen van zuurstof, koolstof en stikstof duiden op een homogene bron voor de allereerste oplossingen. De combinatie van hoge 'overdrukken' en ongeveer constante zuurstof, koolstof en stikstof isotopen duidt sterk op een "magmatisch" fluid in de beginfase. In de eindstadium verschillen de stabiele isotopen van koolstof en zuurstof nogal van eerdere stadia en wijzen op een aanzienlijk aandeel van meteorisch water in de fluids.

TABLE OF CONTENTS

Voorwoord	6
Abstract	9
Samenvatting	11
Table of contents	13
CHAPTER 1 - INTRODUCTION	17
References	19
CHAPTER 2 - GEOCHEMISTRY OF SPECIALIZED GRANITES IN PORTUGAL	21
Geology	23
Mineralizations	24
Description of investigated granitoids	25
Geochemistry	35
analytical techniques	35
interpretation	37
Results and discussion	40
Conclusions	52
References	53
CHAPTER 3 - TRACE ELEMENT DISTRIBUTIONS IN AND AROUND THE PANASQUEIRA TUNGSTEN-TIN DEPOSIT, PORTUGAL	57
Geology	59
Beira shales	59
the Panasqueira granite/greisen	61
quartz veins	62
quartz-cap	62
dolerite dykes	63
Geochemistry	63
analytical techniques	63
Results and discussion	63
CIPW major element trends	63
trace element distributions	68
the Panasqueira granite/greisen	68
granitic trend	68
greisenization trend	72
comparison with other granites	75

the Panasqueira schists	76
drillcores	78
tourmaline zone	80
sericite zone	81
chlorite-sericite zone	85
Conclusions	85
References	87
CHAPTER 4 - SURFACE ANOMALIES AROUND THE PANASQUEIRA TUNGSTEN-TIN DEPOSIT, PORTUGAL	89
Geology	91
Geochemistry	91
sample preparation	91
interpretation	92
Results and discussion	94
surface anomalies	94
Conclusions	104
References	105
CHAPTER 5 - MINERALOGY, FLUID INCLUSIONS AND STABLE ISOTOPES OF THE PANASQUEIRA W-SN DEPOSIT, PORTUGAL	107
Abstract	107
Introduction	108
Geology	108
ore-bearing quartz veins	108
Mineralogy	110
native elements	110
sulphides	110
oxides	112
silicates	114
phosphates	115
tungstates and arsenates	116
fluorite	117
Vein paragenesis	117
Previous work	120
fluid inclusions	120
sulphur isotopes	121

oxygen isotopes	121
carbon isotopes	122
hydrogen isotopes	122
Methods used in this study	122
Fluid inclusions	123
inclusion types	123
occurrence of fluid inclusions	125
homogenization temperatures	127
salinities	129
carbondioxide content	131
Gas compositions	133
Discussion of fluid inclusion data	136
gas compositions	136
boiling of the ore fluids	137
fluid salinities	139
depositional temperatures	139
over-pressures	140
Stable isotopes	141
carbon isotopes	141
oxygen isotopes	143
nitrogen isotopes	145
Discussion of stable isotope data	148
origin of fluids	149
Conclusions	150
the Panasqueira cupola	150
the quartz-cap	151
the hydrothermal tungsten-tin veins	153
origin of the ore fluids	154
References	155
Appendix	159

CHAPTER 1

INTRODUCTION

The northern and western part of the Iberian Peninsula is known for its tin, tungsten and minor tantalum deposits. These deposits are related to granitic belts (Lotze, 1945; Thadeu, 1977; Arribas, 1978) which form the spine of the Hercynian chain. In the Central-Iberian Zone in Portugal the granitoids intruded into a thick meta-sedimentary formation with flyschoid facies, also known as the Beira Schist complex (Thadeu, 1977).

The granitic intrusions are of Hercynian age. K-Ar and Rb-Sr dating indicate three major intrusive phases: the Older granites (320-330 Ma) and the Younger granites (310 ± 10 and 290 ± 10 Ma) (Oen Ing Soen, 1970; Priem et al., 1970; Pinto, 1979; Priem & den Tex, 1982; Priem et al., 1984). Alkaline as well as calc-alkaline characterizes are found in both granitic groups. The initial $^{87}\text{Sr}/^{86}\text{Sr}$ ratios vary between 0.705 and 0.725 (Priem & den Tex, 1982; Pinto, 1983) which indicates S-type granites of sedimentary origin or with a strong crustal contamination (Chappell & White, 1974).

The subject of this thesis is the trace element distribution and behaviour in Portuguese granites and schists, especially in and around the Panasqueira tungsten-tin deposit. In addition, minerals of the Panasqueira deposit were studied for fluid inclusions; stable isotope measurements and gaschromatographic analyses were performed on fluid inclusions in these minerals.

Minor and trace element contents of about 370 samples from different granitoids are treated in Chapter 2. These elements were used in a component analysis to distinguish barren from specialized granites. A one- and a two-component model were used but the two-component model gave the best division into barren, specialized and highly specialized granites. One of these specialized granites was investigated on a more

detailed scale.

The largest tungsten-tin mine in the Iberian Peninsula is the Panasqueira deposit. This deposit consists of sub-horizontal ore veins in the Beira shales and is related to a greisenized granite cupola, only exposed in the mine.

In Chapter 3 major and trace element distributions of granite, greisen and schist samples surrounding the ore veins are investigated. With the aid of component analysis two groups of elements, each with sub-groups, were distinguished in the cupola, namely an altered leucogranite and a greisen deposit.

Chapter 3 also gives the element distribution in schists along the ore veins. A more detailed investigation was carried out on drillcores through the ore zones. The different alteration zones around the individual veins are characterized by increased or decreased contents of several major and trace elements.

In Chapter 4, schist and shale samples, taken from the surface, are used for litho-geochemical exploration purposes. The same elements which outline alteration zones in the mine, occur also at the surface. These elements were used to prepare contour maps of the individual elements. Component analyses was also performed on the surface samples. The component scores are also plotted as contour maps.

Chapter 5, after a brief review of the geology and mineralogy of the Panasqueira mine, gives the results of fluid inclusion and stable isotope studies. While the fluid inclusion study was carried out, the extensive work of Kelly & Rye (1979) was published. Thereafter, fluid inclusions studies were focussed on those parts that were not or incompletely covered by Kelly & Rye. Gas chromatographic analyses were done on gases in the fluid inclusions. Stable isotopes of carbon, oxygen and nitrogen were measured. The combination of the additional fluid inclusion data and stable isotope measurements gives a better understanding of the ore-forming process at Panasqueira.

REFERENCES

- Arribas, A. (1978): Mineral paragenesis in the Variscan metallogeny of Spain. *Studia Geologica*, 14, 223-260.
- Chappell, B.W. & White, A.J.R. (1974): Two contrasting granite types. *Pacific Geology*, 8, 173-174.
- Kelly, W.C. & Rye, R.O. (1979): Geologic, fluid inclusions and stable isotope studies of the tin-tungsten deposits of Panasqueira, Portugal. *Econ. Geol.*, 65, 609-680.
- Lotze, F. (1945): Zur Gliederung der Varisziden der Iberischen Meseta. *Geotekt. Forsch.*, 6, 78-92.
- Oen Ing Soen (1970): Granite intrusion, folding and metamorphism in central northern Portugal. *Bol. Geol. Min. Espana*, 81, 271-298.
- Pinto, M.S. (1979): Geochemistry and geochronology of granitic rocks from the Aveiro and Viseu districts (Northern Portugal). Thesis University of Leeds, pp. 196.
- Pinto, M.S. (1983): Geochronology of Portuguese granitoids: a contribution. Internal report, University of Aveiro, pp. 29.
- Priem, H.N.A. & Boelrijk, N.A.I.M. & Verschure, R.H. & Hebeda, E.H. & Verdurmen, E.A.Th. (1970): Dating events of acid plutonism through the Paleozoic of the western Iberian peninsula. *Eclog. Geol. Helv.*, 63, 255-274.
- Priem, H.N.A. & den Tex, E. (1982): Tracing crustal evolution in the NW Iberian Peninsula through Rb-Sr and U-Pb systematics of Paleozoic granitoids: a review. International Colloquium "Géochimie et Petrologie de granitoids", Clermont-Ferrand, May 1982, Volume of Abstracts.
- Priem, H.N.A. & Schermerhorn, L.J.G. & Boelrijk, N.A.I.M. & Hebeda, E.H. (1984): Rb-Sr geochronology of Variscan granitoids in the tin-tungsten province of Northern Portugal: a progress report. *Ecog VII*, Braunlage, March 1984. Volume of abstracts. *Terra Cognita*, in press.
- Thadeu, D. (1977): Hercynian paragenetic units of the Portuguese part of the Hesperic massif. *Bol. Soc. Geol. Portugal*, 20, 247-276.

CHAPTER 2

GEOCHEMISTRY OF SPECIALIZED GRANITES IN PORTUGAL

The Hercynian granitic belt in Spain and Portugal is known for its tin, tungsten and minor tantalum deposits. These deposits are related to so-called specialized granites or 'tin granites' which contain tin in concentrations above 15 ppm and with increased or decreased contents of other elements (Boissavy-Vinau, 1979). The ore deposits occur in aplitic, granitic or pegmatitic rocks, hydrothermal quartz veins and skarns.

From previous work and literature data two groups of mutually correlating elements can be discerned within tin granites. One group, composed of Rb, Li, Cs, Sn, W, Mo, Nb, Ta, Be, Sb, Bi and As increases in the evolution process of Hercynian magmas; at the same time another group of elements like Ti, Zr, Ba, Sr, Ni, Co, Th, Hf, V, Cr, Sc and Rare Earths generally decrease (Tischendorf, 1977; Boissavy-Vinau, 1979). Other elements such as F, B and P may also correlate positively with the first group of elements.

The present investigation comprises the detailed sampling of granitoids of different composition and areal extent (large batholiths to small domes). The location of a part of the investigated area is indicated in Fig. 1 with more local information in Fig. 2 to 6. Depending upon the accessibility, importance of the occurrence and lateral extent, 5 to 50 samples were collected from each granitoid body by chip sampling. About 370 samples were collected in total and were subsequently analyzed for several minor and trace elements. Although some granites are ore-bearing, suitable concentration processes did occur but did not always result in sizable ore deposits (Table I).

With the aid of trace elements and component analysis, granitoids

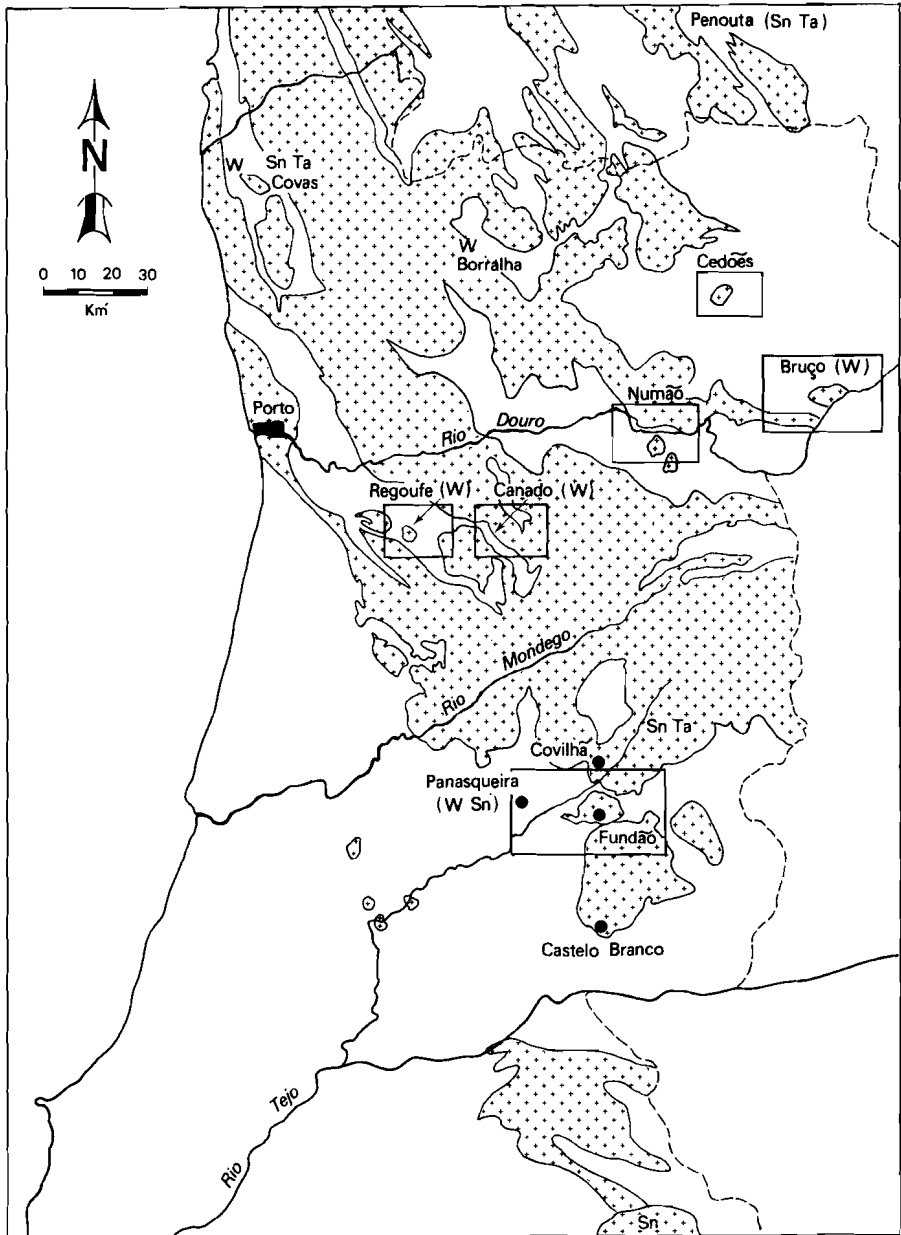


Fig. 1. Location of the investigated granitoids in Portugal and Spain. Granitoid areas are indicated by shading.

can be divided into barren and mineralized granites. A preliminary result of the feasibility of the method is shown in Fig. 7 and Fig. 8 which was developed by Vriend and Oosterom in a technical report (Oosterom et al., 1982).

GEOLOGY

The Hercynian belt of the Iberian Peninsula can be divided into different zones (Lotze, 1945; Thadeu, 1977). The Central-Iberian Zone is the most important one in that it forms the spine of the Iberian Hercynian unit and makes up about half of the northern and central parts of Portugal (Thadeu, 1977). The Central-Iberian Zone is characterized by the occurrence of a very thick meta-sedimentary formation with flyschoid facies which is known as the Beira Shale complex (Thadeu, 1977).

Hercynian granitic magmatism is strongly developed in the Central-Iberian Zone. The Hercynian granites can be divided into two groups: the Older granites (320 - 330 Ma, locally even up to 380 Ma) and the Younger granites (310 ± 10 and 290 ± 10 Ma) (Oen Ing Soen, 1970; Priem et al., 1970; Priem & den Tex, 1982; Pinto, 1983; Priem et al., 1984). The Older granites were supposed to be alkaline whereas the Younger granites had a calc-alkaline nature. Recent results indicate that both granitic groups show alkaline as well as calc-alkaline tendencies (Schermerhorn, 1982). Initial $^{87}\text{Sr}/^{86}\text{Sr}$ ratios in the Younger granites vary from 0.705 to about 0.725 (Priem & den Tex, 1982; Pinto, 1983). Their abundant and varied mineralization seems to indicate a different source in deeper levels or a different mode of generation (Schermerhorn, 1982). The elevated initial $^{87}\text{Sr}/^{86}\text{Sr}$ ratios indicate a sedimentary origin or a strong contamination by crustal material. Albuquerque (1971, 1978) showed with the aid of major elements and rare earth distributions that the Younger granites originated from partial melting of the Beira shales. These Younger granites are often also peraluminous which is reflected by the presence of cordierite,

andalusite, garnet or sillimanite in the granitic rocks. All the data point to S-type granites (Chappell & White, 1974) for the Younger granites in Portugal (Priem & den Tex, 1982; Pinto, 1983).

MINERALIZATIONS

Different types of Sn-W-Ta-Be-Li mineralizations are related to the Younger granites (Thadeu, 1977; Schermerhorn, 1982).

The hydrothermal tin-tungsten veins occur in the endo- and exo-contact zone of the granites but they rarely pass beyond the contact-metamorphic zone (Thadeu, 1973). The ore veins occupy tension cracks with characteristic deuteric alterations in the country rock. Muscovitization, albitization and greisenization occur in granitic rocks and tourmalinization, sericitization and silicification are found in pelitic rocks. Thadeu (1973) distinguishes four hydrothermal tin-tungsten vein types:

- A: Quartz veins with cassiterite, poor in sulphides, moderately rich in muscovite and sometimes containing beryl.
- B: Quartz veins with cassiterite, wolframite and/or scheelite and relatively high sulphide contents (mainly arsenopyrite and pyrite).
- C: Quartz veins with cassiterite, wolframite and/or scheelite, rich in sulphides (mainly arsenopyrite, pyrrhotite, chalcopyrite, sphalerite, pyrite and marcasite but rarely molybdenite) and in some cases siderite and dolomite.
- D: Quartz veins with wolframite and/or scheelite, generally poor in sulphides.

As a rule cassiterite-quartz veins occurring inside the granite pass into cassiterite-wolframite veins across the contact and these again into wolframite veins outside the granite. Sulphides are especially found in the tin-tungsten and tungsten zones (Schermerhorn, 1982). The gangue material is mainly quartz with varying amounts of muscovite, topaz, apatite and fluorite. Cassiterite, wolframite and arsenopyrite were the earliest minerals to form, followed by deposition of sulphides with carbonates as the latest phase. Scheelite appears in deposits

enclosed by granitic rocks as in Borralha (Conde et al., 1971; Noronha, 1974) and in Barruecopardo, Spain (Arribas, 1978, 1980).

In northern Portugal scheelite-wolframite skarns occur in the Beira Shale complex with intercalated volcanics and limestones (e.g. Bruco and Fonte Santa). Thadeu (1973) distinguishes two types:

A: Scheelite skarns almost without sulphides.

B: Scheelite-wolframite skarns rich in sulphides.

Gangue minerals are hornblende (tremolite-actinolite), diopside, clinozoisite, zoisite, vesuvianite, garnets and feldspars. Quartz and epidote may locally be present.

Disseminated tin and tantalum deposits do occur in greisens but their size is generally small. Larger deposits are found in Galicia (Spain); the Penouta kaolinized quartz-albitite with greisen veins contains disseminated cassiterite and tantalite concentrations. Similar deposits in Spain are Laza (Galicia), Losacio (Zamora), Golpejas (Salamanca) and El Trasquilon (Cáceres) (Arribas, 1978, 1980). Their mineralogical assemblage consists of quartz, albite, potassium-feldspar, muscovite, cassiterite, columbite-tantalite, tapiolite, ilmenite, rutile, apatite and occasionally gold and fluorite (Arribas, 1978, 1980). Albitization, muscovitization and also kaolinization may be very intense in these occurrences. The only Portuguese deposit which resembles this type is Argemela near Fundão. Petrologically and chemically Penouta and Argemela are alike but differences are present. Greisen veins crosscut the Penouta body whereas they are lacking in Argemela. The Argemela quartz-albitite is accompanied by a quartz-cassiterite stockwork.

Description of the investigated granitoids

The investigated areas in Portugal and Galicia (Spain) are known for their tin, tungsten, tantalum and uranium deposits. Several investigated deposits (Fig. 1) and their related granitic rocks will be discussed below.

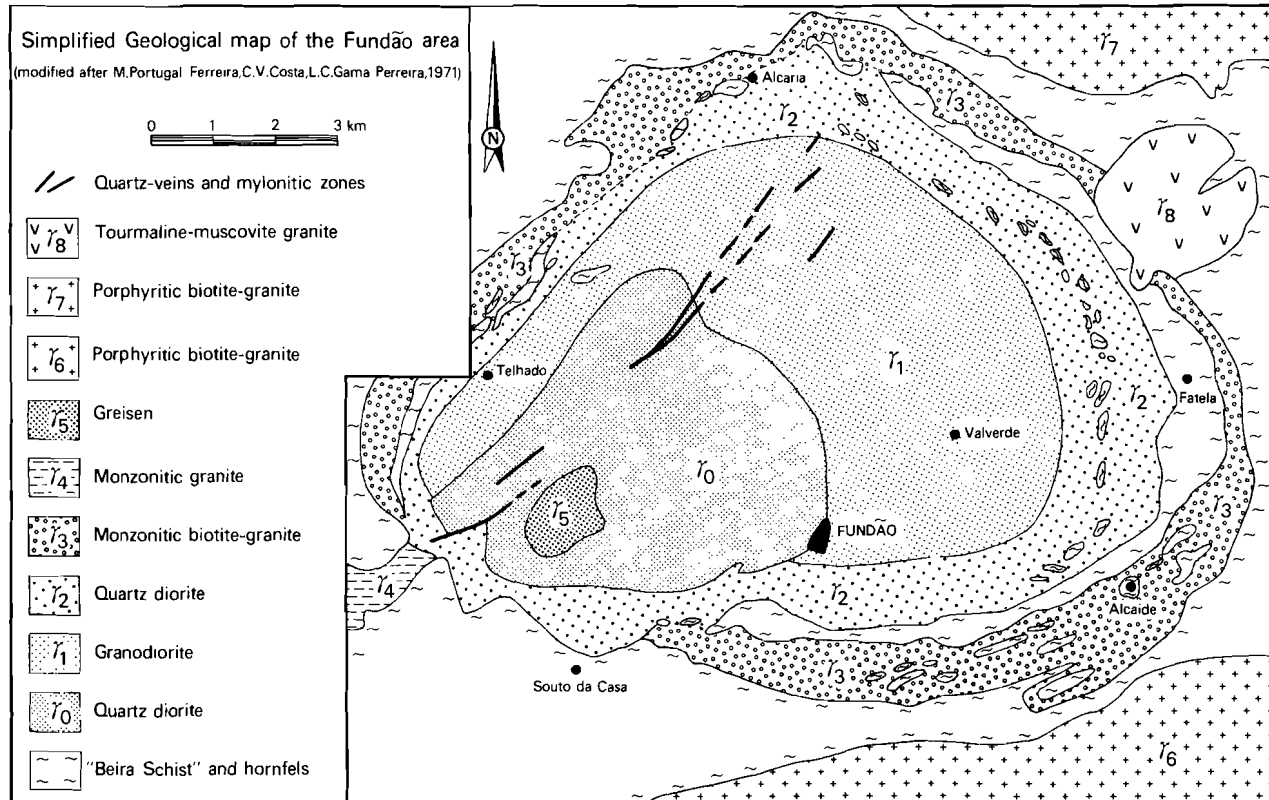


Fig. 2. Simplified geological map of the Fundão (grano)-diorite.

The Fundão region

Fundão is located in the 'Cova da Beira', about 25 km south of Covilha. This 'cova' consists of a deeply weathered granodioritic zoned intrusion, surrounded by hills of contact-metamorphic Beira schists (Fig. 2). The intrusion is composed of a central part with (grano)diorites and an outermost zone of biotite granite (Costa et al., 1971). The intrusive complex belongs to the Older Hercynian granites (Oen Ing Soen, 1970) or to the oldest group of the Younger granites. K-Ar dating on biotites in these rocks gave an age of about 300 Ma after correction for the influence by the Younger porphyritic granites on this complex (Ferreira et al., 1980).

Several satellite bodies occur in the rims of the Fundão intrusion (Fig. 2). The Atalaia granite is of medium grainsize with albite, muscovite or bleached biotite and tourmaline. Potassium-feldspar megacrysts occur in the central parts of the granite. Small Sn-W-bearing quartz veins are found in the granite and a former tungsten mine of some importance is situated in the contact schist near the village of Pero Viseu. The granite of Atalaia probably belongs to the Younger granites (Oen Ing Soen, 1970) and is possibly the uppermost part of a porphyritic two-mica granite. According to Costa et al. (1971) this granite is a satellite of the Belmonte granite in the north. The tungsten mine can be related as well to the porphyritic granite as to the tourmaline-bearing albite-muscovite granite. Both granitic types occur strongly altered in the tungsten mine. Tourmalinization in and around the wolframite-quartz veins is a major characteristic of this mineralization.

Almost in the centre of the intrusion, west of Fundão, lies a small greisenized albite-muscovite granite, the Quinteiros granite. This granite or j-5 in Fig. 2 is crosscut by several quartz veins, surrounded by an intense greisenized zone. In fact, the whole centre is composed of greisens. Although shallow trench-like old workings occur in the greisens, no ores have been found. It thus seems that this greisenization is not accompanied by any mineralization. Even trace elements like rubidium, tin and fluorine are exceptionally low.

Argemela

Argemela is located west of the Fundão intrusion (Fig. 3). The deposit consists of a vertical stockwork of quartz-cassiterite veins in the Beira shales. The mineralization at Argemela differs strongly from that found at Panasqueira. The ore-veins are sub-vertical and occur in a "stockwork". The major ore mineral is cassiterite, wolframite is not present and sulphides only occur in traces. The Beira shales around the quartz-albitite and the ore veins, are characterized by a hydrothermal influence of post-magmatic fluids, especially sericitization. Tourmalinization of schist around the ore veins is negligible compared to Panasqueira (Chapter 3).

The stockwork at Argemela is related to two igneous rock types: first, a quartz-albitite pipe with quartz phenocrysts, albite, potassium-feldspar, muscovite, amblygonite and cassiterite. Its only outcrop is on top of the Argemela hill and it occurs possibly also in the mine. Second, a strongly altered granite which is only exposed in the mine workings. Structural analysis of the hydrothermal quartz-cassiterite veins by Inverno & Ribeiro (1980) indicates the presence of a larger granitic body at depth.

Petrologically, the Argemela quartz-albitite resembles the Penouta deposit in Galicia (Spain). Both deposits consist of quartz-albitite but a later greisenization phase took place only at Penouta. Argemela only suffered a hydrothermal overprint which increased the already high trace element contents.

Panasqueira

The Panasqueira tungsten-tin deposit is located about 35 km WSW of Fundão (Fig. 3). The sub-horizontal tungsten-tin veins in the Beira schists are related to a greisenized granite cupola, exposed in the mine (Fig. 2, Chapter 3). Two types of granitic rocks can be distinguished: first, a greisenized albite-muscovite granite and second, the strongly altered greisen cupola at the top. Greisenization at Panasqueira is variable and intense; the uppermost parts of the granite and the sub-vertical granitic veins are completely greisenized. This is probably due to concentration of fluids in the upper parts of the granite, thereby altering the two-mica granite into a muscovite-

albite leuco-granite and subsequently into a muscovite-quartz greisen. Sulphides like arsenopyrite, sphalerite and chalcopyrite are abundant in the greisen cupola, concentrations of cassiterite are much lower. More detailed geological information about Panasqueira is given in Chapter 3.

Porphyritic biotite granites

The outcrops of the porphyritic biotite granites are the major expressions of the Younger granite series in Central Portugal (Fig. 3). The granites are coarse grained with large potassium-feldspar megacrysts up to 15 cm in size. Biotite is always present, locally accompanied by muscovite. The porphyritic granite of Belmonte, Covilha and Sortelha contains many small pegmatites and quartz veins with tin, niobium, tantalum and tungsten mineralizations. Weathering of these small deposits is responsible for the tin-tantalum placers along the Zèzere and other rivers near Belmonte (Fig. 3).

The occurrence of large potassium-feldspar megacrysts and the age of the batholiths (Ferreira et al., 1980) could indicate that the Belmonte and Covilha granites are related to the Panasqueira granite.

The porphyritic biotite granite of Alpedrinha is part of the Castelo Branco granite. The northern and eastern side is porphyritic, the central part is mainly a fine-grained two-mica granite, possibly belonging to of the Older granites. Considerably less is known about this granitic massif or its possible mineralizations. The geological map of Portugal does not differentiate between these two types.

Capinha

The Capinha granite (Fig. 3) is a fine-grained two-mica granite with some tin-tungsten mineralizations. Shearing of this granite is visible in thin sections by orientated biotite and muscovite zones.

The Capinha granite probably belongs to the Older Hercynian granites. Remnants of these Older(?) granites occur within the porphyritic Younger granitic batholiths.

Bruco and Fonte Santa

The Bruco granite (Fig. 1) is coarse grained with biotite and muscovite. Potassium-feldspar megacrysts are present (Conde et al., 1971). Although weathering only exposes a flat granitic surface,

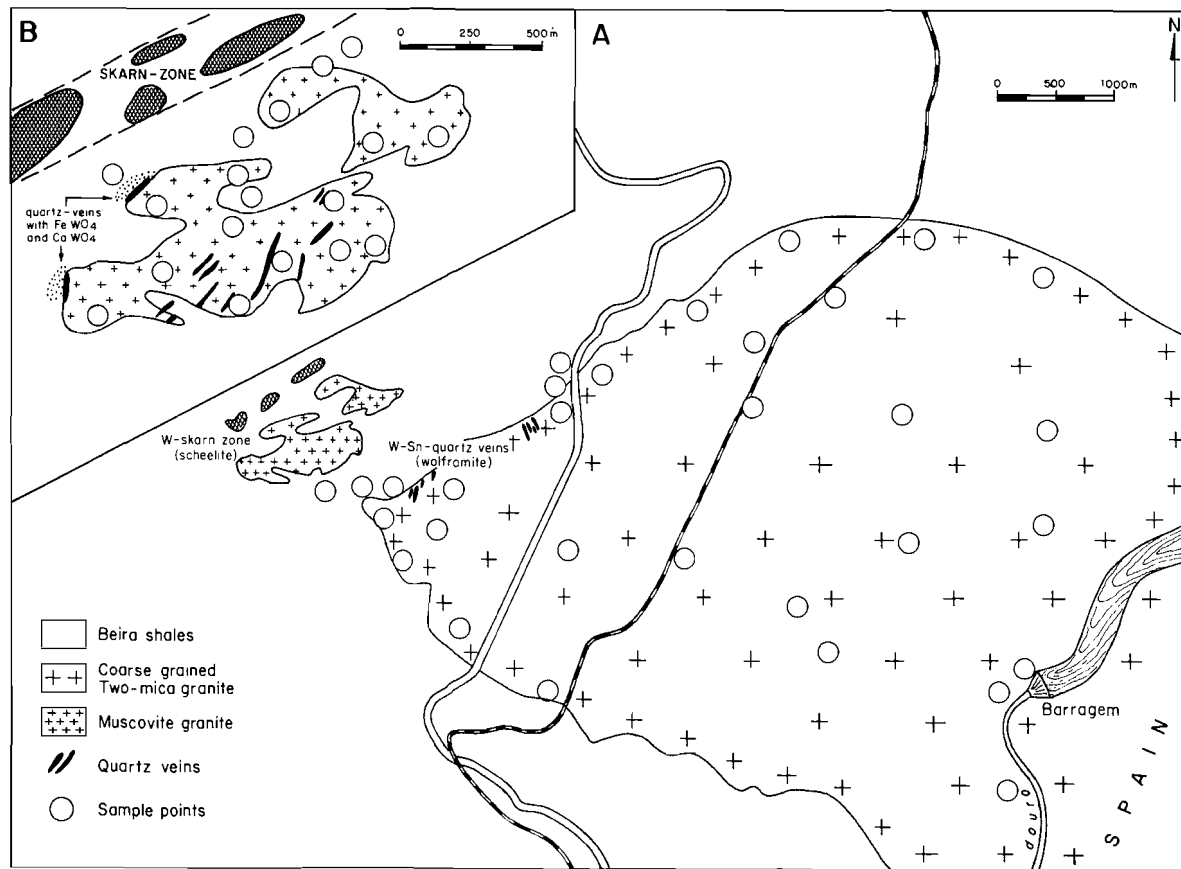


Fig. 5. Simplified geological map of the Bruco and Fonte Santa granites (after Conde et al., 1971).

deeper parts are exposed in the Douro valley, below the dam in the river (Fig. 5).

Mineralizations are rare in this granite although tourmaline-bearing pegmatites occur. In the western part of the granite and in the carbonate-rich Beira shales, some cassiterite- and wolframite-bearing quartz veins with scheelite occur (Fig. 5).

West of the Bruco granite a tourmaline-bearing muscovite granite occurs, the Fonte Santa granite, which is accompanied by cassiterite-wolframite-scheelite quartz veins. The western part of the granite is also known for a large scheelite skarn zone in the carbonate-rich Beira schist. The relation between this skarn zone and the tourmaline-muscovite granite is not clear as the skarn seems to be related to a fault zone in the Beira schists (Fig. 5).

Regoufe

The Regoufe granite (Fig. 1) is a biotite-muscovite granite which grades upwards into a muscovite granite (Fig. 6). Erosion exposes a vertical section of approximately 400 m through the granite. The Regoufe granite was studied in detail by Sluyk (1963) and recently geochemically by Vriend et al. (in press). Geochemically the lower parts are relatively rich in titanium, strontium and barium whereas the upper part is enriched in rubidium, lithium and cesium (Vriend et al., in press).

In and around the Regoufe granite tin- and tungsten-bearing quartz veins occur. Mineralized quartz veins in the granite are surrounded by greisen zones (Sluyk, 1963). Mining occurred on tungsten-rich veins.

Penouta and Laza

The Penouta quartz-albitite (Fig. 1) and Laza leuco-granite in Galicia (Spain) are characterized by disseminated tin-tantalum mineralizations (Arribas, 1978, 1980). Penouta contains greisen zones with quartz-cassiterite veins.

Other granites

Other granites included in the analytical programme are Canadõ, Cedões, Barcarotta and Numõo (Fig. 1). Also included are several French granites like Beauvoir (reference rock sample Ma-N), Monts de Blond, Montebras and Jonchère, all from the Massif Central. These specialized

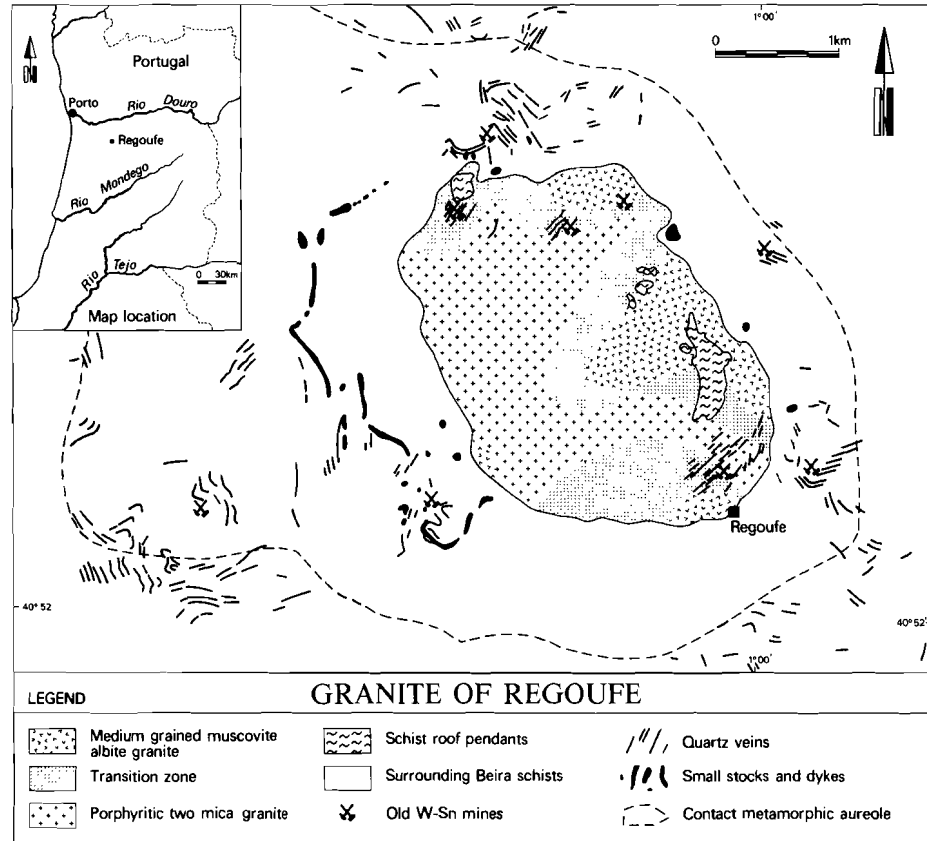


Fig. 6. Simplified geological map of the Regoufe granite (after Vriend et al., in press).

granites were compared with the Portuguese granites but were not used in the computation.

GEOCHEMISTRY

Analytical techniques

Granite samples were collected from surface outcrops and in the mine workings. About 15 to 20 chips were collected over an area of 10 to 40 m². The weight of the samples was between 1 and 7 kg. Initially, some samples were broken with a jaw-crusher coated with tungsten-carbide, thus tungsten values from these samples were deleted from the data set. Later, a Ni-Cr steel jaw-crusher was installed. Samples were split and pulverized in a swing-mill (Ni-Cr steel) to -250 mesh.

The analytical techniques used were:

- 1) X-ray fluorescence for Rb, Sr, Nb, Ta, Sn, Ti, Zr, U, Ba, W, P and Cs in pressed powder briquettes and major elements in glassbeads.
- 2) Atomic-absorption spectrometry for Cu, Zn, Li, Na, K, Ca, Mg, Fe and Mn after dissolution in a mixture of HF, HClO₄ and HNO₃ in teflon pressure vessels.
- 3) Emission spectrometry for B (only semi-quantitative).
- 4) Instrumental neutron activation analysis for the elements K, Sc, Rb, Cs, W, U, Hf, Th, Ta, As, Zn, Ag and REE (La, Ce, Yb, Eu, Tb, Lu).
- 5) The ion-selective electrode technique for the F determination after dissolution in a Na₂CO₃ melt.
- 6) Major elements of some samples were determined by the rapid-rock method of Shapiro (1975).
- 7) Inductively coupled plasma emission spectrometry for the elements Na, K, Ca, Mg, Fe, Li, Ba and Cu.

Several elements were analyzed by two or more different techniques which provided checks on the accuracy of the analyses. The quality of

the analysis was further monitored by inclusion of a wide range of international standard samples in the analytical programme.

Major elements were measured according to the rapid-rock method of Shapiro (1975). In some cases detection limits influence the reproducibility of the method used, e.g. low TiO_2 contents in greisen samples.

For comparison of the reproducibility and accuracy several standards are given in the appendix with proposed values by Gladney et al. (1981) and Abbey (1982). Low TiO_2 values ($< 0.06\%$) in specialized granites were substituted by TiO_2 values obtained by the XRF measurements in briquettes. The major elements are in good agreement with the analyses of the international standards.

Major and trace elements were determined by INAA, XRF, ICP, AAS and ISE. The INAA and XRF analyses were calibrated against international standards and synthetic samples spiked with the elements of interest (e.g. Sn and W).

Several elements were determined by two different techniques, e.g. Ta by INAA and XRF. The low tantalum content in the samples and the relatively high detection limit of the XRF (7 ppm) indicate that INAA values for tantalum are to be preferred over the XRF analyses. Values well above the detection limit of the XRF are in good agreement with the INAA values.

The same problem also holds for W (XRF detection limit: 6 ppm), Ce (XRF: 20 ppm), La (XRF: 20 ppm), Th (XRF: 10 ppm), and U (XRF: 8 ppm). Whenever available, INAA values are preferred for low concentrations of these elements. In greisen samples rare earths are strongly leached, so that low Ce and La values are near or below the detection limit of the INAA.

Cesium gives good agreement between INAA and XRF analyses for contents above 10 ppm, but below 10 ppm XRF analyses tend to be lower.

Rubidium, strontium, zirconium, titanium and phosphorus analyses were all done by XRF. XRF results for niobium at values above 10 ppm are also reliable but below 10 ppm the detection limit is approached (about 6 ppm) with a simultaneous decrease in precision. Analyses of

phosphorus tend to scatter which is probably caused by matrix effects in the samples, combined with several other effects during analysis. This scatter gives a rather large error in the reproducibility.

Barium analyses by XRF are influenced by high titanium contents for which a correction was applied. However, this correction procedure did raise the detection limit to about 50 ppm for high titanium contents. In case of low titanium contents the detection limit of barium is lowered to about 10 ppm.

Tin was calibrated against synthetic standards as tin contents of international standard samples are either too low (< 10 ppm) or extremely high (Ma-N, 800-1200 ppm). Low tin contents are in agreement with standard samples but below 6 ppm the detection limit is approached.

Uranium, tantalum and tungsten in low contents approach the detection limit of the XRF, and INAA values were thus used for these elements, when available.

Copper, zinc and lithium determined by AAS presented no analytical problems. Only copper values below about 10 ppm are around the detection limit and scatter accordingly. Fluorine analyses by ISE pose no problem and are in agreement with the standards. The reproducibility of the results, however, is strongly influenced by the age of the ion-selective electrode which deteriorates with use.

Interpretation

Statistical procedures from the SPSS (Nie et al., 1975) and BMDP (Dixon et al., 1981) computer programme libraries were applied, as well as some other special programmes (Davis, 1973).

First, histograms of the element contents were prepared as a check for outliers, normality or log-normality and multi-modality. With the aid of histograms data points well away from the principal grouping could be detected and accordingly suppressed for later statistical treatment. The trace element distributions have in general a lognormal character, therefore logarithmic values were used for further calculations.

As the data set is not homogeneous, factor analysis seems to be an

Table I: mean values and range of the investigated granitoids in Portugal and Spain.

	N	Rb	Sr	Cu	Sn	F	W	Li	Zr
<u>Highly specialized:</u>									
Beauvoir	1	3600	84	140	1050	17000	70	4900	27
Argemela quartz									
albitite	9	1780 882-2295	70 7-285	21 8- 45	650 190- 890	8500 2930-11100	4 1-10	3200 770-4405	14 9- 25
Montebras	2	1190 1179-1202	95 40-145	28 20- 35	885 790- 980	3220 3200- 3240	17 17-17	650 490- 810	18 10- 26
Panasqueira									
greisen	52	730 464- 986	12 4- 25	320 5-1380	90 41- 205	4500 1990- 6400	25 15-37	340 90- 510	23 18- 35
Regoufe	57	690 500- 950	35 12-115	8 3- 17	55 25- 100	3500 2000- 6880	16 7-35	550 240- 900	35 17- 85
Mts. de Blond	5	680 644- 716	34 25- 45	6 2- 8	60 53- 75	4300 3690- 4710	17 13-19	610 500- 720	45 35- 65
Penouta	6	800 257-1026	33 5-110		340 5- 540	630 250- 1180	4 2- 6	110 40- 240	25 14- 66
Fonte Santa	14	490 360- 648	26 15- 55		45 25- 65	1100 640- 2440	12 11-12	270 105- 655	25 21- 29
<u>Specialized:</u>									
Atalaia j-8	24	495 347- 644	30 10- 50	8 2- 30	40 24- 80	2400 1325- 4680	10 2-17	350 160- 805	40 18- 65
Panasqueira									
granite	24	675 527- 810	35 20- 60	35 4- 310	60 25- 113	6800 3590-10880	20 10-40	690 325-1000	85 40-105
Argemela micro									
granite	4	1050 734-1575	225 110-315	70 45- 95	570 177-1165	7000 4920-10820	38 21-55	1100 645-2145	165 145-180
Cedões	7	950 689-1413	22 10- 60		19 12- 30	220 110- 330	2 1- 4	135 50- 240	19 10- 30
Jonchière	3	565 522- 608	32 25- 35	9 4- 16	45 33- 57	3000 2180- 3680	13 10-19	300 210- 380	75 65- 90
Laza	2	430 414- 446	50 45- 50		65 55- 70	705 650- 760	6 4- 7	405 310- 500	70 65- 70
Atalaia mine	9	280 203- 374	33 5-135	11 5- 30	40 8- 100	1500 580- 6200	19 6-35	26 10- 50	25 11- 40
Numão	5	510 464- 549	32 25- 50		10 2- 20	1400 390- 2300	3 1- 5	185 115- 270	70 50- 95
<u>Barren granites:</u>									
Belmonte									
granites	18	400 279- 509	55 25- 90	9 4- 16	16 2- 85	1700 1230- 2680	5 1- 9	235 160- 330	130 60-190
Capinha	19	325 257- 599	55 10- 70	30 4- 210	17 2- 40	1000 650- 1780	7 1-15	150 70- 250	70 20-135
Canado	27	375 279- 554	85 5-325		18 4- 45	480 120- 1480	7 1-18	105 25- 385	80 20-180
Bruco	28	320 284- 432	160 120-205		16 8- 70	1100 100- 2400	3 2- 6	330 180- 610	100 80-138
Alpedrinha	9	250 225- 302	100 50-150	8 4- 10	11 4- 35	860 430- 1530	12 1-80	155 140- 170	135 15-165
Fundão j-3	5	145 117- 185	140 120-170	8 6- 8	1 1- 3	500 370- 740	1 1- 2	65 45- 85	100 85-125
Quinteiros j-5	11	115 99- 140	50 6-120	35 16- 60	6 1- 25	190 125- 290	8 1-20	17 10- 30	55 25- 95
Barcarrota	19	80 7- 324	80 15-400		2 1- 7	245 80- 500	3 1-11	55 20- 120	375 80-765
Fundão j-012	11	85 50- 135	225 45-320	10 4- 30	2 1- 8	500 480- 520	1 1- 2	55 30- 85	120 95-135

Table I: mean values and range of the investigated granitoids in Portugal and Spain.

	N	Nb	U	Zn	Cs	Ta	Ba	TiO ₂	P ₂ O ₅
<u>Highly specialized:</u>									
Beauvoir	1	173	12	220	640	306	42	.01	1.40
Argemela quartz albite	9	55 35- 65	7 1-17	130 80- 240	200 50-325	50 17- 60	9 2- 35	.01 .01-.01	1.59 1.27-1.84
Montebras	2	110 104-111	8 8- 8	65 60- 65	80 75- 80	120 119-121	2670 1605-3725	.01 .01-.01	.28 .16- .39
Panasqueira greisen	52	30 12- 45	13 1-24	820 30-6150	24 11- 40	16 2- 35	45 15- 165	.02 .01-.08	.33 .17- .49
Regoufe	57	38 19- 60	10 1-20	80 30- 150	50 20-115	15 9- 34	75 12- 180	.06 .01-.21	.45 .27- .71
Mts. de Blond	5	33 31- 34		70 65- 70	100 80-135	8 4- 10	85 80- 95	.10 .09-.13	.34 .28- .44
Penouta	6	45 9- 60			33 2- 50	45 6- 66	85 11- 345	.03 .00-.15	.06 .02- .25
Fonte Santa	14	23 17- 29	12 1-25		32 10-130	11 8- 16	17 8- 40	.04 .02-.08	.41 .23- .52
<u>Specialized:</u>									
Atalaia j-8	24	22 12- 30	8 2-17	60 30- 125	40 15- 80	11 5- 20	70 5- 170	.09 .02-.17	.46 .13- .55
Panasqueira granite	24	18 15- 25	13 9-21	235 35-1560	33 20- 46	3 2- 5	130 40- 205	.21 .07-.28	.56 .35- .85
Argemela micro granite	4	16 6- 25	2 1- 3	55 50- 65	340 265-560	2 1- 3	355 275- 475	.33 .31-.36	1.55 .95-1.76
Cedões	7	14 10- 19	9 6-12		37 16- 67	7 5- 8	17 6- 32	.02 .01-.05	.63 .50- .87
Jonchière	3	24 20- 27		65 50- 70	50 30- 70	5 4- 6	155 90- 210	.14 .12-.15	.26 .10- .40
Laza	2	14 13- 15			28 22- 34	4 1- 7	200 200- 200	.18 .16-.19	.35 .31- .39
Atalaia mine	9	17 10- 20	7 1-15	34 20- 75	4 1- 10	6 3- 10	290 5-1025	.07 .04-.13	1.27 .13-7.56
Numão	5	13 11- 16	16 7-23		30 17- 44	5 1- 10	100 80- 130	.20 .13-.29	.45 .40- .48
<u>Barren granites:</u>									
Belmonte granites	18	17 13- 25	14 1-65	95 65- 180	19 6- 40	6 1- 11	265 110- 560	.29 .13-.53	.27 .15- .34
Capinha	19	14 9- 45	11 2-25	65 25- 90	14 6- 25	5 1- 30	220 30- 395	.19 .01-.25	.31 .14- .41
Canado	27	16 8- 25	7 1-17		25 10- 53	4 1- 9	240 8- 515	.21 .05-.59	.38 .17- .62
Bruco	28	11 9- 12	8 1-16		18 5- 31	6 2- 7	510 370- 660	.28 .22-.39	.35 .29- .51
Alpedrinha	9	13 9- 15	8 2-16	70 65- 75	12 4- 25	3 1- 5	380 95- 550	.34 .04-.44	.36 .32- .43
Fundão j-3	5	7 3- 9	3 1- 7	80 35- 210	5 1- 15	9 5- 13	380 355- 395	.29 .22-.43	.21 .20- .21
Quinteiros j-5	11	7 4- 9	6 3-10	23 12- 40	1 1- 2	2 1- 6	315 195- 405	.12 .06-.20	.17 .08- .23
Barcarrota	19	40 15- 90	2 1-12		1 1- 4	10 1- 21	575 120-2025	.28 .12-.67	.10 .01- .25
Fundão j-012	11	4 1- 6	4 1- 7	50 8- 70	1 1- 4	3 1- 8	435 300- 505	.46 .32-.64	.19 .05- .26

inappropriate technique, so component analysis with Kaiser Varimax rotation was used instead (Davis, 1973; Joreskog et al., 1976). If necessary, weight factors were used to suppress outliers in the data set because they can severely distort the outcome of the component analysis (Davis, 1973; Joreskog et al., 1976). Component analysis is not a real statistical technique and can best be considered as a projection of a N-variable space into a n-variable space whereby $N \gg n$ and a minimum amount of information is lost. The results of the component analysis have to be interpreted as such. The choice of the size of n, or the number of components to be retained, is generally a difficult problem for which no exact criteria exist.

The eigenvalues of the correlation matrix, however, do give some indication of the significance of the components. In this study a first component explains 48% of the variation, a second explains an additional 19%. Further components do not seem important because their eigenvalues are small and decrease in a homogeneous way to zero. With more than one component, a Kaiser Varimax rotation is applied in order to attain a 'simple structure'. The value of the different components should be judged on its geological and geochemical merits.

RESULTS AND DISCUSSION

The mean values and ranges of the investigated granitoids are given in Table I. The granites are divided into barren, specialized and highly specialized types although some overlap between the groups is possible.

A different number of samples was available from each granite that was included in this study. Therefore a weight factor was introduced to give each granite the same influence on the subsequent interpretation. Each granite group was reset to about 1000 samples, apart from the Panasqueira greisens which were set to about 50 samples. The influence of the greisen samples was suppressed as their elevated trace element content could not be compared with the more common

granites.

Trends in a one-component model

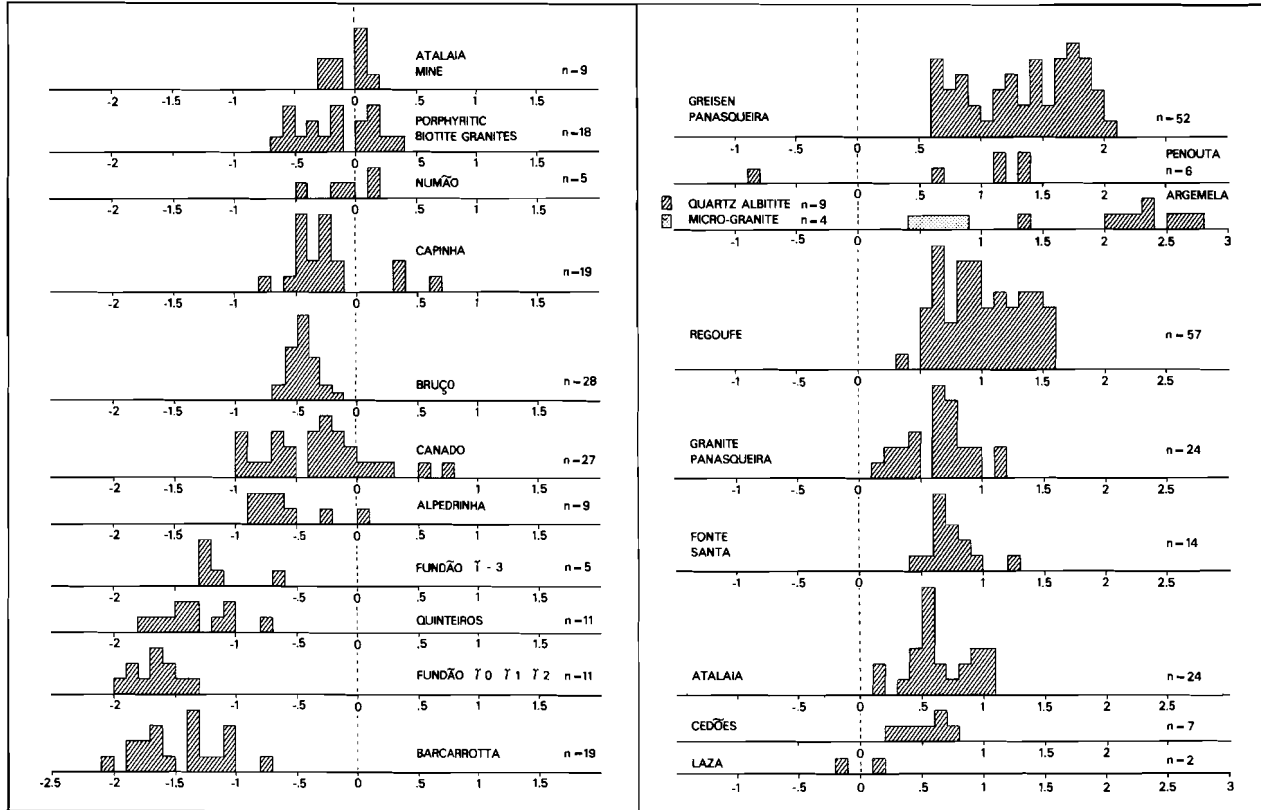
The component loadings of the one-component model are shown in Table II. In this calculation Rb, Sn, Cs, Li, Nb, F, P₂O₅, Ta, Zn and W load positively; Zr, Ba, TiO₂ and Sr load negatively on the component. The first group of elements (Rb to P₂O₅) generally increase in concentration from granodiorite to common granites and from here to specialized granites. The second group (Zr to Sr) decrease simultaneously with the first group.

In Fig. 7 histograms of the component scores of each granite are shown. The granites are arranged from barren types in the left to highly specialized types in the right. The range of the component scores in the individual granites may vary. The plotted histograms show a shift from barren to highly specialized granites which partly coincides with the petrological trend from more basic to more specialized granites, e.g. from the Fundão granodiorite to the Argemela quartz-albitite. This trend interferes with the 'mineralizing' trend and may obscure the distinction between barren and ore-bearing granites in cases of weak mineralizations.

Barcarrotta, Fundão and Quarteiros (Fig. 7) are considered as "barren" granites and granodiorites. Although Quarteiros seems to be a greisen deposit, the element contents and the loadings of the one-component model gives it a "barren appearance". Alpedrinha, Bruco and Capinha (Fig. 7) are already enriched in some trace element contents. Some higher component loadings in Canado and Capinha may point to possible mineralizations. Numão, the porphyritic biotite granites, the Atalaia mine and Laza show a stronger specialization compared to earlier mentioned granites.

Cedões, Atalaia, Fonte Santa, Panasqueira, Regoufe, Argemela and Penouta belong to the highly specialized granites which are also associated with tin and/or tungsten mineralizations. Laza is also supposed to be a specialized granite but this is not clearly observed in Fig. 7 as only two samples were available.

From the results mentioned above it seems that granitoids with



LOADINGS: Rb.92 Sn.90 Cs.85 Li.76 Nb.74 Zr -.73 F.71 Ba -.70 TiO₂ -.70 Ta .61 Zn .51 W.45 Sr-.43 P₂O₅ .40

Fig.7 Histograms of component loadings of individual granites in a one component model.

Table II: Loadings in the one-component model.

	COMPONENT 1
Rb	.92
Sn	.90
Cs	.85
Li	.76
Nb	.74
Zr	-.73
F	.71
Ba	-.70
TiO ₂	-.70
Ta	.61
Zn	.51
W	.45
Sr	-.43
P ₂ O ₅	.40

Eigenvalue before rotation: 6.70

component loadings above -.75 are slightly specialized whereas loadings above about .25 suggest highly specialized granites with mineralizations.

Trends in a two-component model

The results of the component analysis of the one-component model indicate the presence of a second component. The component loadings of the two-component model are given in Table III. A comparison with the one-component model (Table II) indicates a split in the hydrothermally influenced elements. The component loadings suggest that component 1 (F, Li, Cs, Rb, Zn, Sn, P₂O₅, Nb and W) is related to a hydrothermal influence on the granites and that component 2 (TiO₂, Ba, Zr, Sr, -Ta, -Nb, -Rb and -Sn) possibly points to an original magmatic trend. A plot of the component scores of component 1 against component 2 is given in Fig. 8. The granites occur as areas and their position is in accordance with their petrological features. Excluded are samples

Table III: Component loadings in a two-component model.

	COMPONENT 1	COMPONENT 2
TiO ₂		.92
F	.89	
Li	.89	
Ba		.85
Zr		.83
Cs	.82	
Sr		.77
Ta		-.68
Rb	.73	-.57
Zn	.71	
Sn	.70	-.57
P ₂ O ₅	.68	
Nb	.44	-.61
W	.42	

Eigenvalues before rotation: 6.70 and 2.62
 (All data are log-transformed).

which plot far away from their grouping. These outliers are diverted to both sides in the plot. It seems that even slightly mineralized granites contain regions that could be favourable for mineralizations.

Barren granites like Fundão, Barcarrotta and Quinteiros are found at the base of Fig. 8. Slightly specialized granites like Capinha, Alpedrinha, Bruco, Laza, the porphyritic biotite granites and Numão concentrate within one large field (Fig. 8). More specialized granites branch from the aforementioned field. Panasqueira, Regoufe, Atalaia and Fonte Santa plot closely along a more (hydrothermal) enriched trend (Fig. 8). Sodium-rich granites and quartz-albitites also appear in a trend. The Argemela quartz-albitite with quartz-cassiterite veins concentrate in this field, together with the Beauvoir granite (France, reference sample Ma-N) with associated tin-mineralizations. The Penouta tin-tantalum deposit with greisen veins in Galicia does not follow this trend. Penouta also deviates in trace element content

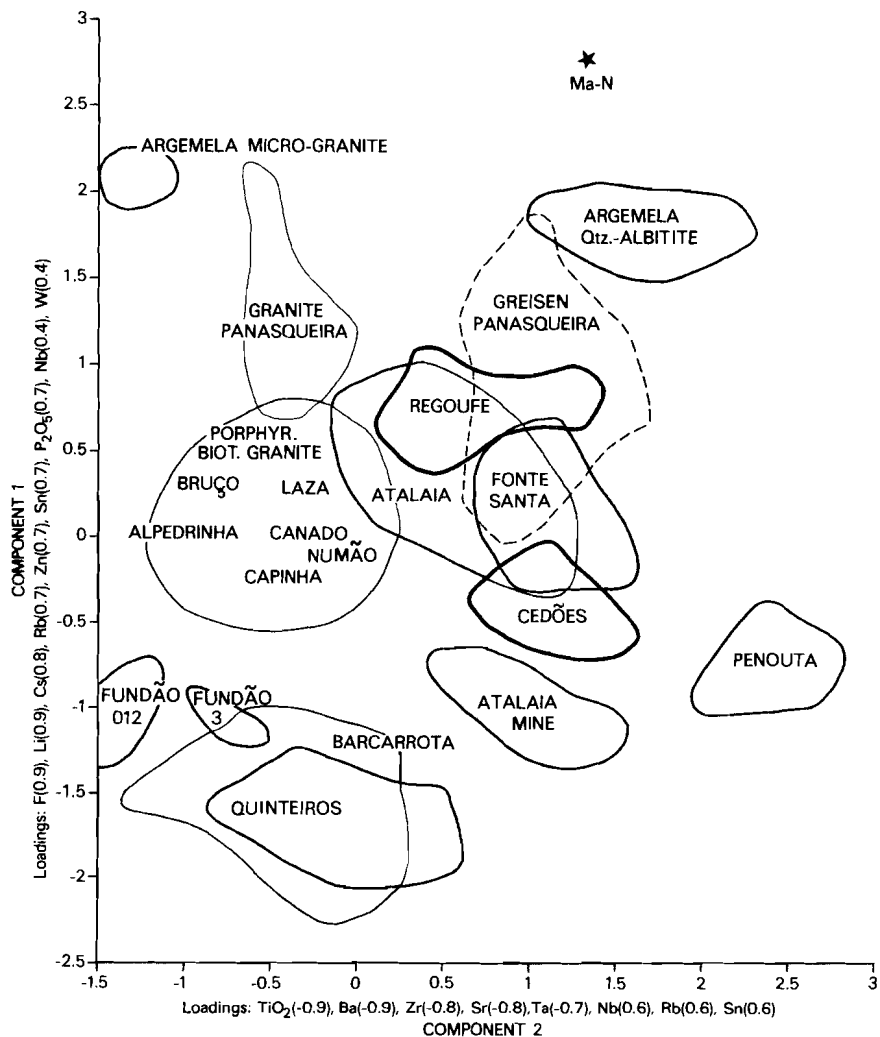


Fig. 8. Component score plot of individual granites of component 1 against component 2.

(much lower P₂O₅, F, Li and Cs contents).

The Quinteiros "greisen" plots in the area of more common granites and granodiorites. Although petrographically a greisen, Fig. 8 indicates that it is possibly a 'pseudo-greisen'. Cedões and samples

from the Atalaia mine deviate more from the hydrothermal trend. The Atalaia mine contains strongly muscovitized porphyritic (biotite) granites, possibly caused by a strong hydrothermal influence without the addition of trace elements.

The French specialized granites plot in the same area as the Portuguese granites with tin-tungsten mineralizations like Fonte Santa, Atalaia and Regoufe. The Beauvoir granite plots close to the Argemela quartz-albite; both granitoids are especially enriched in albite and trace elements.

The trend in Fig. 8 is the result of magmatic differentiations and superimposed post-magmatic fluid activity. The post-magmatic fluids are responsible for the tin-tungsten trend as represented by the Panasqueira greisen, Regoufe and Fonte Santa.

The multi-element model in Fig. 8 indicates the chemical specialization of granites related to tin, tungsten and tantalum deposits in the Iberian Peninsula. With the aid of trace elements a differentiation can be made between barren granites (Fundão, Barcarrotta), weakly specialized granites (Numão, Canado, porphyritic biotite granites) and highly specialized and mineralized granites (Regoufe, Panasqueira, Fonte Santa, Argemela, Penouta). It is a good method for screening large areas for tin-tungsten bearing granites but it does not indicate if ore deposits are present.

The difference between barren and slightly mineralized granites is small but this implies that sample densities within the granite have to be adequate to detect specialized granites.

Trends within granites

This study indicates that differences exist between various types of granites but also that specialized granites differ internally. The Regoufe granite was investigated by Vriend et al. (in press) who found a strong contrast between top and lower parts. Similar results were

obtained from the Atalaia granite which resembles the Regoufe granite. The elements rubidium, lithium, cesium, tin, tungsten, niobium, tantalum, titanium, strontium, barium, zirconium, copper, zinc, sodium, potassium, calcium, magnesium, phosphorus and iron were analyzed in 24 samples of the Atalaia granite, over an area of about 5 km².

The mean values of the Atalaia granite are given in Table IV, together with data of Low-Ca granites by R sler & Lange (1972). Increased Rb, Li, Cs, F, Sn and W values indicate a specialized granite. In accordance with this fact are the low CaO, MgO, TiO₂, Zr, Sr and Ba values. The P₂O₅ values are also higher than in common granites.

Component analysis or contour maps (Chapter 4) were not prepared of the Atalaia granite. The data set was small (24 samples) and not distributed in a sufficiently homogeneous way over this weathered granite. In some areas agriculture prevented the occurrence of suitable outcrops.

The contents of the elements are given individually for each sample point in the Atalaia granite. The amount of a major, minor or trace element is given as a black dot which increases upon an increase of their content. Fig. 9 show these maps for the elements rubidium, lithium, cesium, fluorine, tin, barium, titanium, sodium and magnesium. Titanium, zirconium and barium correlate, giving a NW-SE trend with increased contents.

Lithium, cesium, rubidium and fluorine show a different pattern; they are correlated with each other. These elements give higher values in the southwestern part of the granite. The behaviour of tin deviates from that of lithium and cesium and gives a completely different picture. In specialized granites tin is often correlated with fluorine, rubidium, lithium and cesium but this is not the case in the Atalaia granite.

Two mineralizations are found in the Atalaia granite (Fig. 9), a small greisen occurrence and some small quartz veins with cassiterite. These mineralizations are not characterized by increased trace element contents. Instead, lower contents of fluorine, lithium and rubidium occur in the greisen location. The cassiterite-quartz veins are not

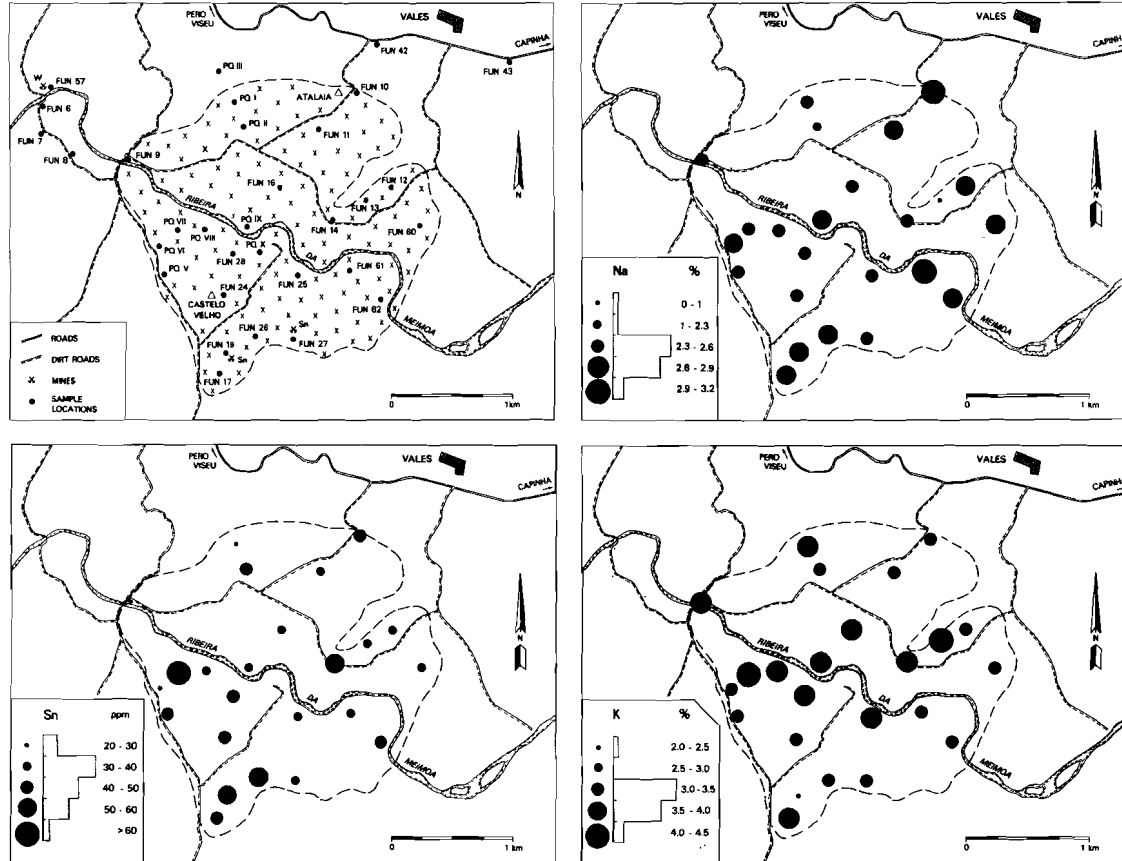


Fig. 9. Simplified geological map of the Atalaia granite and major or trace element contents.

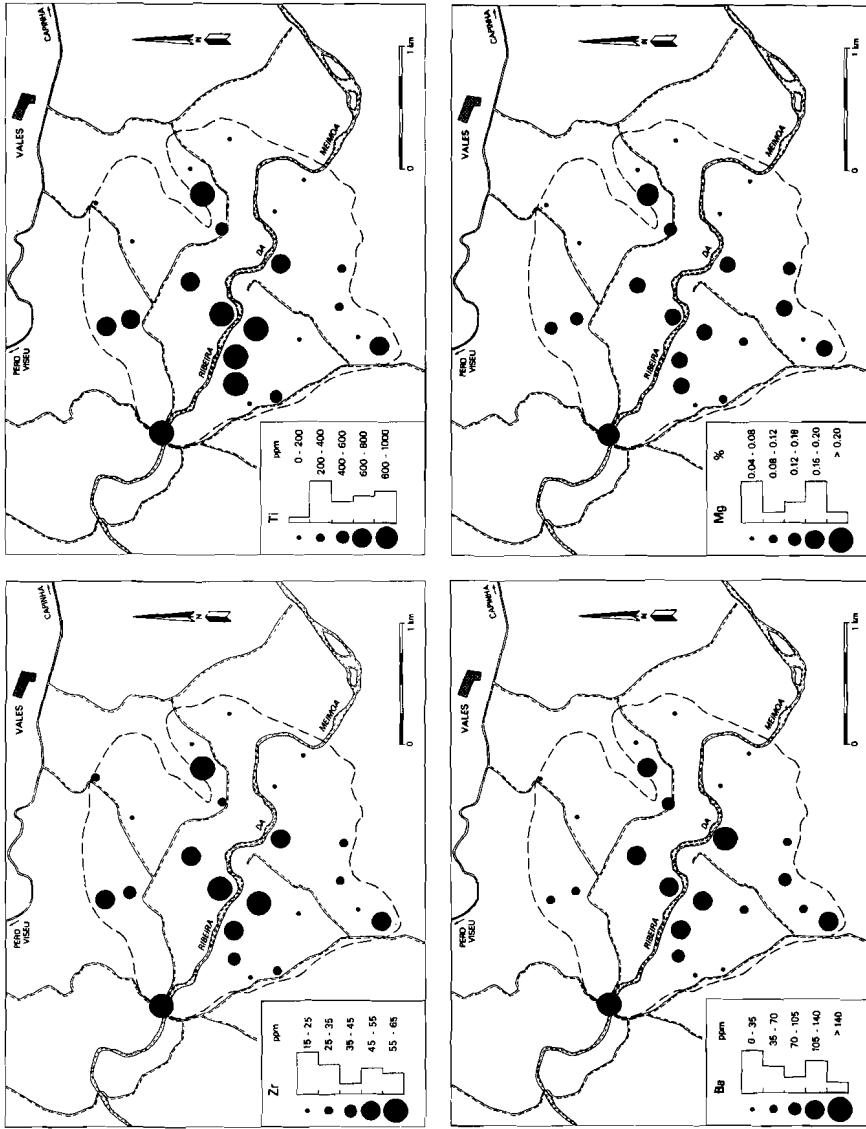


Fig. 9. Major or trace element contents in the Atalala granite.

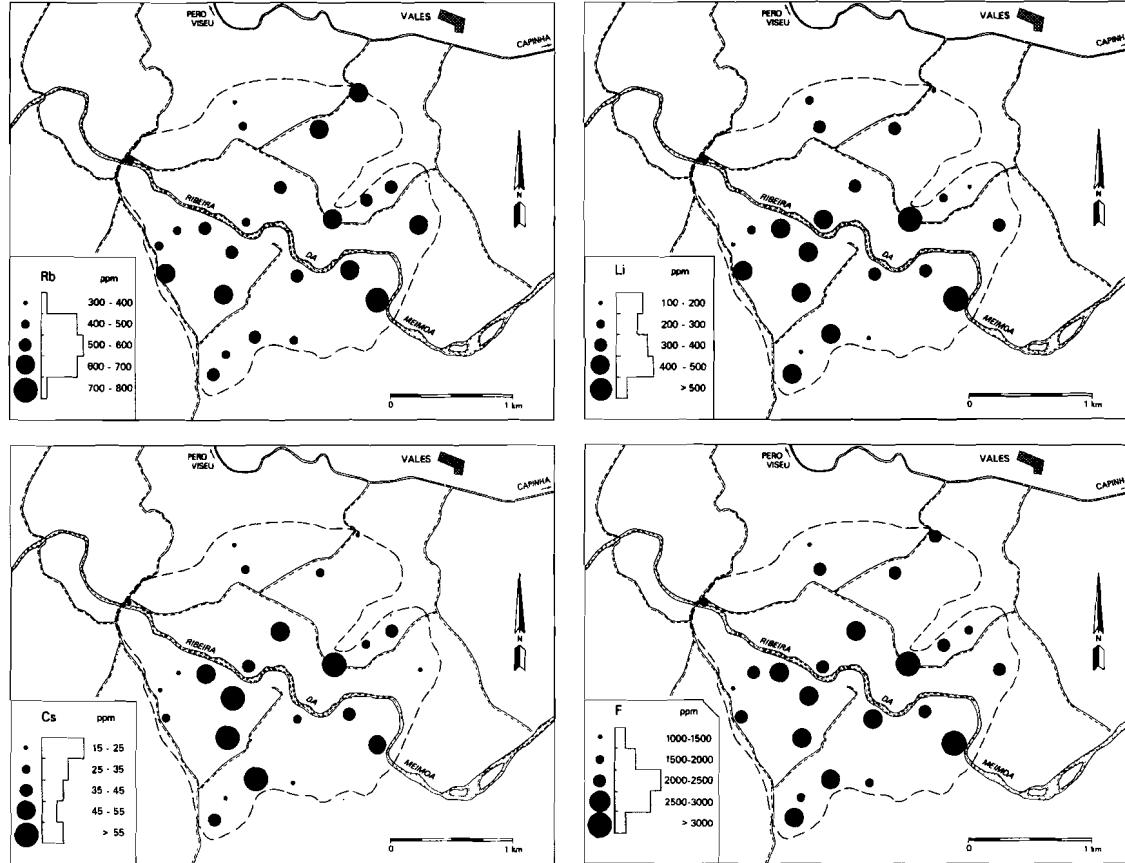


Fig. 9. Major or trace element contents in the Atalaia granite.

Table IV: Mean, standard deviation and range of the Atalaia granite in ppm unless stated otherwise.

	mean	st.dev.	range	Low-Ca granites
CaO %	.24	.08	.06 - .48	2.21
MgO %	.21	.10	.05 - .37	.27
Na ₂ O %	3.32	.72	.39 - 3.92	3.73
K ₂ O %	4.29	.51	2.66 - 4.93	4.02
Fe ₂ O ₃ %	1.47	.36	.90 - 2.06	3.86
P ₂ O ₅ %	.46	.09	.13 - .55	.16
TiO ₂ %	.09	.05	.02 - .17	.38
Rb	495	83	345 - 644	170
Li	350	149	160 - 805	40
Cs	40	19	15 - 80	4
F	2400	715	1325 - 4680	850
Sn	40	11	24 - 80	3
W	10	4	2 - 17	2
Nb	22	4	12 - 30	21
Ta	11	5	5 - 20	4
Zn	60	20	30 - 125	39
Cu	8	7	2 - 30	10
U	8	4	2 - 17	3
Zr	40	16	18 - 65	175
Sr	30	11	10 - 50	100
Ba	70	53	5 - 170	840

characterized at all by trace elements. Some major elements happen to be lower in the southern parts where mineralizations occur but also in the north where no mineralizations are found.

The poor correlation between mineralization and trace element contents is probably due to the erosion level of the granite. The Atalaia tourmaline-muscovite granite has been barely exposed by erosion and a vertical section through the granite as in Regoufe (Vriend et al., in press) is not available. The combination of a relatively horizontal surface and few samples prohibits an interpretation of the trace element contents. The mean values of the granite, however, indicate the presence of a specialized granite (Table IV).

CONCLUSIONS

Specialized granites which produce tin, tungsten and tantalum deposits are also characterized by increased contents of rubidium, lithium, cesium, fluorine, tin, tungsten and sometimes tantalum and phosphorus. At the same time the amounts of titanium, zirconium, barium and strontium are lower.

Component analysis of about 370 granite samples from Portugal and Spain give good results with a one- and two-component model. The component model is well suited for discriminating between barren and specialized granites as it suppresses deviating values in the data set. It combines the different elements in a more homogeneous plot of component scores.

The component loadings in a one-component model gives positive loadings for Rb, Sn, Cs, Li, Nb, F, Ta, Zn, W and P_2O_5 and negative loadings for Zr, Ba, TiO_2 and Sr. Histograms of component scores divide the granites into barren types (Fundão, Barcarrotta, Quinteiros), slightly specialized granites (Alpedrinha, Capinha, Bruco, Canado), specialized granites (Numão, porphyritic biotite granites, Atalaia mine, Laza) and highly specialized granites (Cedões, Atalaia, Fonte Santa, Panasqueira, Regoufe, Argemela, Penouta). The magmatic differentiation trend, however, interferes with the mineralizing trend in this component model. Therefore, slightly specialized granites can be obscured by the differentiation trend in cases of weak mineralizations.

The two-component analysis introduces a split into a magmatic differentiation trend (TiO_2 , Ba, Zr, Sr, -Ta, -Nb, -Rb, -Sn) and a hydrothermal influence (F, Li, Cs, Rb, Zn, Sn, P_2O_5 , Nb, W). The division of the granites in the two-component model is the result of magmatic differentiations and post-magmatic fluids. In this model, granites occur in groups which are in agreement with their petrological features. The differentiation between barren, specialized and highly specialized granites is now easier but additional trends are observed. Barren granites (Fundão, Quinteiros, Barcarrotta) pose no problem. Slightly specialized granites (Capinha, Alpedrinha, Bruco, Laza,

porphyritic biotite granites, Numão) occur in one large field. The more specialized granites branch from this field. Panasqueira, Regoufe, Atalaia and Fonte Santa occur along a hydrothermally enriched trend. Sodium-enriched granites (Argemela, Penouta, Beauvoir) give different trends. Especially Penouta differs from Argemela and Beauvoir which is caused by its rather low trace element contents.

The Atalaia granite was investigated on a more detailed scale. Component analyses or contour maps were not prepared as too few samples were available. Instead, the contents of the elements were plotted for individual samples. Titanium, zirconium and barium give a NW-SE trend in the granite with higher values in the centre of the granite. Rubidium, lithium, cesium and fluorine values are correlated with each other and show higher amounts in the southwestern part of the Atalaia granite. The weak mineralizations in the granite are only characterized by lower amounts of fluorine, lithium and cesium. The poor correlation between trace element content and mineralization phenomena is probably caused by the relatively flat erosion surface of the granite.

REFERENCES

- Abbey, S. (1982): An evolution of U.S.G.S. III. Geostand. Newsletters, 6, April, 47-76.
- Albuquerque, C.A.R. de (1971): Petrochemistry of a series of granitic rocks from Northern Portugal. Bull. Geol. Soc. Amer., 82, 2783-2798.
- Albuquerque, C.A.R. de (1978): Rare earth elements in "Younger" granites, Northern Portugal. Lithos, 11, 219-229.
- Arribas, A. (1978): Mineral paragenesis in the Variscan metallogeny of Spain. Studia Geologica, 14, 223-260.
- Arribas, A. (1980): Mineral paragenesis in the Variscan metallogeny of Spain. Freib. Forsch.-H., C 354, 33-53.
- Boissavy-Vinau, M. (1979): Processus géochimiques de concentrations liés à l'évolution de magmas granitiques. Application aux filons à Sn-W du Massif Central et du Nord Portugal. Thèse 3e cycle, Université P. et M. Curie, Paris. 220 pp.

- Chappell, B.W. & White, A.J.R. (1974): Two contrasting granite types. *Pacific Geology*, 8, 173-174.
- Conde, L.N. & Pereira, V. & Ribeira, A. & Thadeu, D.C. (1971): Jazigos hipogénicos de estanho e volfrâmio. Livro-guia da Excursão No. 7. I congresso Hispano-Luso-Americano de Geologia Económica (Lisbon). Direcção-geral de minas e serviços geológicos. 68-77.
- Costa, C.V. & Pereira L.G. & Ferreira, M.P. & Santos Oliveira, J.M. (1971): Distribuição de oligoelementos nas rochas e solos da região do Fundão. *Mem. Not. Mus. Lab. Min. Geol. da Univ. de Coimbra*, no. 71, 3-37.
- Davis, J.C. (1973): *Statistics and data analysis in geology*. John Wiley & Sons, New York. 550 pp.
- Dixon, W.J. & Brown, M.B. & Engelman, L. & Frane, J.W. & Hill, M.A. & Jennrich, R.I. & Toporek, J.D. (1981): *BMDP statistical software*. University of California Press, Los Angeles, 726 pp.
- Ferreira, M.P. & Costa, V. & Macedo, C.R. & Pereira, L.G. (1977): Datações K-Ar em biotite das rochas granitóides da Cova da Beira (Portugal Central). *Memórias e Notícias, Publ. Mus. Lab. Mineral. Geol. da Univ. de Coimbra*, No. 84.
- Gladney, E. & Goode, W. (1981): Elemental concentration in eight new U.S.G.S. rock standards, a review. *Geostand. Newsletters*, 5, October, 31-64.
- Inverno, C. & Ribeiro, M.L. (1980): Fracturação e cortejo filoneano nas Minas da Argemela (Fundão). *Com. Serv. Geol. Portugal*, 66, 185-193.
- Joreskog, J.A. & Klovan, J.E. & Reymont, R.A. (1976): *Geological component analysis*. Elsevier Publ. Comp. Amsterdam. 178 pp.
- Lotze, F. (1945): Zur Gliederung der Varisziden der Iberischen Meseta. *Geotekt. Forsch.*, 6, 78-92.
- Noronha, F. (1974): Etudes des inclusions fluides dans le quartz des filons du gisement de tungstène de Borralha (Nord du Portugal). *Mus. Min. Geol. Pub. Fac. Sci. Univ. Porto*, no. 85, 4a, 32 pp.
- Nie, N.H. & Hadlai Hull, C. & Jenkins, J.G. & Steinbrenner, K. & Brent, D.H. (1975): *SPSS, Statistical package for the social sciences*. McGraw Hill, New York, 675 pp.
- Oen Ing Soen (1970): Granite intrusion, folding and metamorphism in central northern Portugal. *Bol. Geol. Minero Espana*, 81, 271-298.
- Oosterom, M.G. & Vriend, S.P. & Bussink, R.W. & Moura, M.L. (1982): Geochemistry of tin, tungsten and related elements such as tantalum and niobium. E.E.C. Research programme on primary raw materials, open file report, contract nr. 025.79 MPP NL, 58 pp.

- Pinto, M.S. (1983): Geochronology of Portuguese granitoids: a contribution. Internal report, University of Aveiro, 29 pp.
- Priem, H.N.A. & Boelrijk, N.A.I.M. & Verschure, R.H. & Hebeda, E.H. & Verdurmen, E.A.Th. (1970): Dating events of acid plutonism through the Paleozoic of the western Iberian peninsula. *Eclog. Geol. Helv.*, 63, 255-274.
- Priem, H.N.A. & den Tex, E. (1982): Tracing crustal evolution in the NW Iberian Peninsula through Rb-Sr and U-Pb systematics of Paleozoic granitoids: a review. International Colloquium "Géochimie et Petrologie de granitoids", Clermont-Ferrand, May 1982, Volume of Abstracts.
- Priem, H.N.A. & Schermerhorn, L.J.G. & Boelrijk, N.A.I.M. & Hebeda, E.H. (1984): Rb-Sr geochronology of Variscan granitoids in the tin-tungsten province of Northern Portugal: a progress report. *Ecog VII*, Braunlage, March 1984. Volume of abstracts. Terra Cognita, in press.
- Rösler, H.J. & Lange, H. (1972): Geochemical tables. Elsevier Publ. Company. Amsterdam. 468 pp.
- Schermerhorn, L.J.G. (1982): Framework and evolution of Hercynian mineralization in the Iberian Meseta. *Com. Serv. Geol. Portugal*, 68, 91-140.
- Shapiro, L. (1975): Rapid analysis of silicate, carbonate, and phosphate rocks - revised edition. U.S. Geological Survey, bulletin 1401, 76 pp.
- Sluyk, D. (1963): Geology and tin-tungsten deposits of the Regoufe area, Northern Portugal. PhD thesis University of Amsterdam, 123 pp.
- Thadeu, D.C. (1973): Les gisements stanno-wolframitiques du Portugal. *Ann. Soc. Geol. Belgique*, 96, 5-30.
- Thadeu, D.C. (1977): Hercynian paragenetic units of the Portuguese part of the Hesperic massif. *Bol. Soc. Geol. Portugal*, 20, 247-276.
- Tischendorf, G. (1977): Geochemical and petrographic characteristics of silicic magmatic rocks associated with rare-element mineralizations. In: Stempok, M., Burnol, L. and Tischendorf, G. (editors). *Metallization Associated With Acid Magmatism*. Geological survey of Prague, 2, 41-96.
- Vriend, S.P. & Oosterom, M.G. & Bussink, R.W. & Jansen, J.B.H. (1984): Trace element behaviour in the W-Sn granite of Regoufe, Portugal. *Journ. Geochem. Explor.*, in press.



Sub-horizontal ore vein in the Panasqueira mine.



Splitting of an ore vein to another joint.

CHAPTER 3

TRACE ELEMENT DISTRIBUTION IN AND AROUND THE PANASQUEIRA TUNGSTEN-TIN DEPOSIT, PORTUGAL

The Panasqueira tungsten-tin deposit is located in the Beira Baixa province in Portugal, about 35 km WSW of Fundão. The mining area lies in the foothills of the Serra da Estrela, the highest mountain range of Portugal (Fig. 1, and Fig. 3, Chapter 2).

Mining started in 1898 and currently Beralt Tin & Wolfram S.A.R.L. operates the concession. A crude ore concentrate is produced at Barroca Grande. This concentrate is transported by ropeway to Rio at the Zêzere river (Fig. 1, Chapter 4) where the mill produces high quality concentrates of 75.5% WO_3 , 72% Sn and 22% Cu with about .08% Ag. Production in 1981 amounted to 1808 tons wolframite, 147 tons cassiterite and 2130 tons chalcopyrite concentrate. The total production from 1934 to 1981 was about 75,420 tons wolframite, 4810 tons cassiterite and 16,660 tons chalcopyrite concentrate (McNeil, 1982).

Sub-horizontal ore veins, occurring in swarms around a greisen cupola, range in thickness from 1 to 150 cm but only veins over 20 cm are exploited. The vertical extent of the main economic ore zone is about 75 m (Fig. 2) but increases to about 300 m above the greisen cupola. The ore zone has been exploited over a length of about 1000 m along its extension; further ore zones are developed at deeper levels (Smith, 1979). The ore veins are mined from 4 levels namely Level 0 (675 m), Level 1 (615 m), Level 2 (562 m) and Level 3 (530 m).

The most important mining areas nowadays are Barroca Grande, Panasqueira Deep and Rebordões. Older areas are Rio, Corga Seca, Vale da Ermida and Alvoroso (Fig. 1, Chapter 4). Within these mining

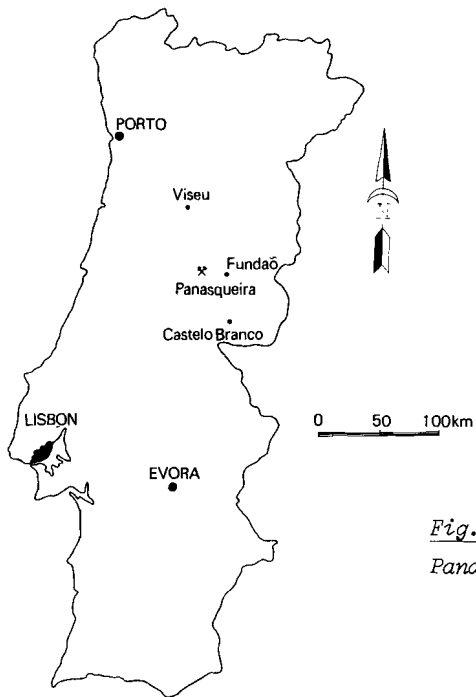


*Fig. 1. Location of the
Panasqueira mining district*

districts tungsten/tin ratios may vary.

Schist and greisen samples were collected from the underground workings and analyzed for major, minor and trace elements. Component analysis was performed on the analytical results of the schist to reveal the influence of the hydrothermal fluids on their host rocks. Component analysis was also used to distinguish between the different greisen or granite varieties. Analytical results of drillcore samples gave more detailed information about the distribution of the elements in fresh schist along the veins.

GEOLOGY

The Panasqueira tungsten-tin deposits occur in sub-horizontal quartz veins in meta-sedimentary rocks. These rocks are the Precambrian Beira shales and Ordovician quartzites (Thadeu, 1951). The mineralized quartz veins emerge from a greisenized granite cupola, exposed in the mine. The separate geological units around Panasqueira are discussed below:

Beira Shales

The Beira shale complex or "Complexo xisto-grauvaquico das Beiras" consists mainly of marine argillaceous shales and graywackes with graded bedding and fine-grained sandstones (Blout & de Wolf, 1953). The rocks are composed of quartz, chlorite, sericite, albite, some carbonate and organic matter (about 0.17%).

Two series can be distinguished within the Beira shales. The lower series of perhaps Precambrian age is formed by a monotonous alternation of slates and graywackes. The upper series of probably Lower Cambrian age consists of conglomerates, acid volcanites and limestone layers in addition to the more abundant shales and graywackes (Thadeu, 1977). An age of about 563 Ma has been obtained by Rb-Sr dating on volcanites in the upper Beira series (Thadeu, 1977). The upper series is found in the Northern and the lower series in the Central and Southern parts of Portugal.

Regional metamorphism during the early stages of the Hercynian orogeny converted the sediments in Beira Baixa into phyllites and fine-grained sandstones (Thadeu, 1951). A vertical schistosity was developed, following the NW-SE Hercynian direction. Locally, some irregular quartz masses are found in the shales which were probably formed during the Hercynian regional metamorphism (Thadeu, 1951). These barren quartz masses, "Seixo Bravo", are mostly parallel to the schistosity and at Panasqueira are crosscut by the later tungsten-tin veins.

Contact-metamorphism converted the Beira shales into biotite-chlorite-cordierite hornfelses, the so called "spotted schist". Andalusite is found close to the granitic contact. The size of the

metamorphic area suggests that more extensive granitic bodies occur at depth. Contact-metamorphism and greisen veins point to a second cupola below the Zêzere river at Rio (Fig. 1, Chapter 4).

After contact metamorphism by the granite, hydrothermal alteration took place along the ore veins. Especially cordierite is strongly altered by the later fluids, leaving ore rims with sericite, muscovite or chlorite in its former texture (Bloot & de Wolf, 1953; Clark, 1964). Locally, andalusite is altered into topaz.

Alteration along the ore veins includes tourmalinization and sericitization. Tourmaline is found in the first 10 to 30 cm around veins, giving a brown colour to the rocks. Schist inclusions in the ore veins are almost completely tourmalinized. Tourmaline alteration zones can suddenly end at the contact between different schist layers. Outwards from the veins, tourmalinization is followed by sericitization. This sericitization gives a silky appearance to the schists. The extension of the alteration zone strongly depends upon host rock composition and available joints; extensions of 0.5 to 2 m are frequent.

Arsenopyrite and apatite are occasionally found in the alteration zone. It is interesting to note that tourmalines in the schist and in the ore veins have different colours. Tourmaline in the schists is mostly brown, whereas in the ore veins it is red, blue, green or brown.

The Panasqueira granite/greisen

The known granite at Panasqueira is a biotite-muscovite granite with large potassium-feldspar megacrysts up to 6 cm in size. This granite grades upwards into an albite-muscovite granite. The top of the granite and the subvertical granitic veins are altered into an equigranular, medium grained, quartz-muscovite greisen. Topaz occurs in the albite-muscovite granite and strongly altered topaz occurs in the greisen. The greisen cupola does not crop out but is exposed in the mine workings (Fig. 2). The composition of the greisen is about 40% muscovite and 60% quartz (Bloot & de Wolf, 1953). In the greisen and to a lesser extent in the albite-muscovite granite, arsenopyrite,

chalcopyrite and sphalerite occur. Below the 530 m level large blocks of schist are found, metamorphosed to quartzitic hornfelses, in the granite.

Muscovites of the granite, greisen and ore veins give a Hercynian age of 289 ± 5 Ma by K-Ar dating (Clark, 1970). Altered granite samples from below the 530 m level give an age of 289 ± 4 Ma by whole-rock Rb-Sr dating (Priem & den Tex, 1982). Initial $^{87}\text{Sr}/^{86}\text{Sr}$ ratios of the granite samples are about 0.713, indicating an S-type granite (Chappell & White, 1974).

Quartz veins

The ore-bearing veins follow a sub-horizontal joint-system which was developed after intrusion of the granite but before and during the main mineralization (Thadeu, 1951; Bloot & de Wolf, 1953; Clark, 1964, 1965; Kelly & Rye, 1979; Marignac, 1982). This joint-system occurs in the whole region, but it is very pronounced at Panasqueira. The veins are found in and outside the contact-metamorphic aureole and crosscut the bedding and schistosity of their schist host rocks, including the greisen cupola. Only around the greisen cupola some sub-vertical ore veins occur, the so called "Galos". Almost no ore veins are found at depth in the granite. More detailed information about the hydrothermal ore veins is given in Chapter 5.

Quartz-cap

The top of the greisen cupola is overlain by a sheeted mass of quartz, approximately 14 m thick, the so-called quartz-cap (Fig. 2). The quartz-cap shows a sharp contact with the Beira schist and the greisen cupola. According to Kelly & Rye (1979) this cap is formed by filling of a large cave which was formed upon retreat of the granitic magma. The formation of the quartz-cap represents the first stage of vein development (Chapter 5). High fluid pressures during formation of the quartz-cap may have lifted the schist cover off the granite (See Chapter 5). From this quartz-cap horizontal quartz veins (1 to 2 m thick) penetrate into the surrounding Beira schists. Arsenopyrite and wolframite occur as large isolated blocks in these veins and in the quartz-cap.

Dolerite dykes

Dolerite dykes are common in the district; they are near-vertical and range in thickness from 0.5 to 25 m. The dykes consist of labradorite and altered pyroxene. This alteration took place upon intrusion of the granite (Thadeu, 1951). Some dolerite dykes are younger in age as they occur as veins in the Younger granites.

GEOCHEMISTRY

Analytical techniques

Granite and schist samples were collected at the surface but also from drillcores and in mine workings. About 15 to 20 chips were collected at outcrops over 10 to 30 m². The weight of the treated samples is between 0.5 and 1 kg. In underground workings a sampling distance of about 2 m was used.

As contamination is a serious problem, ultrasonic cleaning was necessary before crushing and grinding. Initially, some samples were broken with a jaw-crusher coated with tungsten-carbide, thus tungsten values from these samples were deleted from the data set. Later, a Ni-Cr steel jaw-crusher was installed. About 100 gram was split from the bulk sample with a Jones splitter and pulverized in a swingmill (Ni-Cr steel) to -250 mesh. The analytical techniques are given in Chapter 2.

RESULTS AND DISCUSSION

CIPW major element trends

Major elements were used to calculate the CIPW-norm of the different granitic types. The specialized granites contain sometimes excess values of P₂O₅, F and CO₂ which were not considered during the CIPW-norm calculations.

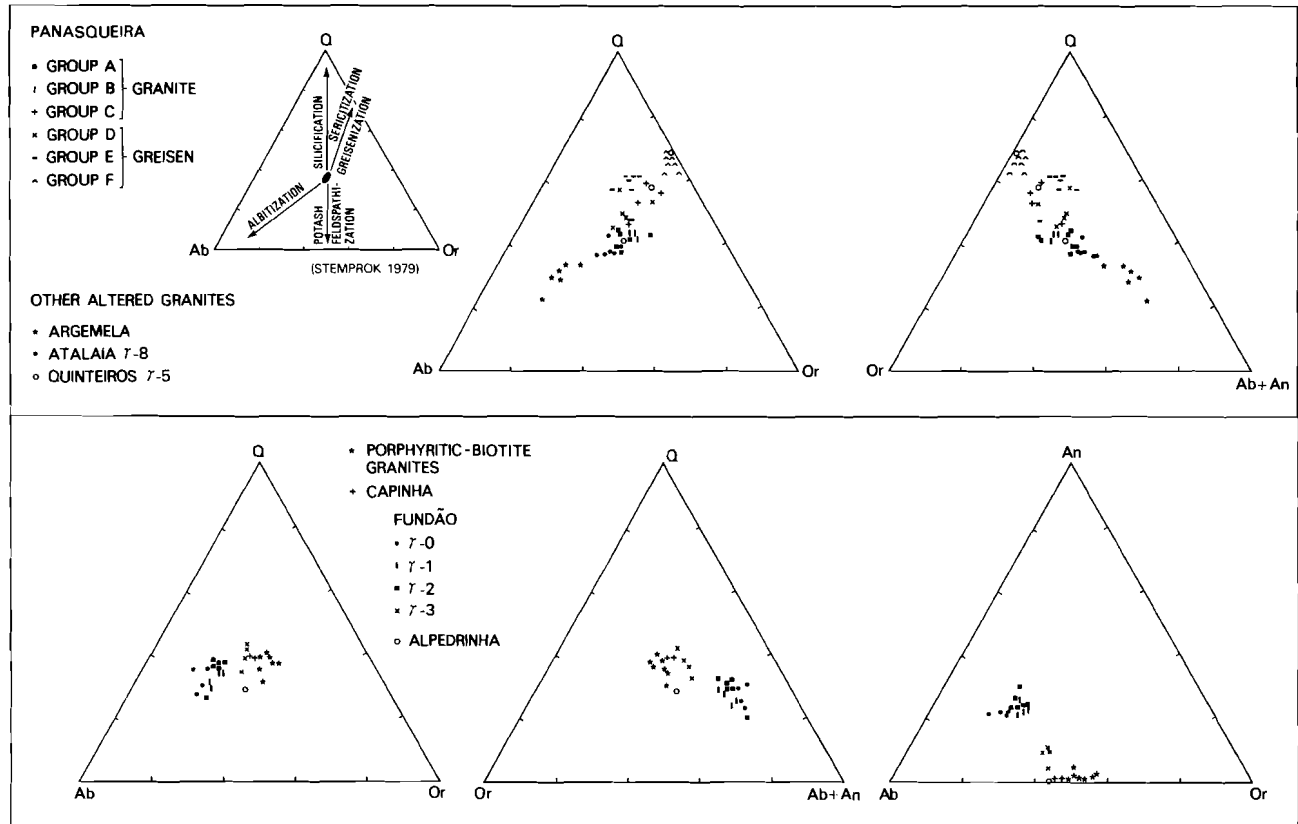


Fig. 3. Modal analyses (CIPW) of granites in the Fundao region.

Fig. 3 shows the modal analyses in the Q-Ab-Or, An-Ab-Or and Q-Or-AbAn triangles for Fundão, Capinha and the porphyritic biotite granites of Covilha, Belmonte, Caria and Alpedrinha. More detailed information about these granitoids is given in Chapter 2. Additional data of Fundão were obtained from Costa et al. (1971). The granites in Portugal are high-level intrusions (Oen Ing Soen, 1970) therefore a fluid pressure of about 2 kbar is proposed for the eutectic of these granites. The porphyritic and Capinha granites are close to the eutectic for anatectic granites ($P_{H_2O} = 2$ kbar). The granodiorites of Fundão are located to the more Ab-rich side which may be caused by a higher fluid pressure in the ring intrusion as is indicated by the high biotite content. The different plots of the Fundão intrusives show an intrusion sequence from quartz-diorite (j-0) to biotite-granite (j-3) (Fig. 3).

This figure also shows the modal analyses of the specialized granites which may contain excess values of P_2O_5 , F and sometimes CO_2 . Stemprok (1979) indicated processes which may have occurred during Sn-W and other mineralizations (see inset Fig. 3). These processes can also be recognized in the modal analyses. The Panasqueira, Atalaia and Quinteiros granites are close to the eutectic ($P_{H_2O} = 2$ kbar). The quartz-albitite of Argemela follows the albitization trend although the rocks were influenced by a later hydrothermal overprint. The Panasqueira granites are close to the eutectic but the greisenized granites and greisens shift to the Q-Or boundary as indicated by the greisenization trend (Stemprok, 1979). The same also holds for the Quinteiros granite, the "greisen" samples of this occurrence plot between the greisen samples of Panasqueira.

The clearly distinct groups of the Panasqueira granites and greisens, obtained by component analysis (see below), are only vaguely recognized in the Q-Ab-Or and Q-Or-AbAn plots. Greisen samples should be concentrated in the quartz-rich corner but the CIPW-norm recalculates the amount of muscovite into normative orthoclase (which is not present in the greisen). The component ferrosilite is also calculated in the CIPW-norm but in greisen samples in our case the Fe^{2+}

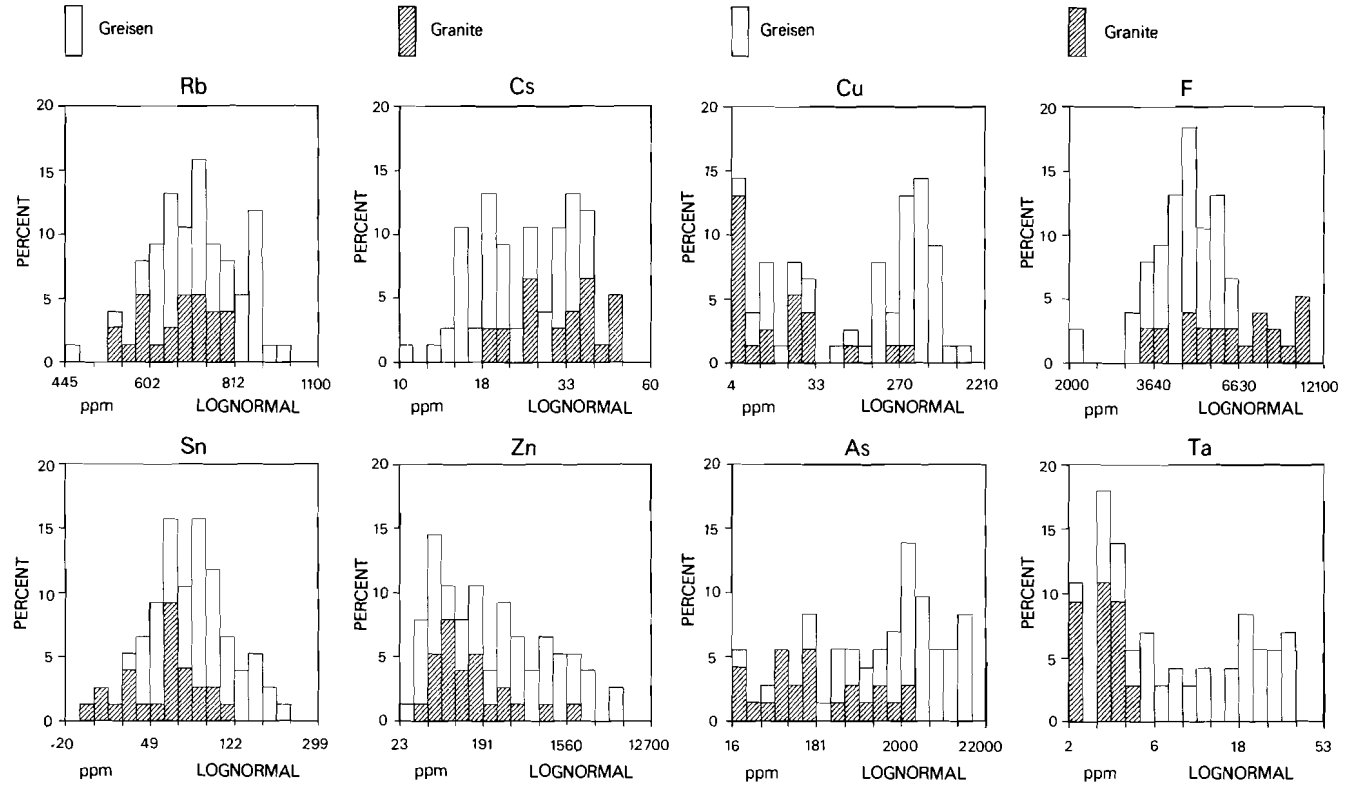


Fig. 4. Histograms of major and trace elements of the Panasqueira granite and greisen samples.

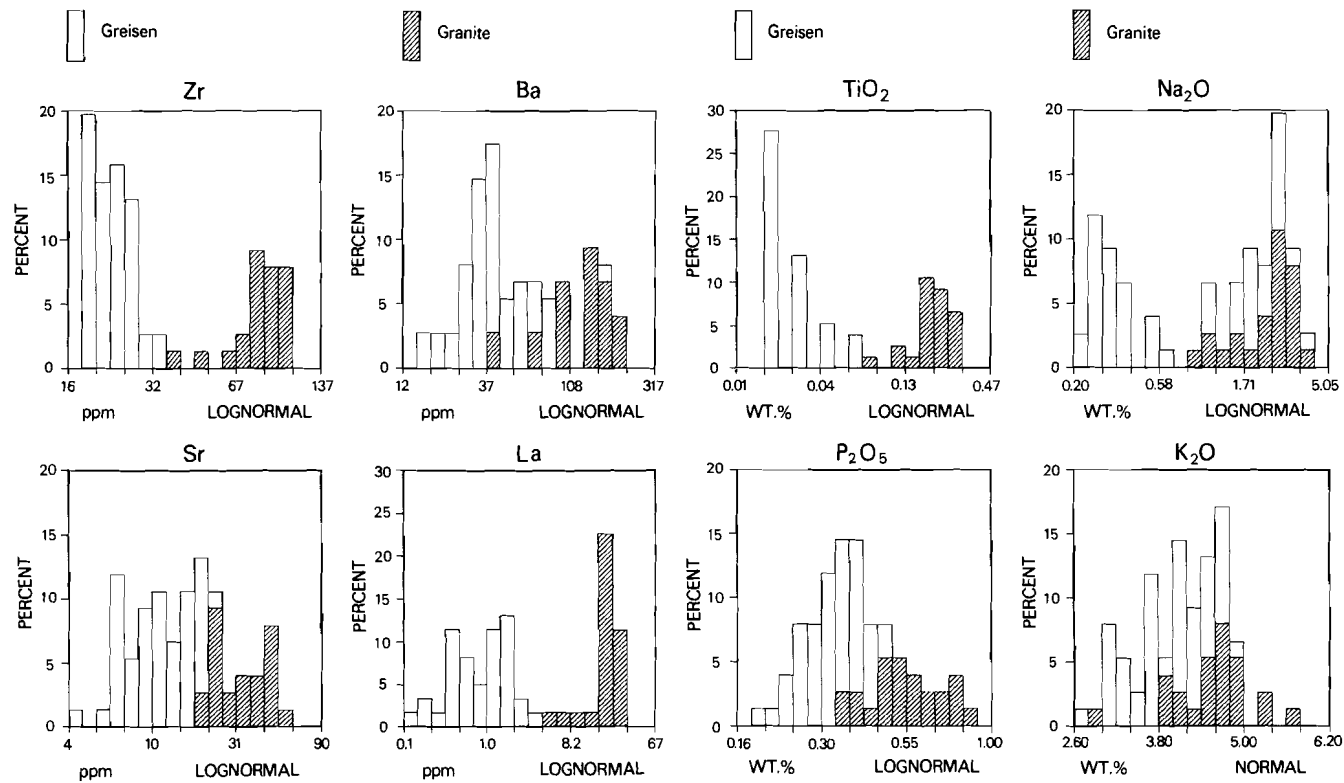


Fig. 4. Histograms of major and trace elements of the Panasqueira granite and greisen samples.

is fixed in sulphides. Unfortunately, sulphur analyses were not available.

Trace element distributions

The Panasqueira granite/greisen

The distribution of the investigated elements in granite and greisen samples is given in Fig. 4. With component analysis one-, two- and three-component models were computed for 76 granite and greisen samples. In this case the two-component model (Table I) gave geochemically the best interpretable results. A first component explains 56% of the variation, a second explains an additional 22%. In the three-component model the third component would have mainly been composed of U and K₂O. Component scores were computed for each sample and plotted (Fig. 5).

As is apparent from Fig. 5, the data set consists of several distinct trends, which each can be subdivided into three groups. First, a "granitic" trend (A-B-C) from biotite-muscovite granite (A) up to leucogranite (C), and secondly, a greisen trend (D-E-F) from greisenized muscovite granite (D) to greisen (F). The two trends point to different processes within the granites. The granitic trend originated from metasomatic processes after crystallization of the granitic body but before opening of the joint system. The greisen trend was formed after opening of the joint system which provided channels for the elements leached during greisenization of the granite (see Chapter 5).

Granitic trend

The alteration in the granitic trend (A-B-C) in Fig. 5 is mineralogically characterized by the alteration of brown biotite (subgroup A) through green biotite (subgroup B) to a mixture of sphene, muscovite, apatite and carbonate (subgroup C). The muscovite content in this trend increases while the potassium-feldspar megacrysts are present throughout the whole sequence. Albite rims, which are formed

Table I: Loadings of component 1 and 2 in granite and greisen samples.

	COMPONENT 1	COMPONENT 2
Na ₂ O		-.89
Fe ₂ O ₃		.86
CaO *	.75	
MgO *	.73	-.49
P ₂ O ₅ *	.80	
TiO ₂ *	.83	-.46
F *	.77	.40
Li *	.92	
Rb *		.88
Cs *	.70	.65
Sr *	.67	-.62
Ba *	.78	
Sc *	.57	-.74
La *	.85	-.50
Ce *	.89	-.42
Yb *	.63	-.56
Th *	.94	
Zr *	.89	
Hf *	.73	
Nb *		.83
Ta *	-.49	.78
W *		.67
Sn *		.88
Cu *	-.49	.67
Zn *		.77
As *		.71

Eigenvalues before rotation: 14.46 and 5.77
 (* log-transformed values used)

around the plagioclase crystals (about 10% An), disappear. Topaz is also present in the granite, especially in the leucogranite (Group C).

The means of the subgroups were calculated with the winsorizing technique (see BMDP manual, Dixon et al., 1981) which gives a more robust estimate of the mean (Table II). The changes in major and trace

Table II: Winzorized mean of the elements for the different granite and greisen subgroups. Major elements and F in percentages, others in parts per million.

	Group A n=11	Group B n=6	Group C n=7	Group D n=12	Group E n=15	Group F n=25
Na ₂ O %	3.05	2.56	1.49	2.40	1.65	.31
Fe ₂ O ₃ %	2.11	2.63	3.53	1.67	2.61	3.88
CaO % *	.48	.75	.72	.35	.37	.27
MgO % *	.33	.44	.60	.19	.19	.09
K ₂ O % *	4.86	4.69	4.20	3.88	3.51	4.28
P ₂ O ₅ % *	.44	.66	.66	.34	.35	.30
TiO ₂ % *	.20	.19	.24	.03	.03	.01
F % *	.46	.73	.95	.36	.41	.52
Li *	432	843	957	280	330	365
Rb *	597	706	771	626	662	811
Cs *	24	37	43	15	20	31
Sr *	33	49	25	18	12	9
Ba *	112	155	108	48	32	41
Sc *	3.9	3.3	3.8	1.9	1.5	.4
La *	18	22	25	1.9	1.2	.4
Ce *	37	42	50	5.4	4.2	3.0
Eu	.38	.53	.47	.20	<.10	<.10
Tb	.38	.38	.43	.10	<.06	<.06
Yb *	1.1	1.0	1.2	.6	.6	.3
Lu	.19	.14	.25	.11	<.05	<.05
Th *	9.4	10.4	12.5	.9	1.0	1.5
Zr *	78	80	95	25	24	22
Hf *	2.9	3.1	3.4	1.9	1.9	2.6
Nb *	17	19	19	18	25	38
Ta *	3	3	3	4	8	24
W *	18	16	27	19	24	30
Sn *	40	67	88	53	70	115
Cu *	8	9	28	18	233	436
Zn *	80	184	153	52	195	890
Ag	<2	<2	<2	<2	18	18
As *	68	103	1225	459	1680	4750
U *	14	12	12	14	16	12

(* geometrical mean used)

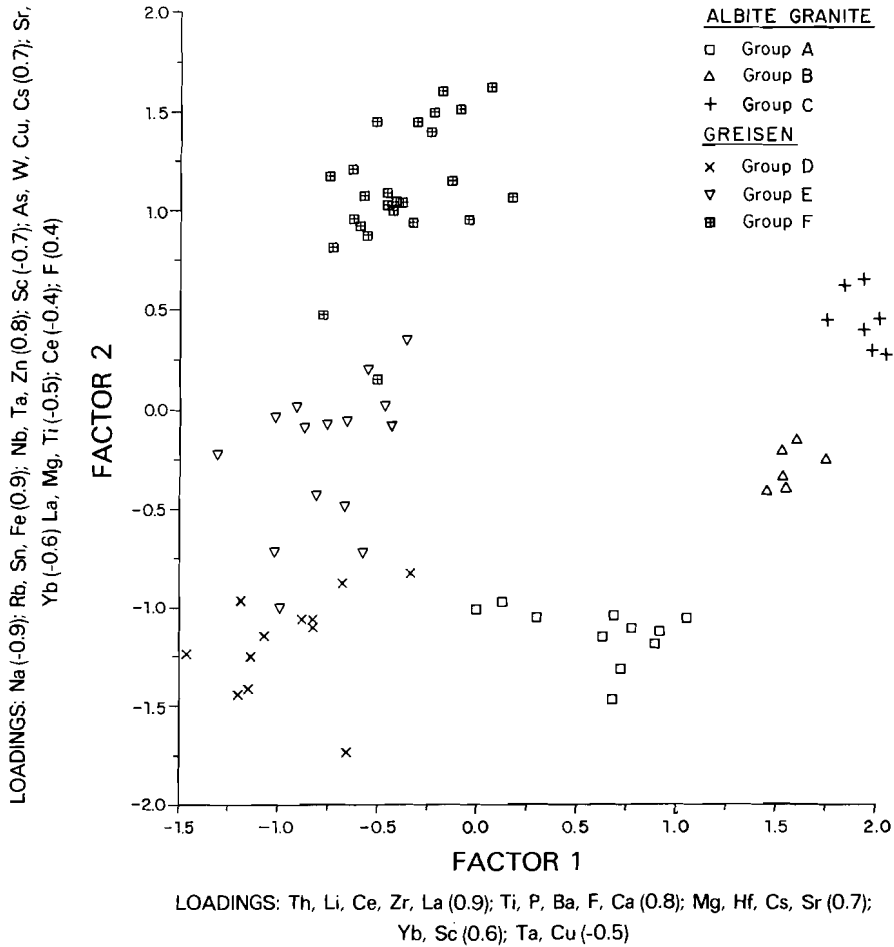


Fig. 5. Component score plot of component 1 against component 2 for the Panasqueira granite and greisen samples.

element content for the individual subgroups are shown in Fig. 6. The contents of Sn, Rb, Li, W, Fe₂O₃, P₂O₅, MgO, La, Ce, Zr, Zn, As, CaO, F, Cs and Cu increase from biotite-muscovite granite to leucogranite whereas the contents of Sr and Na₂O decrease.

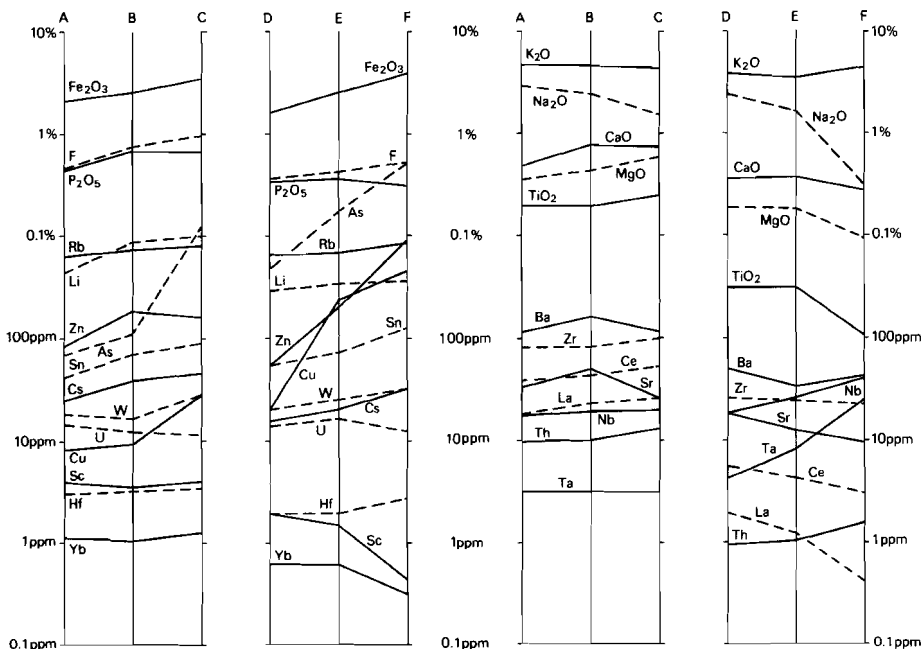


Fig. 6. Plot of the mean values for the different granite and greisenization phases at Panasqueira. Subgroup A: (biotite)-muscovite granite; B: muscovite granite; C: leucogranite; D: greisenized muscovite granite; E: greisen Level 2; F: greisen Level 1.

Greisenization trend

The greisen trend (D-E-F in Fig. 5) is characterized by the absence of biotite and potassium-feldspar. Muscovite, plagioclase (albite) and quartz are the major constituents of these altered granites. With increasing greisenization plagioclase is strongly altered; albite rims are dissolved (subgroup D) and finally plagioclase disappears almost completely. Remnants of albite are found only in quartz in the upper parts of the greisen cupola (subgroups E and F in Fig. 5). Topaz is present as corroded grains in the greisen. The leaching of feldspars is reflected by a change in the concentrations of Na₂O and CaO. The

greisen veins crosscut the altered biotite-muscovite granite as well as the leucogranite.

In the greisen trend Na_2O , CaO , MgO , Sr , Zr and TiO_2 contents are decreasing whereas Rb , Sn , Li , F , Zn , Fe_2O_3 , W , Cu , Ag , Cs , Nb and Ta contents are increasing. Rare earths are leached, only Ce and La are detectable in the greisen samples. The amount of K_2O does not change, the breakdown of potassium-feldspar occurs simultaneously with new formation of muscovite. A reducing environment during ore deposition caused the mobility of uranium to be very low (see Chapter 5).

Although ilmenite, rutile and zircon are generally considered as very refractory minerals, their lower contents in the greisen indicate that the open system is capable of leaching these minerals from the granite (Table II).

Rb , Li , F and P_2O_5 contents increase both in the granitic and in the greisen trend but a clear difference in concentration level occurs between these two trends. Apparently, these elements are enriched in the leucogranite but in later processes during greisenization they are leached.

The granitic group is only slightly altered, compared to the greisen group, possibly as a result of different fluid quantities moving upwards through the granite. The intense greisenization indicates large quantities of fluid passing through sub-vertical joints in the granite, thereby altering the albite-muscovite granite into greisen. The albite-muscovite granite probably represents the original granite but with an intense hydrothermal overprint. The early alteration in the granite probably occurred as the veins were not yet opened and as the fluids were concentrated in the upper parts of the granite. After opening of the sub-horizontal ore veins, an intense fluid flow caused greisenization in the uppermost part of the granite and in deeper sub-vertical joints or fluid channels.

The difference between the granitic trend (A-B-C) and the greisen trend (D-E-F) can be explained by leaching of elements from the altered albite-muscovite granites. Especially Th , Li , Ce , Zr , La , TiO_2 , P_2O_5 , Ba , F , CaO , MgO , Hf , Cs , Sr , Yb , Eu , Tb and Lu are lower in the greisen than in the albite-muscovite granite (Table II). Stable minerals like

Table III: Mean values of several granites around Panasqueira.

	Atalaia	Quinteiros	Argemela	Panasqueira greisen	Panasqueira granite	Capinha	Porphyritic biotite gr.	Fundão	Alpedrinha	Low-Ca granites (Rösler et al., 1972)
	n=24	n=11	n=9	n=52	n=24	n=19	n=18	n=11	n=9	
Rb	495	115	1780	730	675	325	400	85	250	170
Sr	30	50	70	12	35	55	55	225	100	100
Cu	8	35	21	320	35	30	9	10	8	10
Sn	40	6	650	90	60	17	16	2	11	3
F	2400	190	8500	4500	6800	1000	1700	500	860	850
B	120			50	40					10
W	10	8	4	25	20	7	5	1	12	2
Li	350	17	3200	340	690	150	235	55	155	40
Zr	40	55	14	23	85	70	130	120	135	175
Nb	22	7	55	30	18	14	17	4	13	21
U	8	6	7	13	13	11	14	4	8	3
Zn	60	23	130	820	235	65	95	50	70	39
Cs	40	1	200	24	33	14	19	1	12	4
Ta	11	2	50	16	3	5	6	3	3	4
Ba	70	315	9	45	130	220	265	435	380	840
P ₂ O ₅ %	.46	.17	1.59	.33	.56	.31	.27	.19	.36	.14
TiO ₂ %	.09	.12	.01	.02	.21	.19	.29	.46	.34	.20

P₂O₅ and TiO₂ in percentages, others in parts per million.

ilmenite and zircon are leached from the granite, possibly caused by the large amounts of fluorine in the fluid. Sr and Ba contents are lower in the greisens which is due to the breakdown of potassium-feldspar.

Major elements confirm the trends but not so pronounced as trace elements. Especially Na_2O , CaO , TiO_2 and MgO are characteristic for the greisenization (Table II).

The elements Nb, Ti and Ta are mobilized at Panasqueira during the greisen trend but not during the granitic trend (see Table II). Boissavy-Vinau & Roger (1981) suggest a TiO_2/Ta ratio as a characteristic for Sn-mineralized granites because Ta is enriched and Ti depleted by end-stage magmatic processes and not changed by post-magmatic fluids. This fact was questioned by Lehmann (1981). The mobility of Ti and Ta by hydrothermal fluids is also confirmed by the analyses of Panasqueira (see Table II).

Comparison with other granites

Hall (1971) analyzed major and trace elements in the greisenized Cligga Head granite with tungsten mineralizations. His findings partly coincide with the results in Panasqueira. In Cligga Head and Panasqueira, the greisen deposits show increased As, F, Li, Rb, Sn, W and Zn values and decreased Ba, Sr, Zr and TiO_2 values. Boron is strongly enriched in the Cligga Head granite while in the Panasqueira granite or greisen boron contents are low but extensive tourmalinization occurs in schist along the ore veins.

Neiva (1974) investigated greisenization of a muscovite-biotite albite granite in northern Portugal. Greisenization is accompanied by increased F, W, Nb, Sn, Pb and Rb contents and a decrease in Li, Zr and Sr contents. However, greisenization accompanied by increasing albitization shows decreasing values of Rb, Li, Zr, Sr and Ba. These results are partly confirmed at Panasqueira as F, W, Nb, Sn and Rb but also Li increase during greisenization whereas Zr, Sr and Ba decrease.

According to Tischendorf (1977) tin-tungsten and other specialized

granites are characterized by certain increased trace element contents whereas major elements change only within limited values. In Table III data of low-Ca granites (Rösler & Lange, 1972) are compared with the granitoids in and around Panasqueira (see also Table I in Chapter 2).

THE PANASQUEIRA SCHISTS

The Beira schists around veins at Panasqueira are severely affected by the hydrothermal fluids. Although most of the shales have undergone contact-metamorphism, later alteration by the ore veins is much more intense. About 150 schist samples were sampled underground along galleries and drives. Major and trace elements were analyzed of these schists (Table IV and VI).

Component analysis of the sub-surface schists give the best results in a two-component model (Table V). Component 1 (Rb, Li, F, Sn, Cs, B, -Na₂O) indicates the influence of the ore fluids in the veins on the

Table IV: Analyses of Beira schists at Panasqueira.

	PQ 392	PQ 511	PQ 505	Schist HST.
SiO ₂	59.55	58.63	72.61	63.96
TiO ₂	.91	.92	.71	.83
Al ₂ O ₃	18.78	19.84	12.81	17.43
Fe ₂ O ₃	7.27	6.98	4.53	6.61
MnO	.05	.04	.03	.07
MgO	2.36	2.61	1.65	2.25
CaO	.34	.29	.23	.27
Na ₂ O	1.93	1.04	1.64	1.31
K ₂ O	3.44	4.32	2.32	4.03
P ₂ O ₅	.22	.20	.17	.17
L.O.I.	3.32	3.76	2.37	3.04
	98.17	98.57	99.05	99.97

Analyses by XRF; Fe₂O₃ is the sum of Fe₂O₃ + FeO.

Table V: Component loadings of sub-surface schists

	COMPONENT 1	COMPONENT 2
Na ₂ O	-.50	
K ₂ O	.47	.62
MgO		.86
Fe ₂ O ₃		.86
TiO ₂		.79
B *	.82	
F *	.90	
Li *	.91	
Rb *	.94	
Sn *	.89	
Zr *		-.54
Cs *	.87	

Eigenvalues before rotation: 5.86 and 3.30
 (* log-transformed values used)

surrounding Beira schist and is dependant upon host rock composition and available joints. Component 2 (MgO, Fe₂O₃, TiO₂, K₂O, -Zr) is determined by the composition of the Beira schists. A plot of the component scores of component 1 did not give any new information of the vein distribution underground. The component scores are not easily interpretable as even small veins (0.1 to 5 cm) gave alteration halos with associated elevated trace element contents. Component 2, which is governed by the composition of the Beira schist, only gave the compositional differences between the individual shale/graywacke layers.

The Argemela quartz-cassiterite veins occur in a stockwork in the Beira shales. Sericitization is the major alteration process of these shales. Tourmalinization of the shales, compared to Panasqueira, is negligible.

Sericitization is responsible for the strongly increased Rb, Li, Cs and F contents (Table VI). The contents of Rb, Li, Cs, F, Sn and W in

Table VI: Geometrical mean and range of Beira schist and shales at Panasqueira and Argemela.
Values in parts per million unless stated otherwise.

	Panasqueira anomalous n=64	Panasqueira background n=18	Argemela anomalous n=15	Argemela background n=11
Li	380 (152-1880)	95 (52-125)	1150 (345-2080)	90 (45-215)
B	1570 (200-8000)	100 (50-200)		
F	3800 (1320-17400)	570 (340-970)	8300 (2980-14130)	680 (460-1400)
Cu	55 (8-205)	23 (5-90)	70 (40-110)	45 (30-70)
Zn	190 (70-1160)	140 (70-390)	110 (50-150)	125 (95-200)
Rb	510 (230-1116)	130 (72-220)	810 (374-1184)	125 (99-165)
Sr	45 (18-140)	55 (25-130)	70 (40-120)	45 (30-55)
Zr	200 (161-275)	210 (175-360)	200 (165-250)	210 (185-245)
Nb			13 (9-20)	12 (10-14)
Sn	50 (23-135)	2 (1-6)	95 (30-390)	1 (1-2)
Cs	85 (35-195)	4 (1-10)	285 (45-865)	3 (1-10)
W	27 (10-55)	< 6 (1-10)	18 (10-95)	< 6 (1-7)
P ₂ O ₅ %	.22 (.12-.76)	.14 (.07-.30)	.22 (.07-.77)	.08 (.04-.16)
TiO ₂ %	.93 (.68-1.26)	.92 (.61-1.14)	.93 (.80-1.43)	.91 (.78-1.03)
CaO %	.45 (.16-2.01)	.26 (.14-.70)		
MgO %	2.19 (.86-6.22)	2.08 (1.29-2.67)		
Fe ₂ O ₃ %	6.37 (3.89-9.41)	5.83 (3.43-7.95)		
K ₂ O %	4.38 (1.24-7.52)	2.08 (1.29-2.67)		
Na ₂ O %	1.42 (.23-3.07)	1.93 (1.28-2.84)		

the Argemela surface shales attain higher Rb, Li, Cs and Sn values and also a greater extension outwards from the veins, compared to Panasqueira.

Drillcores

Drillcores from the mine with well developed and separated alteration zones were sampled and analyzed. The conclusions below were drawn from DDH 139-H but also from DDH 115, 99 and 34-E. The sampling distance was however much smaller in 139-H than in core 115 and 99.

Similar conclusions were obtained from DDH 34-E and a macroscopical study of DDH 72-K (Dekker, 1979).

A study of these drillcores indicates three different coloured zones. In the first 2 to 30 cm around a vein a brown coloured tourmaline-rich zone occurs. This zone is strongly dependant on the veins; wider veins have tourmaline zones about 30 cm thick, smaller veins may also have smaller zones. However, muscovite filled veins (1 to 5 cm) may be surrounded by thick tourmaline zones, up to 20 cm. Other quartz veins are surrounded by a purple coloured tourmaline-sericite zone. Some veins do not have a tourmaline-rich zone. It seems that tourmalinization of the host rock along the veins was time controlled, only schist along the early opened joints or veins underwent tourmalinization. Small joints with tourmalinization continue into wider ore veins, also with tourmalinization. The tourmalinized schist contains arsenopyrite, wolframite and cassiterite.

The brown-coloured tourmaline zone is followed outwards by a purple coloured sericite-rich zone. Along some veins the tourmaline and sericite zone may overlap. The sericite zone consists mainly of sericite, quartz, altered cordierite and occasionally tourmaline or topaz.

The sericite zone is outwardly followed by a green coloured zone which consists mainly of chloritized Beira schist with sericite. This is the common background for schists surrounding the veins, it continues until the next vein assemblage.

Component analysis as well as plots were made of the element distribution in drillcores through the ore zone. The host rock composition is variable. This explains partly why in the drillcores different alteration zones are found.

Especially DDH 139-H showed well developed and separated alteration zones (Fig. 7). Between 14 and 25 m this core showed all alteration patterns observed and element distributions in this core are given in Fig. 7 and 8. Component analysis on DDH 139-H revealed three components (Table VII). Component 1 represents the sericite zone with increased contents of K_2O , Rb, Li, Cs, Ba and lower contents of Fe_2O_3 and Na_2O . Component 2 represents the tourmaline zone which is

Table VII: Loadings of component analysis on DDH 139-H.

	COMPONENT 1	COMPONENT 2	COMPONENT 3
CaO		.50	.53
K ₂ O	.83	-.51	
Fe ₂ O ₃	-.80		
Na ₂ O	-.86		
P ₂ O ₅		.68	.50
TiO ₂			.80
Cu *		.76	
Li *	.88		
Rb *	.86	-.41	
Sn *		.87	
Sr *		.84	
Zn *	-.45	.83	
Zr *			.89
Cs *	.91		
Mn *		.70	
Ba *	.73	-.59	

Eigenvalues before rotation: 7.20, 3.78 and 1.79

* log-transformed values used

characterized by higher Sn, Sr, Zn, Cu, Mn and P₂O₅ contents. Component 3 is the background of the unaltered Beira schists and is characterized by TiO₂, Zr, CaO and P₂O₅.

Tourmaline zone

The brown coloured tourmaline zone is characterized by higher Sn, Cu, Zn, Mn, Sr, W and P₂O₅ values but also by lower Rb, Li, Cs, Ba and K₂O values (see Fig. 7 and 8). From the element distributions several conclusions can be drawn. Rb, Li and Cs values are high in the sericite zone but not in the tourmaline zone. Obviously, this tourmaline (Dravite) is rich in Fe₂O₃ and Na₂O and not in Rb, Li or Cs as is the case with the green, red and blue tourmalines in the veins. CaO and P₂O₅ values are erratic but still higher in the tourmaline zone which is caused by the occurrence of apatite in this zone. Cu and Zn occur as sulphides in the tourmaline zone, especially along cracks in

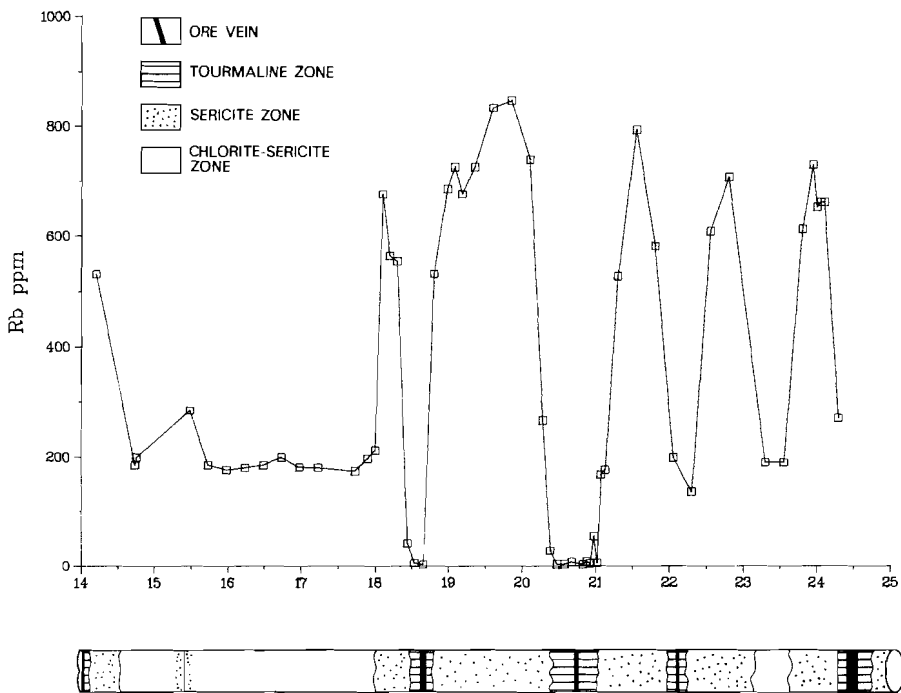


Fig. 7. Profile of Rb contents along DDH 139-H from 14 to 25 m.

the schist together with cassiterite and wolframite.

Analyses of uncontaminated drillcores indicate that tungsten is concentrated in the tourmaline zone but much less in the sericite zone. In the chlorite-sericite zone tungsten values are below the detection limit of the XRF (about 6 ppm). It seems that the mobility of tungsten is very low in the schist environment, compared to other elements like Sn, F, Li and Rb. Introduction of tungsten in the schist occurred as wolframite in small cracks and joints.

Sericite zone

The purple coloured sericite zone is high in Rb, Li, Cs and K₂O and somewhat higher Ba. Fe₂O₃ and Na₂O values are lower than in the unaltered Beira schist (Fig. 7 and 8). Li however differs somewhat from Rb, Cs and K₂O. Between individual veins Li values decrease again

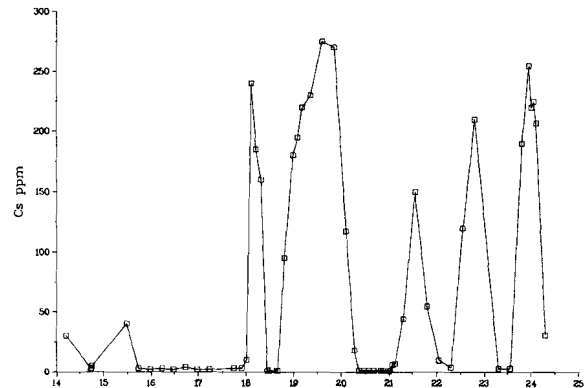
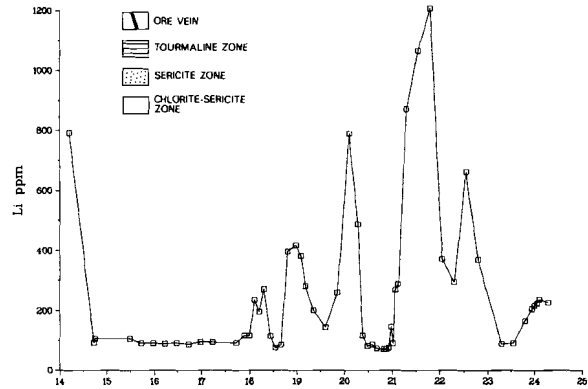
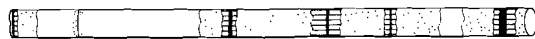
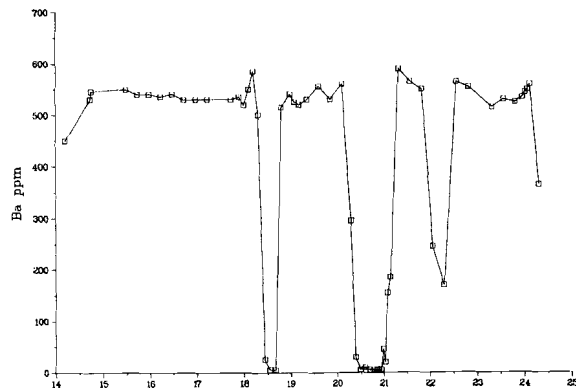
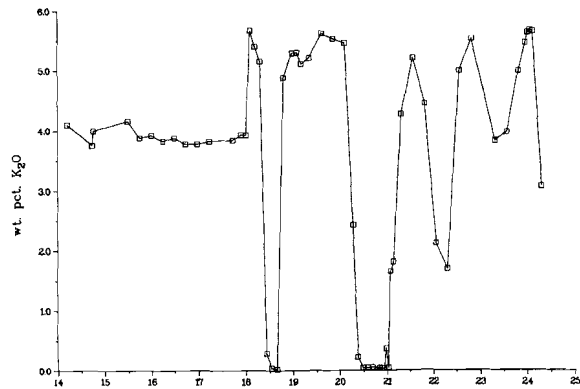


Fig. 8. Profiles of several element contents along DDH 139-H from 14 to 25 m.

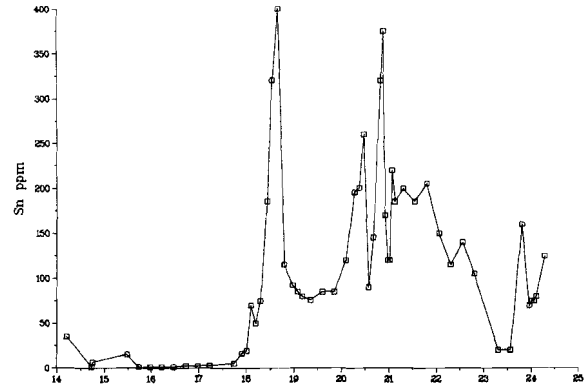
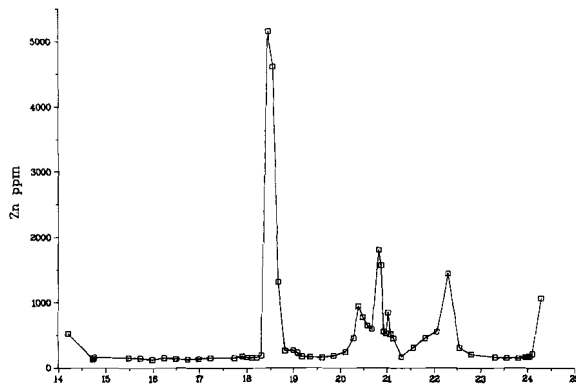
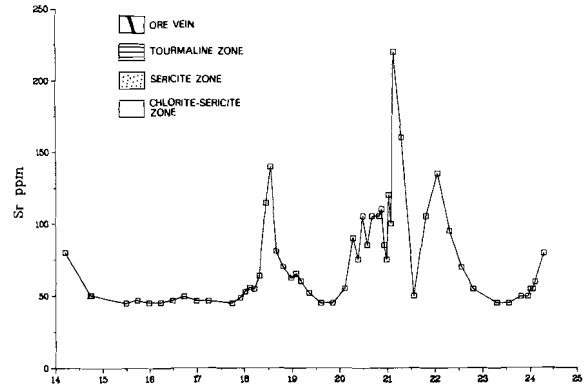
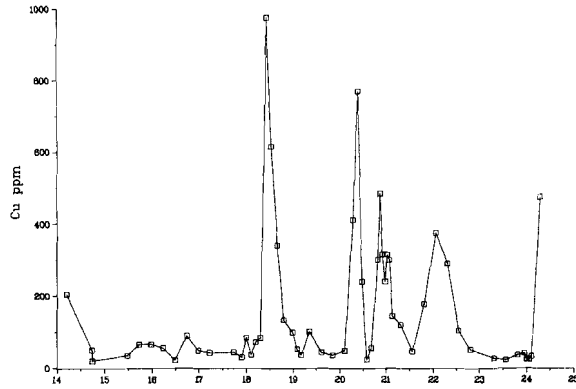


Fig. 8. Profiles of several element contents along DDH 139-H from 14 to 25 m.

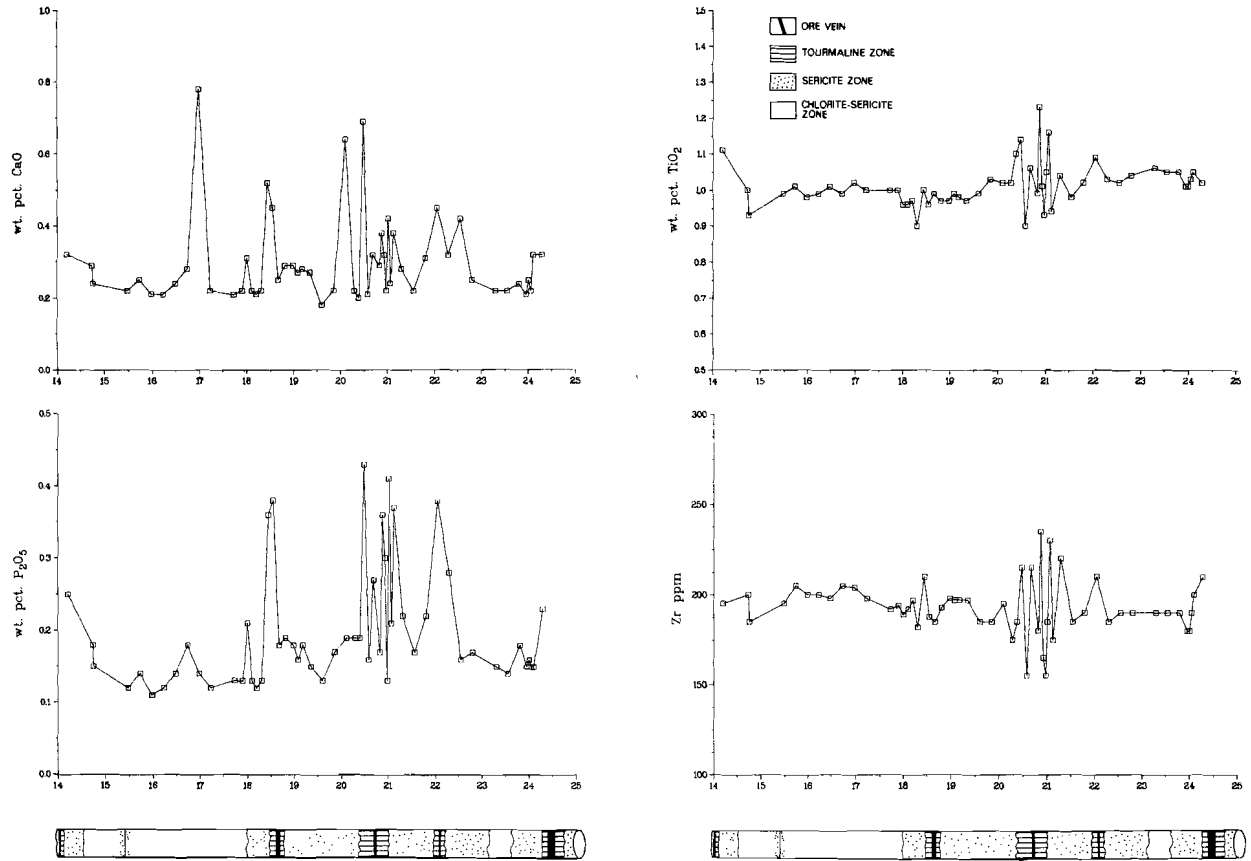


Fig. 8. Profiles of several element contents along DDH 139-H from 14 to 25 m.

whereas Rb, Cs and K_2O values remain high. From this it appears that two sericite generations may be present in this zone, one with high Rb and Cs values and another with high Li values. Thus in the sericite zone Rb, Cs, Li and K_2O were fixed in newly formed sericite with a removal of Na_2O and Fe_2O_3 , probably to the tourmaline zone.

Chlorite-sericite zone

The green coloured chlorite-sericite zone represents the local background schist in the mine. The values of all determined elements attain their "normal" values in this zone, compared to the unaffected Beira schists. Zr and TiO_2 stay at about the same level in drillcore 139-H, even in the sericite and tourmaline zone and both elements represent shale/graywacke layers in the Beira shale complex. Different host-rock compositions explain why Zr and TiO_2 differ only slightly in DDH 139-H but scatter as in DDH 115.

The analyses of the sub-surface schists and drillcores indicate different mobilities for the investigated elements. Whereas Rb, Li, F and Cs show high mobilities, elements like Cu, Zn, W and Ba have much lower mobilities. The mobility of Sn is between those of the above mentioned elements and may depend upon the F concentration in the fluid. The low mobilities of Cu and Zn (and possibly As) can be explained by their deposition as sulphides. Most likely, elements like Rb, Li and Cs are transported as chlorides which explains their much higher mobilities in the schist environment (see Chapter 5). These elements are especially concentrated in the newly formed muscovite and sericite in the sericite zone.

CONCLUSIONS

The Panasqueira tungsten-tin deposit consists of sub-horizontal ore veins which are related to a greisenized granite cupola. Greisenization especially mobilizes Na_2O , apart from other major elements. Component analysis of major and trace elements in the

granite and greisen samples indicates a complex (re)mobilization within the different granitoid phases at Panasqueira. Two trends, each with different sub-groups, can be distinguished: a granitic trend (albite granite) and a greisen trend. Both trends show an increase in Sn, Fe₂O₃, Rb, Nb, Ta, W, Cu, Zn and As contents and a decrease in Na₂O, caused by the post-magmatic greisenizing fluids. The difference between the two trends is characterized by different concentration levels of Th, Li, Zr, Ce, La, TiO₂, P₂O₅, Ba, F, CaO, MgO, Hf, Cs, Sr and Sc. The origin of the two trends seems to be related to the status of the hydrothermal system, i.e. closed or opened (see also Chapter 5).

The schist composition in the Panasqueira mine is influenced by the post-magmatic fluids in the veins. Schist samples are characterized by their MgO, Fe₂O₃, TiO₂, K₂O and Zr contents which may reflect the different schist layers. The influence of the hydrothermal fluids on the schists consists of increased Rb, Li, F, Sn, Cs and B contents and lower Na₂O contents. The hydrothermal aureole is fairly independent on the vein size. Earlier veins (even small ones) have thicker tourmaline zones than later ones. It rather seems that the hydrothermal "overprint" is time controlled.

Investigations of drillcores indicate two alteration zones around the veins. First, a tourmaline zone which is followed outwards by a sericite zone. The outermost zone consists of the local background, the chlorite-sericite schist. The tourmaline zone has increased Sn, Cu, Zn, Sr, W, Mn and P₂O₅ values but decreased Ba, Rb, Li, Cs and K₂O values. The sericite zone contains increased Rb, Li, Cs and K₂O and somewhat higher Ba values. Na₂O and Fe₂O₃ are somewhat lower than in the unaltered schist. The chlorite-sericite schist is the local background in the schist aureole around the cupola and adjacent veins.

The mobilities of the individual elements in the surroundings of a vein system differ strongly. Li, Rb, Cs, F and Sn are much more mobile than elements like Cu, Zn, As, W and Ba. These mobilities are only valid in the schist environment; alteration of encasing granitoid rocks may produce a different picture.

REFERENCES

- Bloot, C. & de Wolf, L.C.M. (1953): Geological features of the Panasqueira tin-tungsten ore occurrence (Portugal). *Bol. Soc. Geol. Portugal*, 11, 1-58.
- Boissavy-Vinau, M. & Roger, G. (1980): The TiO_2/Ta ratio as an indicator of the degree of differentiation of tin granites. *Min. Deposita*, 15, 231-236.
- Chappell, B.W. & White, A.J.R. (1974): Two contrasting granite types. *Pacific Geology*, 8, 173-174.
- Clark, A.H. (1964): Preliminary study of the temperatures and confining pressures of granite emplacement and mineralization, Panasqueira, Portugal. *Trans. Inst. Min. Metall.*, 73, section B, 813-824.
- Clark, A.H. (1965): Author's reply to discussion of 1964 paper. *Trans. Inst. Min. Metall.*, 74, section B, 217-223, 296, 663-672.
- Clark, A.H. (1970): Potassium-Argon age and regional relationships of the Panasqueira tungsten-tin mineralization. *Com. Serv. Geol. Portugal*, 53, 243-261.
- Costa, C.V. & Pereira L.G. & Ferreira, M.P. & Santos Oliveira, J.M. (1971): Distribuição de oligoelementos nas rochas e solos da região do Fundão. *Mem. Not. Mus. Lab. Min. Geol. da Univ. de Coimbra*, no. 71, 3-37.
- Dekker, C.A. (1979): A geochemical study of rocks in the Panasqueira mine, Portugal. Internal report, Dept. of Geochemistry, State University of Utrecht, 89 pp.
- Dixon, W.J. & Brown, M.B. & Engelman, L. & Frane, J.W. & Hill, M.A. & Jennrich, R.I. & Toporek, J.D. (1981): BMDP statistical software. University of California Press, Los Angeles, 726 pp.
- Hall, A. (1971): Greisenization in the granite of Cligga Head, Cornwall. *Proc. Geol. Ass.*, 82, 209-230.
- Kelly, W.C. & Rye, R.O. (1979): Geologic, fluid inclusion and stable isotope studies of the tin-tungsten deposits of Panasqueira, Portugal. *Econ. Geol.*, 74, 1721-1822.
- Lehmann, B. (1981): A discussion of the paper by M. Boissavy-Vinau and G. Roger "The TiO_2/Ta ratio as an indicator of the degree of differentiation of tin granites". *Min. Deposita*, 16, 329-331.
- Marignac, Chr. (1982): Geologic, fluid inclusion and stable isotope studies of the tin-tungsten deposits of Panasqueira, Portugal. - A discussion. *Econ. Geol.*, 77, 1263-1266.
- McNeil, M. (1982): Panasqueira - The largest mine in Portugal. *World Mining U.S.A.*, 52-55.

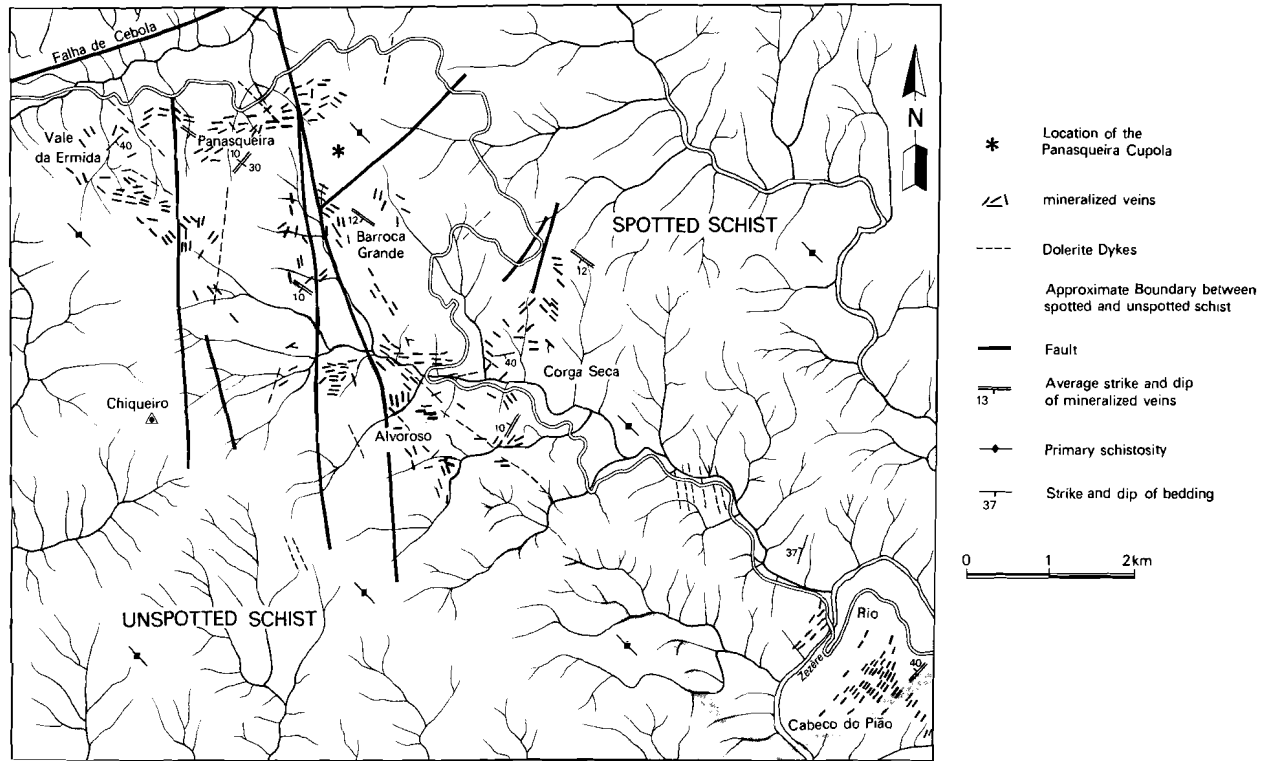
- Neiva, A.M.R. (1974): Greisenization of a muscovite-biotite albite granite of northern Portugal. *Chem. Geol.*, 13, 295-308.
- Priem, H.N.A. & den Tex, E. (1982): Tracing crustal evolution in the NW Iberian Peninsula through Rb-Sr and U-Pb systematics of Paleozoic granitoids: a review. *International Colloquim "Géochimie et Petrologie de granitoids"*, Clermont-Ferrand, May 1982, Volume of Abstracts.
- Rösler, H.J. & Lange, H. (1972): *Geochemical tables*. Elsevier Publ. Company. Amsterdam. 468 pp.
- Smith, A. (1979): Mining at Panasqueira mine, Portugal. *Trans. Inst. Min. Metall.*, 88, section A, 108-115.
- Stemprok, M. (1979): Mineralized granites and their origin. *Episodes*, no. 3, 20-24.
- Thadeu, D.C. (1951): *Geologia do couto minero da Panasqueira*. *Com. Serv. Geol. Portugal*, 32, 1-64.
- Thadeu, D.C. (1977): Hercynian paragenetic units of the Portuguese part of the Hesperic massif. *Bol. Soc. Geol. Portugal*, 20, 247-276.
- Tischendorf, G. (1977): Geochemical and petrographic characteristics of silicic magmatic rocks associated with rare-element mineralizations. In: Stemprok, M., Burnol, L. and Tischendorf, G. (editors). *Metallization Associated With Acid Magmatism*. Geological survey of Prague, 2, 41-96.

CHAPTER 4

SURFACE ANOMALIES AROUND THE PANASQUEIRA TUNGSTEN-TIN DEPOSIT, PORTUGAL

The Panasqueira tungsten-tin deposit is located in the Beira Baixa province in Portugal, about 35 km WSW of Fundão, in the foothills of the Serra da Estrela, the highest mountain range of Portugal (Fig. 1, Chapter 3). Mining started in 1898 and currently Beralt Tin & Wolfram S.A.R.L. operates the concession. Ore concentrates are produced in Rio at the Zêzere river (Fig. 1)

The purpose of this study was to investigate the expression of the dispersion aureole around the mineralization at the surface. Due to extensive mining at Panasqueira, soils, commonly used for detailed exploration, are strongly contaminated with the ore-related elements. Therefore schist samples, the least weathered possible, were taken from surface outcrops. The schists were analyzed for several minor and trace elements. The results are compared with schist samples collected underground. Contour maps were prepared for the relevant elements. The contour maps of the element concentrations give the extent of the dispersion aureole of the different elements. Component analysis was performed to reveal interrelations between the analyzed elements. The component scores were plotted and compared with the contour maps of the individual elements.



(Modified after Conde et al. 1971 and Kelly & Rye, 1979)

Fig. 1. The Panasqueira mining district.

GEOLOGY

The Panasqueira ore body consists of sub-horizontal quartz veins in the Beira shales (Fig. 2, Chapter 3), surrounding a greisenized granite cupola. A sub-horizontal joint system was developed after intrusion of the granite (Thadeu, 1951; Bloot & de Wolf, 1953; Clark, 1964, 1965; Kelly & Rye, 1979; Marignac, 1982). This joint system was opened by the fluids with subsequent ore deposition. The veins are found in and outside the spotted schist area (Fig. 1) and crosscut the bedding and schistosity of their host rocks, including the greisen cupola (Thadeu, 1951; Conde et al., 1971).

Alteration along the ore veins includes tourmalinization and sericitization. The extent of the alteration zone around veins strongly depends upon host rock composition and available joints; normally the width of the alteration zones is between 0.5 and 2 m (see Chapter 3). More detailed geological information about the granite, greisen and schists is found in Chapter 3.

The ore veins are cut by later vertical faults (Fig. 2). The Cebola fault was supposed to terminate the ore zone in the northwest of the mining concession (Kelly & Rye, 1979). However, similar sub-horizontal ore veins have been found across this fault in new road cuts.

GEOCHEMISTRY

Sample preparation

Some 180 schist and shale samples were collected at the surface by sampling 15 to 20 chips at outcrops over 20 to 50 m². The weight of the samples was between 0.5 to 1 kg. Care was taken not to include small quartz or muscovite veinlets. The samples were collected above the underground veinage system but also at a distance, up to several kilometers from the known ore fields (Fig. 2). The chip sampling technique provides a more representative sample of the composition of the sampled outcrop than can be achieved by one large hand specimen.

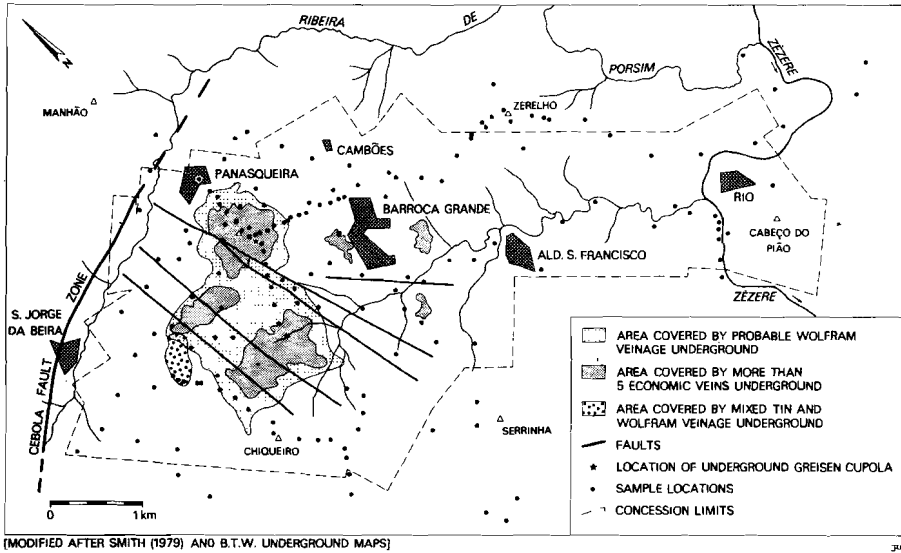


Fig. 2. Surface map with sample locations and underground areas with 2- and 5-vein limits.

Initially, some samples were broken with a jaw-crusher coated with tungsten-carbide, thus tungsten values from these samples were deleted from the data set. Later, a Ni-Cr steel jaw-crusher was installed for sample preparation. The crushed samples were split and pulverized in a swingmill (Ni-Cr steel) to ~250 mesh. More information about the analytical techniques is given in Chapter 2.

Interpretation

The analytical results of the surface schist samples were studied with the aid of univariate and multivariate statistical techniques. Statistical procedures from the SPSS (Nie et al., 1975) computer programme library were applied, as well as some special programmes not included in this library. More information about mapping and other multivariate techniques is given by Howarth (1983).

First, histograms and cumulative frequency curves of the element

contents were prepared as a check for normality or log-normality and multi-modality. From the cumulative frequency curves it appeared that the trace elements have a lognormal distribution, therefore logarithmic values were used for further calculations.

Probability plots (Sinclair, 1976) showed that several populations occur within the data sets which could be separated by their inflection points. In the tin, tungsten and cesium data sets the lowest population was influenced by the detection limit of the analytical method used. Detection limits for these elements were respectively 4, 7 and 3 ppm.

The SYMAP computer package (Dougenik & Sheehan, 1976) was used to prepare contour maps of the investigated elements. Class intervals, identified by the populations in the probability graphs, were used as contour fields. Large class intervals were split into two intervals of equal size.

The surface samples are not homogeneously distributed over the sampled area; many samples were collected close to mineralized veins or at a considerable distance from veins. Lack of suitable outcrops also influenced the sample distribution. A more homogeneous distributed data set was prepared by adding aggregated data to the original data set. The aggregated data were obtained by non-overlapping, non-weighted moving average with a square window (SPSS programme, Nie et al., 1975; Davis, 1973). The extended data set was used in the subsequent component analysis but the aggregated data were given an arbitrary weight factor of 10 thereby suppressing the included original data set.

With component analysis, a first component explains 49% of the variation, a second explains an additional 15% and it appears that only the first component is of real geological importance (Table II).

Table I: Geometrical mean and range of sub-surface and surface schists.
 Values in parts per million except for P₂O₅ and TiO₂.

	Sub-surface anomalous n=64	Sub-surface background n=18	Surface anomalous n=19	Surface background n=62
Li	380 (152-1880)	95 (52-125)	280 (165-665)	70 (28-135)
B	1570 (200-8000)	100 (50-200)	1130 (150-7000)	47 (10-200)
F	3800 (1320-17400)	570 (340-970)	3700 (1715-9640)	445 (200-890)
Cu	55 (8-205)	23 (5-90)	45 (24-95)	34 (10-68)
Zn	190 (70-1160)	140 (70-390)		
Rb	510 (230-1116)	130 (72-220)	330 (225-518)	105 (54-145)
Sr	45 (18-140)	55 (25-130)	39 (25-70)	26 (10-45)
Zr	200 (161-275)	210 (175-360)	210 (190-245)	220 (185-270)
Nb			12 (8-13)	10 (7-13)
Sn	50 (23-135)	2 (1-6)	45 (25-140)	2 (1-6)
Cs	85 (35-195)	4 (1-10)	55 (30-245)	3 (1-9)
W	27 (10-55)	<6 (1-10)	12 (3-40)	<6 (1-10)
P ₂ O ₅ %	.22 (.12-.76)	.14 (.07-.30)	.14 (.07-.22)	.10 (.04-.21)
TiO ₂ %	.93 (.68-1.26)	.92 (.61-1.14)	1.00 (.68-1.14)	.91 (.50-1.14)

RESULTS AND DISCUSSION

The contents of surface samples of Rb, Li, Cs and other elements, are comparable to those of fresh schists samples taken underground (see Chapter 3 and Table I). Although the variable degree of weathering of the samples possibly sometimes results in lower amounts, this is not to such a degree that surface schists can not be used for geochemical exploration purposes.

Surface anomalies

Single element dispersions around the sub-horizontal ore veins at the surface are shown in Fig. 3 for the elements tin, fluorine, rubidium, tungsten, lithium, boron, cesium, titanium, copper and zirconium. The elements tin, fluorine, rubidium, lithium, cesium,

boron and to a lesser extent tungsten, exhibit a broad similarity in distribution pattern with higher anomalies where concentrations of ore veins occur (Fig. 5). Tin, rubidium, lithium, cesium and fluorine give a considerably better representation of the mineralized areas, compared to tungsten and boron. Apparently, they are much more mobile than tungsten in the schist environment and produce a distinct dispersion pattern. However, the boron contour map suffered from missing data which makes the resulting map less reliable. The same is true for tungsten as contaminated tungsten values were deleted from the data set. In the case of Panasqueira rubidium, lithium, cesium, fluorine, boron and tin can be used as 'pathfinders' for the tungsten mineralization (Oosterom et al., 1982).

The contour maps of rubidium, lithium, cesium, tin and fluorine produce large and fairly contrasting patterns of anomalies which outline the outcropping vein swarms. The lithium contours are similar to those of tin, fluorine, rubidium and cesium but its contrast is much weaker. For copper, which is of importance in the ore deposit, even less is revealed by the contour maps. The contour map gives a poor reflection of the ore zone, only the highest copper values may show some correlation. Contour maps of titanium, strontium and zirconium, although consistent by themselves, are not related to the mineralization processes which is confirmed by results of Chapter 3. These elements reflect the original sedimentary composition of the Beira shales. Strontium also reflects this composition but it is remobilized along the veins, thereby correlating slightly with the vein related elements like rubidium.

For exploration purposes tin and cesium are the best indicators for the tungsten mineralization at Panasqueira. Both elements attain more than tenfold their background values close to the mineralization. For practical reasons lithium also can be mentioned. Lithium is easily determined by AAS and can be used instead of tin or cesium.

Results from Chapter 3 and 5 indicate that the Beira schists had a low permeability, apart from the opened joints which acted as vein channels (Kelly & Rye, 1979). This low permeability in the schists

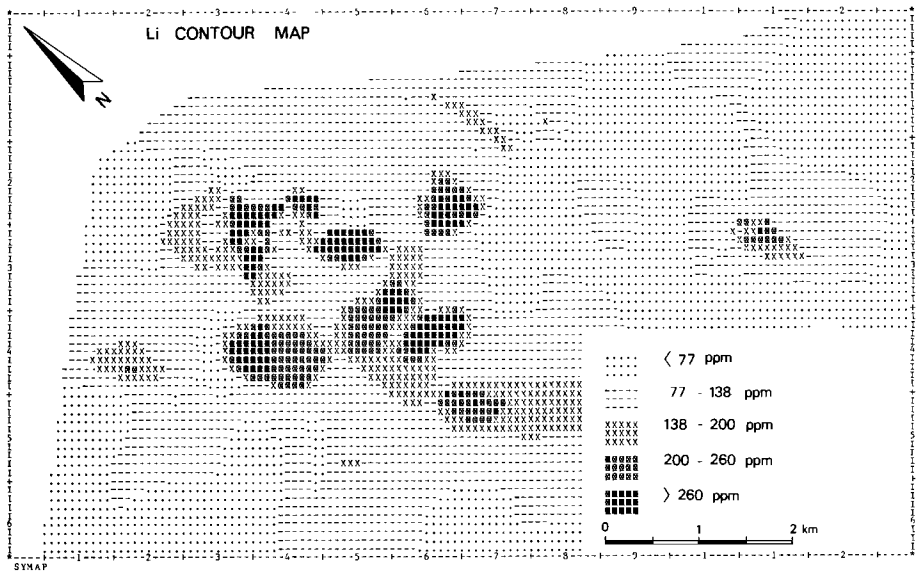
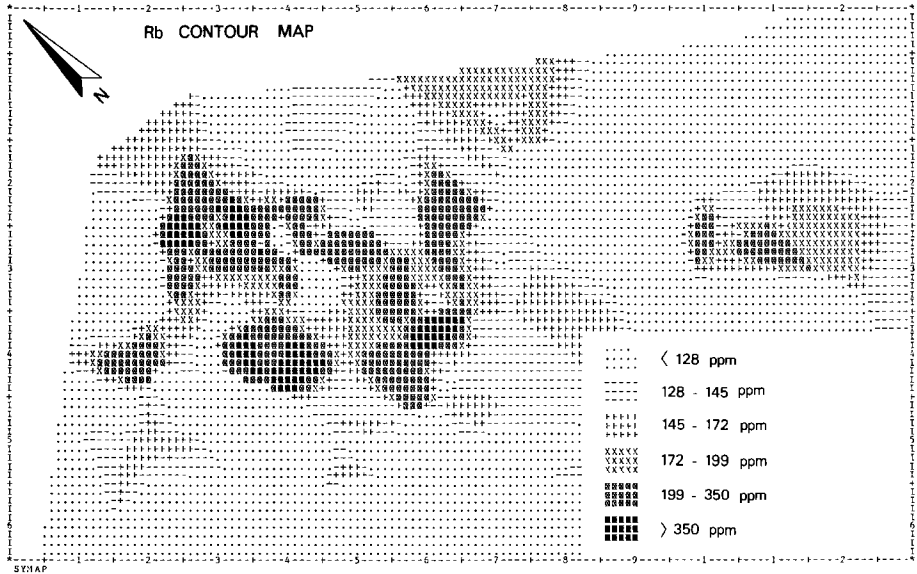


Fig. 3. SYMAP contour maps of the individual elements.

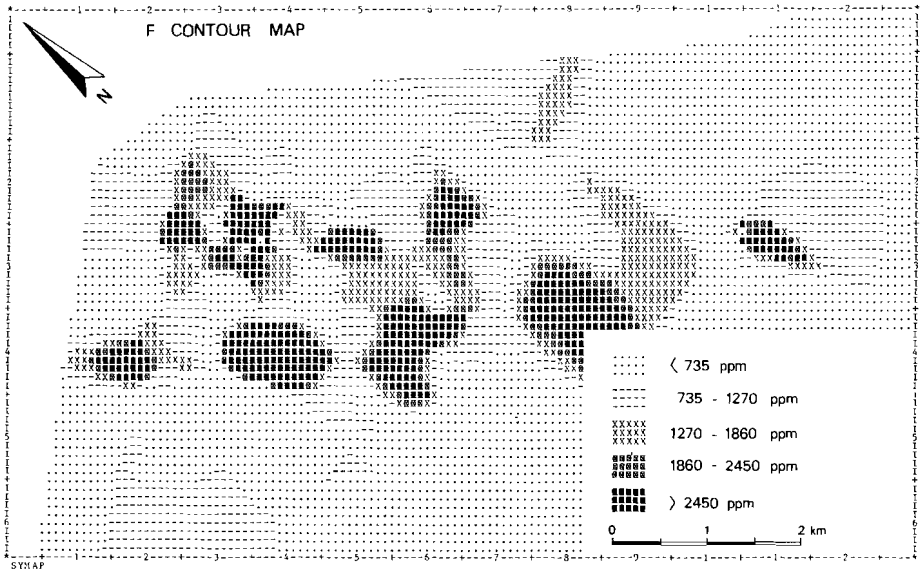
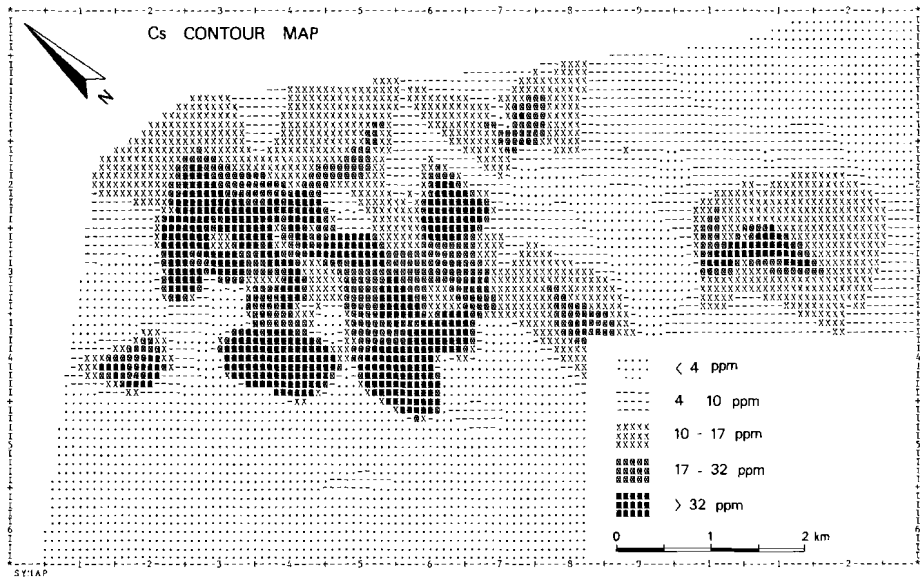


Fig. 3. SYMAP contour maps of the individual elements.

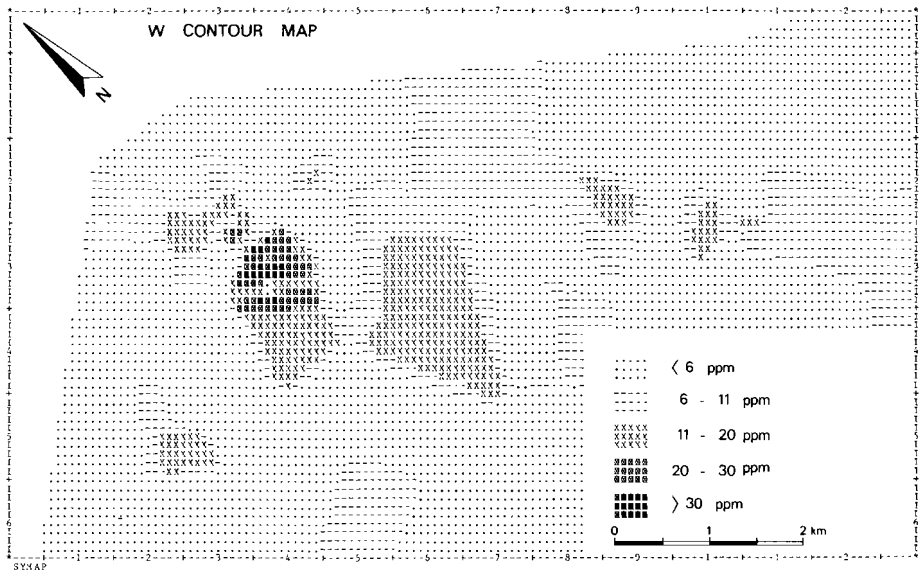
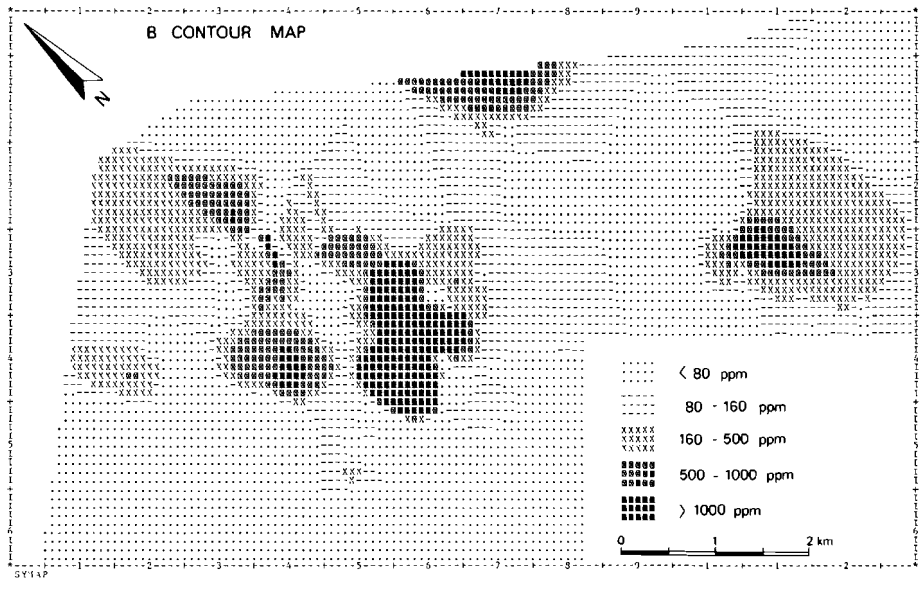


Fig. 3. SYMAP contour maps of the individual elements.

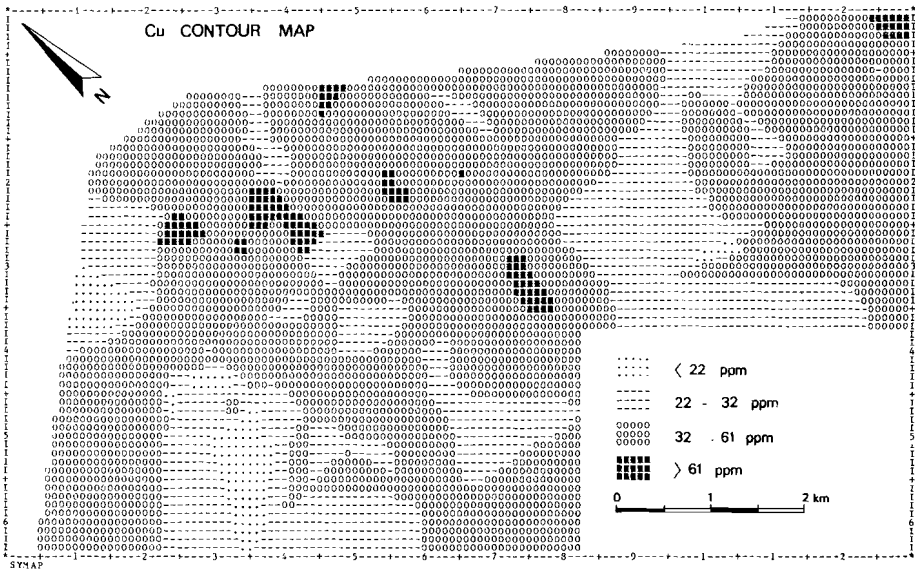
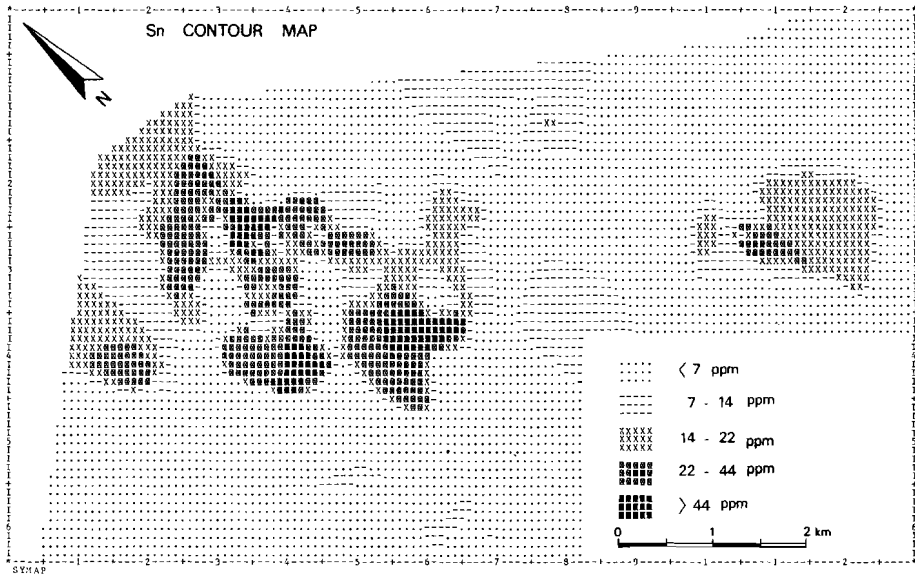


Fig. 3. SYMAP contour maps of the individual elements.

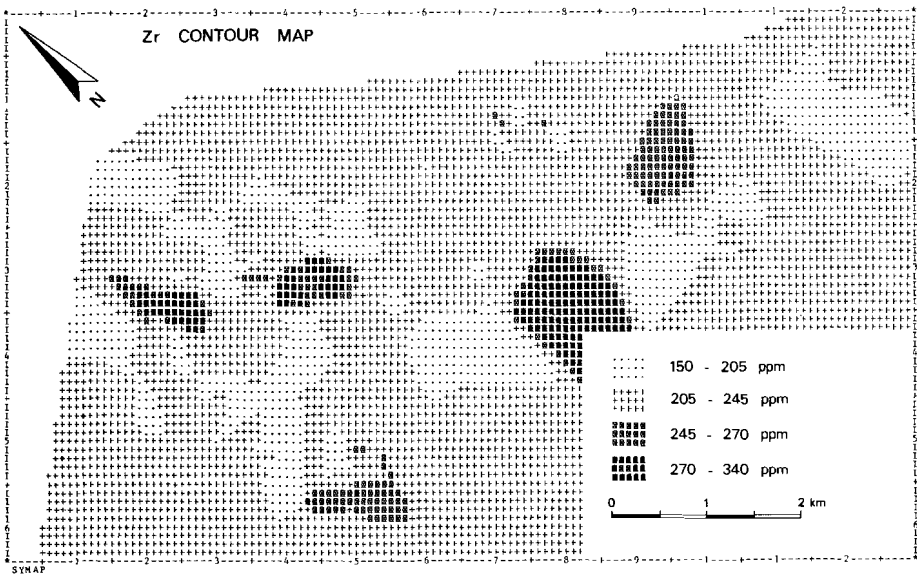
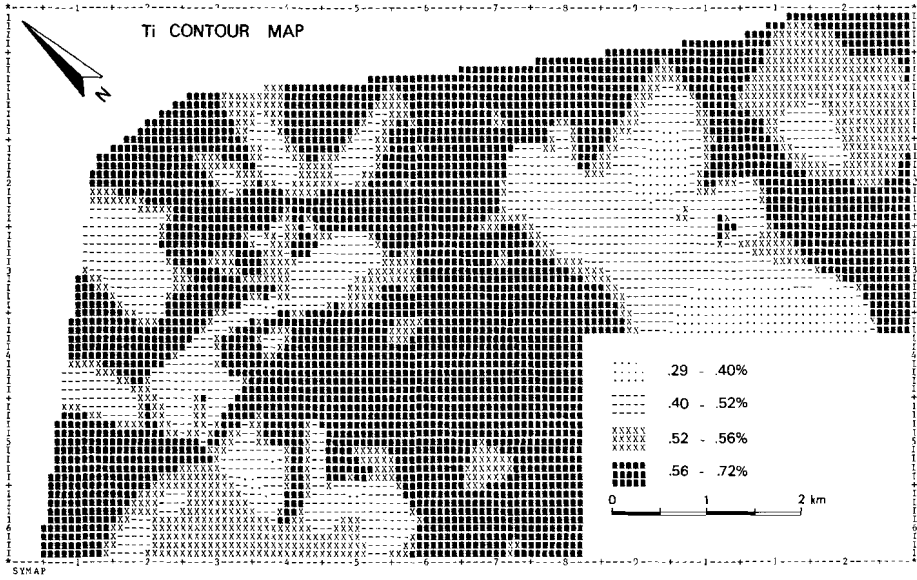


Fig. 3. SYMAP contour maps of the individual elements.

caused the anomalies around the ore veins to be small.

The alteration zones are the results of diffusion and infiltration processes. At Panasqueira infiltration along the sub-horizontal joints is of more importance than diffusion into the schists. For exploration purposes diffusion aureoles are of importance because these are sampled and analyzed. Although the diffusion zones are small, the combination of extended infiltration along joints with the diffusion zones gives a large alteration zone around the vein swarms.

The anomalies around ore veins do not exceed about 2 m (Chapter 3) but the combination of several veins with many smaller surrounding veinlets offers a much larger anomalous zone which can easily outrange the metasomatic zone of one economic vein. Mineralized economic veins are always accompanied by many smaller veins and veinlets, resulting in a large hydrothermally altered aureole.

Component analysis with the SPSS programme (Nie et al., 1975) reveals two components in the surface samples (Table II). Component 1 (Sn, Cs, B, F, Rb, Li, W, Sr, P₂O₅) points to a "mineralization" factor and component 2 (TiO₂, Nb, Cu) possibly represents the schist composition. The association of lithium, fluorine, rubidium, cesium and tin with the hydrothermal aureoles is confirmed by the results of Chapter 3.

The multi-element presentation of the component scores of component 1 (Fig. 4) gives a better representation of the contours as it suppresses deviating values of the original elements, combining the individual maps into a more homogeneous map. The multi-element presentation is superior to the single element plot and shows a relation between anomalies and vein density at the surface (Fig. 5). The anomalies are found around sub-horizontal mineralized joints and indicate the location of outcropping or nearby ore zones.

The sub-horizontal ore veins are about 400 m below the Chiqueiro hill; here, no surface patterns are found, apart from some occasionally occurring veins. Obviously, the distance from the ore veins to the surface is too large. Comparison with other ore zones indicates a

Table II: Component loadings of the Panasqueira surface schists.

	COMPONENT 1	COMPONENT 2
Rb *	.82	.48
Sr *	.56	
Cu *		.67
Sn *	.88	
F *	.83	
W *	.59	
B *	.86	
Li *	.77	
Nb *		.85
Cs *	.87	
TiO ₂		.88
P ₂ O ₅	.45	

Eigenvalues before rotation: 5.89 and 1.77

(* logarithmic values used)

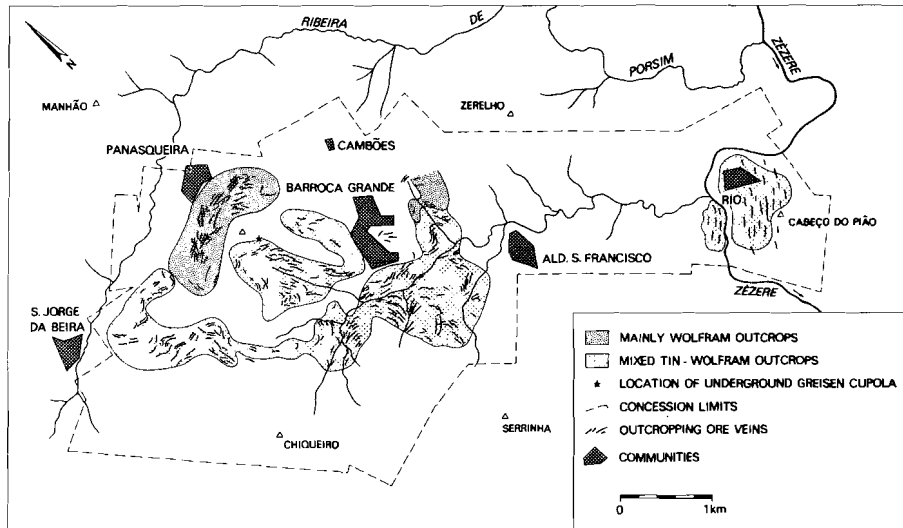


Fig. 5. Surface map with outcropping ore veins, combined with their major mineralizations.

maximum extent of the alteration zone of about 50 m around economic vein swarms.

Northeast of Barroca Grande, somewhat higher rubidium, lithium, tin and cesium values occur (Fig. 3). This anomaly is not related to any known ore zone. Ore veins may be present below the surface but the anomaly may also be caused by the proximity of the granite/schist contact at depth.

CONCLUSIONS

The contour maps of the elements tin, cesium, boron, fluorine, rubidium, lithium and to a lesser extent tungsten, strontium and phosphorus, show a clear relation with the occurrence of sub-horizontal ore veins at Panasqueira. The representation of component 1 (Sn, Cs, B, F, Rb, Li, W, Sr, P₂O₅) gives a better expression of the geochemical contours as it suppresses deviating values in the data set, thereby combining the individual maps into a more homogeneous map. The dispersion of individual elements like tin, cesium, boron, fluorine, rubidium, lithium and tungsten is fairly small (0.5 to 2 m around veins, Chapter 3) but the combined anomalies of vein swarms outline the zones of ore dispersion very well. Obviously, the anomalies are indications for vein swarms and not of individual veins.

The anomalies at the surface but also underground, are the results of diffusion and infiltration processes along the sub-horizontal joints. Thin cracks penetrate to some extent into the schist but their length is small. Mineralized economic veins are always accompanied by many smaller veins which results in a large hydrothermally altered aureole. The altered zone surrounding these veins offers a good target for geochemical prospection. The inhomogeneity of veinlets in this aureole requires a large sample area for detection, e.g. a composite sample is much better than only one large hand specimen.

In the southwestern area covered by the contour maps the absence of ore zones is indicated, only locally some veins occur (e.g. Fonte das

Lameiras). This area also contains the Chiqueiro hill under which ore zones deflect to deeper levels. The distance from the ore zone to the surface is obviously too large to cause a geochemical anomaly. Contour maps show two distinct anomalous areas, one around Rio at the Zèzere river and the largest one around Panasqueira and Barroca Grande, coincident with the distribution of the major ore fields.

REFERENCES

- Blout, C. & de Wolf, L.C.M. (1953): Geological features of the Panasqueira tin-tungsten ore occurrence (Portugal). Bol. Soc. Geol. Portugal, 11, 1-58.
- Clark, A.H. (1964): Preliminary study of the temperatures and confining pressures of granite emplacement and mineralization, Panasqueira, Portugal. Trans. Inst. Min. Metall., 73, section B, 813-824.
- Clark, A.H. (1965): Author's reply to discussion of 1964 paper. Trans. Inst. Min. Metall., 74, section B, 217-223, 296, 663-672.
- Conde, L.N. & Pereira, V. & Ribeira, A. & Thadeu, D.C. (1971): Jazigos hipogénicos de estanho e volfrâmio. Livro-guia da Excursao No. 7. I congresso Hispano-Luso-Americano de Geologia Económica (Lisbon). Direcção-geral de minas e serviços geológicos. 68-77.
- Davis, J.C. (1973): Statistics and data analysis in geology. John Wiley & Sons, New York. 550 pp.
- Dougenik, J.A. & Sheehan, D.E. (1976): SYMAP user's reference manual. Harvard University, Mass. 5th edition.
- Howarth, R.J. (1983): Mapping. In: Statistics and data analysis in geochemical prospecting. Handbook of exploration geochemistry. Volume 2. Elseviers Publ. Comp. Amsterdam. 437 pp.
- Kelly, W.C. & Rye, R.O. (1979): Geologic, fluid inclusion and stable isotope studies of the tin-tungsten deposits of Panasqueira, Portugal. Econ. Geol., 74, 1721-1822.
- Marignac, Chr. (1982): Geologic, fluid inclusion and stable isotope studies of the tin-tungsten deposits of Panasqueira, Portugal. - A discussion. Econ. Geol., 77, 1263-1266.
- Nie, N.H. & Hadlai Hull, C. & Jenkins, J.G. & Steinbrenner, K. & Brent, D.H. (1975): SPSS, Statistical package for the social sciences. McGraw Hill, New York, 675 pp.

- Oosterom, M.G. & Vriend, S.P. & Bussink, R.W. & Moura, M.L. (1982):
Geochemistry of tin, tungsten and related elements such as
tantalum and niobium. E.E.C. Research programme on primary raw
materials, open file report, contract nr. 025.79 MPP NL, 58 pp.
- Sinclair, A.J. (1976): Application of probability graphs in mineral
exploration. The association of exploration geochemists. Special
volume No. 4, 95 pp.
- Thadeu, D.C. (1951): Geologia do couto minero da Panasqueira. Com.
Serv. Geol. Portugal, 32, 1-64.

CHAPTER 5

MINERALOGY, FLUID INCLUSIONS AND STABLE ISOTOPES OF
THE PANASQUEIRA W-SN DEPOSIT, PORTUGAL(*)

ABSTRACT

The Panasqueira tungsten-tin deposits occur in sub-horizontal veins related to a Hercynian granitic intrusion in the Beira shales.

Fluid inclusions indicate relatively low temperatures, ranging from 325°C in the first formed minerals through 250°C during the pyrrhotite alteration stage with salinities from 5 to 10 wt% NaCl to about 120°C with salinities below 5 wt% NaCl in the late carbonate stage. High CO₂ contents (up to 17 mol%) are observed in the early stages. Fluid pressures were about 1500 bars in the earliest stage but rapidly dropped to values between 100 and 200 bar during opening of the joint system, causing vigorous boiling in the ore veins at a depth of about 1800 m.

The gas composition of fluid inclusions in quartz, topaz and wolframite is 65-80% CO₂, 10-20% CH₄ and 10-17% N₂ on a H₂O free basis.

The $\delta^{18}\text{O}$ values of the fluids indicate extensive exchange with the granite. The $\delta^{13}\text{C}$ values of CO₂ from fluid inclusions in quartz, topaz and wolframite are between -12 and -4 per mil; most of this CO₂ was probably derived from the granite. The high initial pressures, combined with stable isotope data, show that the mineralizing fluids had a "magmatic" origin. Only in the late carbonate stage a meteoric water component becomes apparent.

(*) A condensed version of this chapter will be published in Bulletin de Minéralogie

INTRODUCTION

A comprehensive study of fluid inclusions and stable isotopes of the Panasqueira deposit has already been published by Kelly & Rye (1979). This paper reports fluid inclusion and heating/freezing data related to aspects of the Panasqueira W-Sn deposit not covered by Kelly & Rye (op. cit.), and gas chromatographic analyses of the fluid inclusions.

Stable isotopes of carbon, oxygen and nitrogen in fluid inclusions were also analyzed. These new data, combined with fluid inclusions, permit a better understanding of the formation of the Panasqueira ore deposit.

GEOLOGY

The Panasqueira tungsten-tin deposits occur in sub-horizontal ore veins in meta-sedimentary rocks and are related to a greisenized granite cupola. More detailed information about the geology is given in Chapter 3.

Ore-bearing quartz veins

Characteristic of the Panasqueira W-Sn deposit is the sub-horizontal ore-vein system. The ore veins follow a horizontal joint system which was developed after intrusion of the granite as it crosscuts the Panasqueira greisen cupola (Thadeu, 1951; Bloot & de Wolf, 1953; Clark, 1964, 1965a; Kelly & Rye, 1979; Marignac, 1982). Drillcores indicate that ore veins are virtually absent in deeper parts of the granite (Fig. 2, Chapter 3). Quartz veins follow the horizontal joints but the greisenized granite veins are always steeper according to a more vertical dipping joint system.

The dip of the ore veins is between 0° and 40° but the average is about 10° . Occasionally steeper dipping veins occur near the greisen cupola, the so-called "Galos". This vein system is connected with the thicker quartz veins which are related to the quartz-cap.

Ore veins follow a particular joint over some distance, mostly 10 to 200 m, then the veins pinch out and continue in another joint, 10 to

100 cm higher or lower. The ends of the ore veins wedge out as "eel-tails" and continue as small quartz or muscovite veinlets. The ends of the veins are often strongly mineralized.

Sometimes the connection between two overlapping veins is visible. By changing from one joint to another, the vein system is capable of reaching a large lateral extent. Although many joints are present, ore veins always follow the flattest joint-set available (Kelly & Rye, 1979). Splitting of ore veins is a common phenomenon which is clearly visible in pillars in the stopes. According to Bloot & de Wolf (1953) ore veins cross each other without any sign of discontinuity or enrichment in mineralization. However, some wolframite-quartz veins are later than topaz-cassiterite veins as they split off into different joints.

In the border zone of the ore veins small quartz veinlets occur. These veinlets, about 1 to 5 mm thick, are the remnants of the first vein developments and occur along veins in the whole mine. Euhedral crystals and large vugs are indications for open-space filling of the ore veins.

Kelly & Wagner (1977) studied fission-tracks in apatites from Panasqueira. Their study indicates that the veins were reheated at least once and probably twice in their post-Hercynian history. About 152 Ma ago (Late Jurassic), the apatites were heated to temperatures above 150°C. A second thermal event may have occurred about 79 Ma ago (Late Cretaceous) whereby the temperatures probably stayed below 105°C (150°C according to Kelly & Wagner). The authors ascribed the first thermal event to a cooling or uplift age of the Hercynian basement in Portugal. Kelly & Wagner related the second thermal event to the vertical Alpine faults which are filled by carbonates, sulphides and quartz. Fluid inclusions in these carbonates indicate temperatures between 100 and 140°C (Kelly & Rye, 1979).

MINERALOGY

In the mine several blocks can be distinguished, according to their mineralogical contents (Orey, 1967). Some minerals are found only in special areas, e.g. Ag-sulfosalts in Vale da Ermida.

Sampling of the ore specimens was restricted to the newer areas as some older areas are nowadays closed (Corga Seca, Vale da Ermida).

Generally, the ore veins contain a selvage of muscovite or topaz along the walls. Cassiterite, wolframite and arsenopyrite generally occur near the walls of the veins, in and on the muscovite and topaz selvages. Arsenopyrite is also found in the centre of the veins, together with chalcopyrite, sphalerite and pyrrhotite. The rest of the vein is filled by quartz.

Native elements

Orey (1967) reports native silver and gold in the ore veins but these elements were not observed in the present study. Although native silver is commonly found in galena in Vale da Ermida, it is lacking in the rest of the mine.

Native bismuth is common, it occurs in arsenopyrite and is associated with bismuthinite. It also occurs together with sphalerite and chalcopyrite.

Sulphides

Arsenopyrite

Arsenopyrite is a common mineral in the Panasqueira ore veins. It shows spectacular crystals up to 8 cm in size. Arsenopyrite was the first ore mineral which was deposited in the veins. Arsenopyrite without bismuth minerals preceded wolframite and cassiterite deposition but arsenopyrite with bismuth minerals is later (Orey, 1967). Arsenopyrite also occurs in the greisen and close to the veins in the Beira schist.

Bismuthinite

Bismuthinite is almost always associated with native bismuth. Together they occur as small spots in arsenopyrite, wolframite, sphalerite and chalcopyrite (Bloot & de Wolf, 1953; Orey, 1967; Clark, 1964, 1965a; Kelly & Rye, 1979). Bismuthinite is always later than bismuth.

Chalcopyrite

Chalcopyrite is at the moment the only sulphide of economic importance at Panasqueira. Although it is widely distributed in the veins, it mostly occurs with sphalerite and pyrrhotite. Exsolution stars of sphalerite are often found in the chalcopyrite, together with exsolution blebs of stannite and cubanite. Chalcopyrite also occurs with siderite, mostly in small crystals.

Analyses of chalcopyrite revealed a variable content in silver, mostly between 0.03 and 0.14% Ag. This silver is probably hosted within the chalcopyrite lattice because no silver minerals were observed.

Marcasite

Marcasite is an alteration product of pyrrhotite and is always accompanied by pyrite and sometimes siderite. Fine-grained aggregates of pyrite/marcasite often contain remnants of pyrrhotite. Marcasite also fills veinlets and occurs as separate crystals on older minerals, together with pyrite and siderite crystals.

Pyrite

Pyrite is formed as an alteration product of pyrrhotite but is also deposited together with sphalerite, chalcopyrite and pyrrhotite. The older pyrite crystals have no pyrrhotite relicts and are also not the fine-grained and irregular aggregates associated with marcasite. Pyrite deposition started with the sphalerite and pyrrhotite deposition and continued until after the siderite deposition.

Pyrrhotite

Pyrrhotite was once a common mineral in the veins but most of it is altered into a mixture of pyrite/marcasite with siderite, hematite and magnetite. Pyrrhotite occurs, not altered, as blebs and large spots exsolved in sphalerite and chalcopyrite, together with stannite.

Sphalerite

Sphalerite occurs in aggregates and large massive blocks, together with chalcopyrite, arsenopyrite and pyrrhotite. Within sphalerite exsolution blebs of chalcopyrite, stannite, pyrrhotite and cubanite occur. Sphalerite is older than siderite, marcasite and other pyrrhotite alteration products as they cover the sphalerite. Sometimes coatings of chlorite and oxy-chlorite are found on sphalerite. As the sphalerite is an iron-rich variety it is not recovered during flotation of the ore.

Stannite

Minor stannite occurrences are found, associated with chalcopyrite, sphalerite and pyrrhotite. It also occurs as an exsolution product within sphalerite and chalcopyrite. Within marcasite/pyrite alteration products, remnants of stannite can be found. Alteration of stannite locally produces intergrowths of needle tin, chalcopyrite and covellite (Orey, 1967). This alteration was not observed in the present study.

Other sulphides

Freibergite, pyrargyrite and stephanite occur in Vale da Ermida, together with acanthite and native silver. Apart from these minerals others are found in small quantities: stibnite, chalcocite, covellite, cubanite, gudmundite, loellingite, molybdenite, pentlandite and mackinawite (Thadeu, 1951; Clark, 1964, 1965a, 1965b; Orey, 1967).

Oxides

Cassiterite

Cassiterite crystals are mostly dark coloured, their size is about 1 cm but rarely exceeds 3 cm. In transmitted light cassiterite crystals show distinct zoning with clear and colourless bands. Cassiterite is one of the earliest vein minerals. It occurs along the walls of the veins, together with muscovite, arsenopyrite and topaz. The time relationship of the wolframite and cassiterite deposition is not clear. In some parts of the mine cassiterite-topaz veins are clearly earlier than wolframite-quartz veins. Hosking (1973) reports wolframite coated with cassiterite crystals. In cassiterite crystals strongly corroded

grains of rutile occur, especially in crystals at some distance from the cupola (Orey, 1967). The distribution of cassiterite in the veins is very irregular, Vale da Ermida, Alvoroso, Corga Seca and areas close around the greisen cupola are known for their increased cassiterite contents.

Iron oxides

Hematite and magnetite are associated with the pyrrhotite alteration. They are especially found in the pyrite/marcasite aggregates and sometimes with siderite.

Quartz

Quartz is the most abundant mineral in the veins. In vugs crystal length may reach about 40 cm. The crystals are often clear but may become cloudy at the bottom. This phenomenon is attributed to a high fluid inclusion content.

Quartz was deposited during several periods in the mineralization. Without doubt it was the first mineral formed in the quartz-cap and continued until the end of the sphalerite-chalcopyrite deposition. Deposition of the quartz was not continuous as muscovite flakes, tourmaline needles, mineral debris and small wolframite or cassiterite crystals mark several stages within a crystal. Two main periods of quartz deposition occur: one before wolframite-cassiterite deposition and another after the wolframite-cassiterite deposition until the end of the sphalerite-chalcopyrite deposition. Siderite, marcasite and dolomite are not covered by quartz.

Rutile

Rutile was found as strongly corroded grains within cassiterite in Vale da Ermida, Rebordões and Panasqueira. The rutile grains occur only in cassiterites at some distance from the greisen cupola (Orey, 1967).

Carbonates

Carbonates occur in the ore veins as well as in the vertical Alpine veins. Siderite and dolomite are the major carbonates, calcite and ankerite are rare (Kelly & Rye, 1979). Siderite, the most abundant one, is associated with pyrite and marcasite as it formed from iron release during the alteration of pyrrhotite (Kelly & Turneure, 1970). Siderite occurs as vein filling in older minerals but also as discrete

crystals up to 10 cm in size. Chalcopyrite may occur in these crystals. Dolomite and calcite were the last minerals to precipitate in the veins. They form small crystals on almost all other minerals.

Silicates

Chlorite/oxy-chlorite

Chlorite and oxy-chlorite appear as green-black coatings on sphalerite and siderite. It was deposited after the pyrrhotite alteration until the formation of calcite. According to Kelly & Rye (1979) late fluorite and chlorite show reversed age relations in different specimen.

Muscovite

Muscovite is a very common mineral in the ore veins at Panasqueira. It forms selvages up to 5 cm thick along the borders of the veins. But it also formed coatings on other minerals during ore deposition. Arsenopyrite, cassiterite, topaz, wolframite and fluorite are sometimes coated by thin muscovite layers. Sphalerite and chalcopyrite are not coated by muscovite, instead they corrode the older muscovite layers. Muscovite is also strongly concentrated in the so-called "eel-tails". Muscovite-filled eel-tails may continue as muscovite veinlets along mineralized joints. Veins with thick muscovite selvages also have a higher wolframite content (Orey, 1967), for which an explanation is still lacking.

Topaz

Kelly & Rye (1979) were the first to report topaz. Our findings indicate that topaz is a common mineral in the Rebordões and Barroca Grande sections of the mine where it crystallized along the walls. It forms light-green altered masses with clear crystal fragments. In the mentioned mine sections topaz forms the equivalent of early muscovite selvages. Topaz is corroded by muscovite of the later fluids.

In the mine a muscovite-topaz zoning occurs. Close to the greisen cupola muscovite is the more common mineral and at greater distances topaz is the dominant earlier mineral.

Tourmaline

Tourmaline is uncommon in the ore veins but occurs mainly as a metasomatic mineral in the wall-rock (Kelly & Rye, 1979). In the ore veins tourmaline occurs as brown, green or blue needles which concentrate along the walls of the veins. Other minerals like muscovite, apatite, sphalerite, siderite and calcite are suspended in and on these tourmaline needles (Kelly & Rye, 1979). Tourmaline needles also occur within quartz crystals and sometimes in the fluid inclusions. The deposition started together with the early muscovite selvages and probably continued until pyrrhotite deposition.

There are, however, also other varieties of tourmaline. Yellow, red and pink lithium tourmalines occur within a topaz-fluorite vein which happens to be vertical. The yellow, red, blue and pink tourmalines predate the more common brown tourmalines in veins and schist.

Other silicates

Beryl was described by Thadeu (1951) who found it in Corga Seca. Although beryl is rare, it is still found in veins in the Rebordões and Barroca Grande sections of the mine. Bertrandite was reported by Clark (1965b); it forms fine-grained crusts on beryl and apatite.

Phosphates

Apatite

Apatites from Panasqueira are known for their excellent crystal shape and size. The mineral is widespread in the veins and mainly occurs within vugs, together with cassiterite, wolframite, arsenopyrite, sphalerite and chalcopyrite. The crystals vary in colour from deep green to almost colourless in some growth zones. Other colours do occur but are rare. The size of the apatite crystals is mostly 1 to 3 cm but can increase up to 10 cm. The colourless zones within the apatite crystals fluoresce bright yellow under ultraviolet light (Blout & de Wolf, 1953; Kelly & Rye, 1979). According to Kelly & Rye (1979) apatite is contemporaneous with sphalerite and predates siderite deposition.

Other phosphates

Phosphates like althausite, isokite, vivianite and wolfeite were reported by Kelly & Rye (1979) and the new minerals thadeuite and panasqueiraite by Isaacs et al. (1979, 1981). The triplite of Gaines & Thadeu (1971) was probably wolfeite, together with wagnerite. All these phosphates (apart from vivianite) occur together and are closely related to the topaz selvages.

Tungstates and arsenates

Wolframite

Wolframite is the principal ore mineral at Panasqueira. Its main composition is ferberite but some specimen do have a more wolframitic composition. Crystal size can be as large as 30 cm but the common length is between 5 and 15 cm. Radiating groups of wolframite crystals are normally found in and on the muscovite and topaz selvages. Isolated and corroded crystals occur within the vein mass. Cassiterite is slightly older than wolframite as wolframite-quartz veins split off from cassiterite-topaz veins. Some cassiterite is contemporaneous with wolframite; Hosking (1973) reports wolframite crystals from Panasqueira coated by cassiterite crystals. The vugs in the ore veins often contain spectacular crystal groups of arsenopyrite, wolframite, quartz, apatite and siderite.

Hubnerite/ferberite ratios of wolframites have been investigated by Saraiva (1971). The hubnerite/ferberite ratio increases towards the Panasqueira greisen cupola. The variance within a single wolframite crystal, however, was just as large as in the entire vein system. No systematical trend from core to rim could be detected in the wolframite crystals.

Scheelite

Clark (1965b) reported scheelite as a weathering product on the mine dumps of Rebordões. Recently, scheelite was discovered in the tungsten-tin veins. This occurrence is restricted to a vein which crosscuts a very thick (35 m) dolerite dyke (R. de Barros, pers. comm. 1981). The stability of scheelite in the veins is restricted by the

low CaO content of the schist (about 0.30% CaO) and by the occurrence of phosphates and fluorite. The pre-ore dolerite dyke was the only source for the excess CaO. Unfortunately, no exact place within the paragenesis can be given for this scheelite.

Other tungstates and arsenates

Clark (1965b) reports scorodite, tungstite and hydrotungstite from the dumps. Scorodite was also discovered in the mine on strongly corroded arsenopyrite masses.

Fluorite

Fluorite is the only halide mineral, it is rare in the vein system but locally it is concentrated. In Vale da Ermida it was known for its large size up to 7 cm (Thadeu, 1951; Gaines & Thadeu, 1971). According to these authors fluorite is a late stage mineral which crystallized after siderite but before the calcite deposition (Kelly & Rye, 1979). There is also an earlier generation of fluorite in the vein system. It occurs in some extreme sections of the mine. This fluorite generation was common which is confirmed by many perfect cubic-shaped hollow coatings in siderite. Some of these early fluorites are strongly corroded, leaving only hollow skeletons. This fluorite was dissolved by later fluids or perhaps even remobilized. In some mine sections this early fluorite is still preserved. It forms blue, green and pink crystals on wolframite, topaz and muscovite. Fluid inclusions in this fluorite generation give much higher homogenization temperatures in this study than reported by Kelly & Rye (1979).

VEIN PARAGENESIS

The paragenesis of the tungsten-tin veins at Panasqueira is rather complex. The main problem is the time correlation between minerals within the ore veins in different areas of the mine. Another problem is the occurrence of minerals only in restricted parts of the mine (Orey, 1967). Vale da Ermida, for instance, was known for its unusual paragenesis with silver minerals. Several authors gave mineral sequences for the Panasqueira mine. The paragenesis given here

STAGES

- I Opening
- II Oxide-silicate
- III Main sulphide
- IV Pyrrhotite alteration
- V ?
- VI Late carbonate

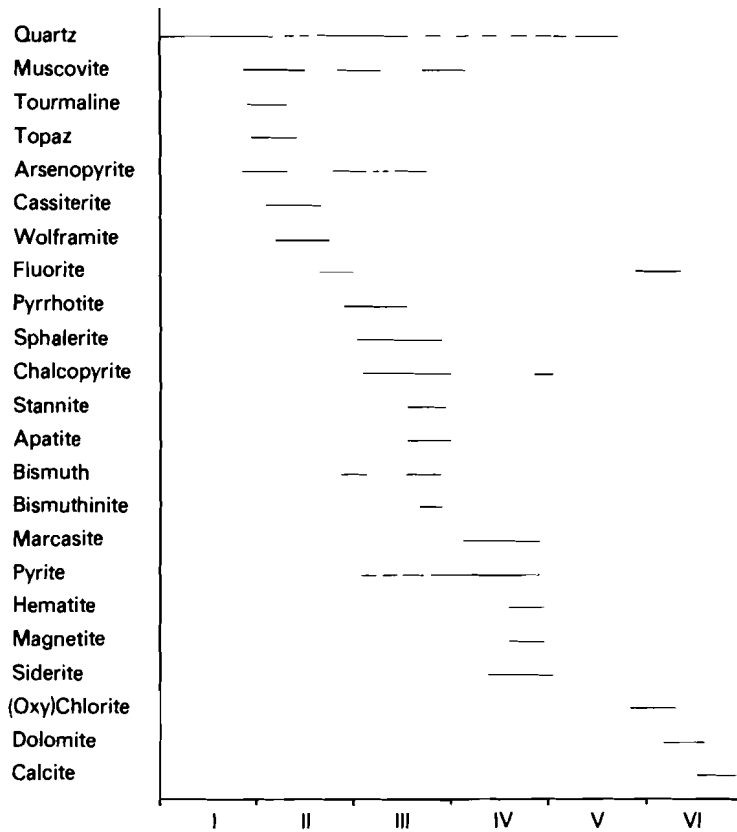


Fig. 1. Mineralization stages in the Panasqueira and Barroca Grande sections of the Panasqueira mine.

(Fig. 1) is a combination of the work of these authors (Thadeu, 1951; Bloot & de Wolf, 1953; Clark, 1964, 1965a; Orey, 1967; Kelly & Rye, 1979) with additional data of the present work. Vale da Ermida and Corga Seca are excluded from the paragenesis as these parts of the mine are no longer accessible. In the veins five principal stages can be recognized:

Opening stage

This stage started with filling of the quartz-cap and opening of the vein system. Quartz was deposited together with some arsenopyrite, wolframite and possibly cassiterite.

Oxide-silicate stage

This is the economically most important period in the vein system. During this period muscovite, topaz, quartz, wolframite, cassiterite and arsenopyrite were deposited. The oxide-silicate stage started with muscovite and topaz selvages, followed by intergrowths of coarse quartz, muscovite, topaz, cassiterite, wolframite, fluorite and arsenopyrite. The rare Ca-Mg-Fe phosphates are found in and close to these topaz selvages. Muscovite growth zones in quartz crystals are an indication of several periods of growth. The first muscovite generation forms selvages on the walls, the second one forms coatings on quartz, wolframite, cassiterite and late arsenopyrite. Muscovite can show a reversed age relationship with the other minerals. Wolframite, cassiterite and arsenopyrite are early minerals, they all form euhedral crystals in the veins. Deposition of tourmaline started together with the muscovite selvage and probably diminished during the oxide-silicate stage.

Main sulphide stage

This stage started with the deposition of arsenopyrite, together with chalcopyrite, sphalerite, pyrrhotite and possibly some pyrite. The sulphides mostly filled the vugs in the veins. Sphalerite and chalcopyrite exsolved variable amounts of stannite, sphalerite, chalcopyrite and pyrrhotite. Again some quartz was deposited. During the main sulphide stage the famous green apatites of Panasqueira were formed.

Pyrrhotite alteration stage

In this stage pyrrhotite was thoroughly altered by the later fluids into porous pyrite and marcasite aggregates. By-products were siderite, hematite and magnetite. The euhedral siderite crystals are somewhat later than pyrite and marcasite; they sometimes contain chalcopyrite crystals.

Late carbonate stage

Siderite deposition is much later followed by a late carbonate stage. Dolomite is the major mineral during this period. Dolomite formed rims on the siderite crystals (Kelly & Rye, 1979). Deposition of the late fluorite and chlorite followed. Calcite was the last mineral formed in the veins. It occurs as small crystals on all other minerals. Pyrite deposition continued until this last stage.

PREVIOUS WORK

The results of the extensive work of Kelly & Rye (1979) will be briefly reviewed below.

Fluid inclusions

Three inclusion types are distinguished:

Type I inclusions are water-rich with a gas phase of 10 to 30 vol% CO₂.

Type II inclusions are gas-rich and contain 70 to 80 vol% CO₂.

Type III inclusions are water-rich and contain a small gas bubble, normally less than 5 vol%.

The association of type I and II inclusions, close to each other in the same crystal, indicates boiling of the ore fluids. Boiling was especially found in Corga Seca, Vale da Ermida and around the greisen cupola.

Homogenization temperatures of fluid inclusions range from 365°C in the quartz-cap to 250°C in the pyrrhotite alteration stage. Homogenization temperatures in the late carbonate stage are much lower,

about 150°C for fluorite and between 120 and 80°C for dolomite and calcite.

Salinities of the early stages range from 5 to 10 wt% NaCl; the late carbonate stage has lower salinities of about 3 wt% NaCl. Kelly & Rye (1979) did electron microscope studies on evaporites from opened type I inclusions and showed that the salts were predominantly NaCl with small amounts of KCl.

Pressures in the hydrothermal ore veins were about 80 to 150 bar from the oxide-silicate stage to the pyrrhotite alteration stage. The oxide-silicate stage started with much higher pressures, up to about 900 bar. In the late carbonate stage pressures were about 60 bar. From the pressure in the fluids, obtained from boiling type I and II inclusions, a mineralization depth of 660 to 1300 m was calculated.

Sulphur isotopes

Sulphides of the opening, oxide-silicate, main sulphide and pyrrhotite alteration stage all show a narrow range of $\delta^{34}\text{S}$ values from -0.9 to 2.0 per mil. This narrow range indicates a single homogeneous sulphur source and H_2S dominant fluids (Ohmoto & Rye, 1979). The estimated $\delta^{34}\text{S}$ values of the fluid are typical for sulphur derived from igneous sources.

Sulphides of the late carbonate stage show a much wider range of $\delta^{34}\text{S}$ values from -13 to +12 per mil. The large spread may be caused by non-homogeneous sources, e.g. the Beira shales.

Oxygen isotopes

The $\delta^{18}\text{O}$ values of quartz, muscovite, cassiterite, wolframite, siderite, dolomite and calcite were used to calculate the $\delta^{18}\text{O}$ values of the fluids. During the opening, oxide-silicate, main sulphide and pyrrhotite alteration stages $\delta^{18}\text{O}$ values of the fluid were 6 ± 2 per mil. These values reflect magmatic and/or highly exchanged meteoric water. The $\delta^{18}\text{O}$ values of the fluids of the late carbonate stage range from 4 to -4 per mil and indicate a dominant meteoric water component in the fluid.

Carbon isotopes

The $\delta^{13}\text{C}$ values of the carbonates range from -8 to -14 per mil. The $\delta^{13}\text{C}$ values of CO_2 from fluid inclusions in quartz are between -9.3 and -10.8 per mil. The relatively low values possibly indicate an exchange with organic matter of the Beira shales.

Hydrogen isotopes

The δD values of the Panasqueira fluids fluctuate between -40 and -124 per mil and are contradicting. Some sulphide minerals and cassiterite gave values as low as -124 per mil whereas contemporaneous other minerals showed values of -40 to -70 per mil. A serious problem with hydrogen isotopes is furthermore that the δD ranges of meteoric and magmatic waters overlap.

METHODS USED IN THIS STUDY

Doubly polished plates, 1 mm thick, were used to study the fluid inclusions in mineralized quartz veins, quartz-cap and greisen. Heating and freezing runs were made with the Chaixmeca stage described by Poty et al. (1976). Calibration was done on the triple point of CO_2 in natural inclusions. Artificial standards were also used, mercury, distilled water, NaNO_3 and Merck organic standards.

For a quantitative check of the gas composition in fluid inclusions, several minerals were crushed under vacuum in steel tubes. The techniques for crushing, gas analyses and stable isotope measurements are summarized in Kreulen & Schuiling (1982). A blank analysis, showing background levels in the analytical procedure was obtained by crushing inclusion-free quartz. The water content was not determined because of the strong adsorption effects. Apart from CO_2 , CH_4 and N_2 , Ar was also detected. CO was not detected in the samples and Ar was close to the detection limit. Small amounts of oxygen were also found but are ascribed to air leakage during sample handling. The amount of oxygen was used to correct the nitrogen quantity for air leakage but

such corrections were minor in most cases.

CO₂ from carbonates was prepared with H₃PO₄ according to McCrea (1950). Oxygen for isotope determination was prepared through reaction of silicates with BrF₅ at temperatures around 550°C (Clayton & Mayeda, 1963). Standard sample NBS 28 gave a δ ¹⁸O value of 9.25 per mil with a CO₂-H₂O fractionation of 1.0412, in good agreement with data of Ito & Clayton (1983).

Nitrogen isotopes were measured in N₂ liberated from the fluid inclusions by decrepitation at about 900°C in the presence of CuO to oxidize methane. Excess oxygen was removed by slowly cooling to about 700°C whereby CO was converted into CO₂. Nitrogen was collected in small sample bottles with Porapak-Q at liquid nitrogen temperatures. CO₂ was collected to determine the total carbon composition of the fluids.

FLUID INCLUSIONS

Crystals in the veins are well suited for fluid inclusion studies. Fluid inclusions were studied in quartz, cassiterite, fluorite, topaz, apatite and siderite.

Before heating or freezing, inclusions were optically studied and classified. Criteria for primary, secondary and pseudo-secondary inclusions were used according to descriptions by Roedder (1979). Most of the primary inclusions are large and occur randomly distributed in their host mineral or are correlated with growth zones. Many inclusions occur in trails and bands and are classified as secondary or pseudo-secondary.

Inclusion types

In the Panasqueira minerals three major types of fluid inclusions can be recognized:

Type I inclusions are water-rich with a CO₂ phase (liquid and/or gas) which occupies 10 to 35 vol% (Fig. 2a). This inclusion type homogenizes by solution of the CO₂ into the

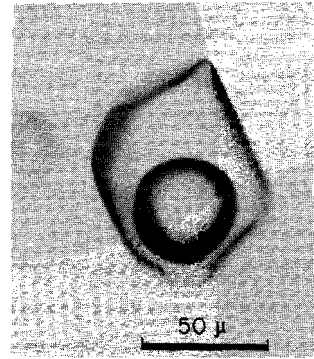
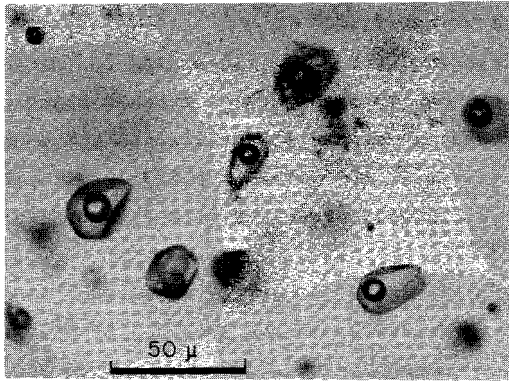


Fig. 2a Type I inclusions with 10 - 35 vol% CO₂.

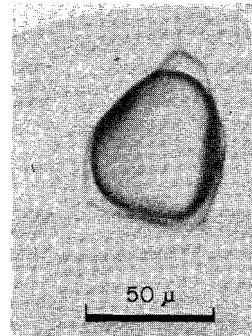
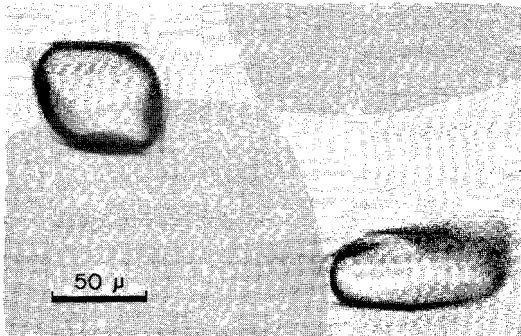


Fig. 2b Type II inclusions with 70 - 80 vol% CO₂.

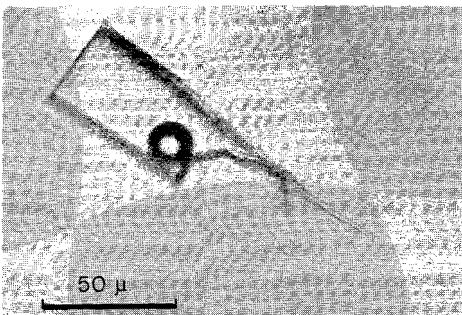


Fig. 2c Type III inclusions with less than 5 vol% vapour

aqueous phase.

Type II inclusions are CO₂-rich and contain 70 to 80 vol% CO₂ (liquid and/or gas) (Fig. 2b). Upon heating these inclusions homogenize by evaporation of the aqueous phase.

Type III inclusions are water-rich with a small gas bubble, normally less than 5 vol% (Fig. 2c).

Type I and III inclusions can be found in all minerals at Panasqueira. Type II inclusions were found in quartz, fluorite and topaz.

Various daughter minerals and captives were observed in type I and III inclusions. Captives occur in the host crystal but also partly or completely within the fluid inclusions. The captives are muscovite, tourmaline needles, ore particles and other unknown phases. Halite daughter minerals occur in late high-salinity type III inclusions.

Occurrence of fluid inclusions

Quartz

Several quartz crystals contain growth zones which are delineated by muscovite flakes. Sometimes these growth zones contain wolframite crystals parallel to it. Such samples help establishing time relations between fluid inclusions and ore deposition. Type I inclusions are the major type of inclusions, they are primary, pseudo-secondary and secondary inclusions. These inclusion types may all show negative crystal shapes.

In some quartz crystals, especially crystals of the oxide-silicate stage, primary and pseudo-secondary type II inclusions occur. They are always associated with the primary type I inclusions. Some inclusions contain intermediate compositions, probably as a result of trapping of non-homogeneous fluids during boiling (see below). Homogenization temperatures of these inclusions are much higher (above 400°C) than those of the associated type I and II inclusions. The association of type I and II inclusions suggests that the ore fluids were "boiling" during the oxide-silicate stage (see below). Later mineralization stages lack the occurrence of type II inclusions. According to Kelly &

Rye (1979) the associated type I and II inclusions are abundant at Vale da Ermida, Corga Seca and close to the greisen cupola. The associated type I and II inclusions are also common in the rest of the vein system.

Along the ore veins small quartz veinlets occur (about 3 mm thick) which contain an association of liquid CO₂-rich type I and II inclusions. These early veinlets are the first indications of vein formation and are related to the quartz-cap. The quartz-cap and its fluid inclusions will be discussed separately.

Fluorite

Fluorite crystals contain excellent fluid inclusions. Colour zoning is common; blue, violet and purple zones alternate with colourless zones.

The first generation of fluorite shows the normal type I inclusions with about 20 to 25 vol% gas. Type II inclusions may occur in this early fluorite. Both types have homogenization temperatures which fit in the oxide-silicate stage (Fig. 3). The second generation of fluorite contains type III inclusion. Homogenization temperatures are much lower than those of the earlier generation.

Topaz

Fluid inclusions in topaz are mostly type I and sometimes type II; type I inclusions contain several large daughter minerals which did not dissolve upon heating. The time of entrapment of these inclusions is uncertain but is probably pseudo-secondary.

Apatite

Primary inclusions in apatite crystals can be related to zoning. These inclusions are type I but their shape is very irregular. They display curved shapes and tabular extensions which could indicate some form of necking-down (Kelly & Rye, 1979). But all these primary inclusions along growth zones gave about the same homogenization temperatures and salinities. Trails with pseudo-secondary inclusions crosscut these growth zones.

Siderite

Inclusions in siderite are mainly type I. Due to the perfect cleavage of siderite many inclusions leaked during the heating runs. Many fluid inclusions in siderite follow the cleavage planes in the host, thus

criteria for primary or secondary origin could not be made. Secondary inclusions crosscut all other zones or cleavage planes. These inclusions contain a small gas phase and belong to the late low-salinity type III inclusions. Kelly & Rye (1979) reported acanthite in siderite with attached fluid inclusions.

Calcite

As the last mineral in the tungsten-tin mineralization calcite only contains the low-salinity type III inclusions (Kelly & Rye, 1979).

Quartz-cap

Quartz crystals are milky white due to their fluid inclusion content. Almost all inclusions are type I and II. Type III inclusions are rare. The difference between type I and II inclusions in the quartz-cap compared with those in the tungsten-tin veins, is their higher CO₂ density. Instead of gaseous CO₂, liquid CO₂ is the major gas phase at room temperature. Most type I and II inclusions are randomly distributed in quartz and are probably primary (Roedder, 1979), although pseudo-secondary and secondary inclusions occur.

Greisen cupola

Large quartz grains in the greisen have similar inclusion contents as the ore veins. Associated type I and II inclusions with liquid and/or gaseous CO₂ are common and might be primary although no proof can be given. Inclusions of magmatic origin were not observed, they were probably destroyed during the intense greisenization of the uppermost part of the granite. Kelly & Rye (1979) report magmatic inclusions (solidified melt) in zircons.

Metamorphic quartz

According to Kelly & Rye (1979) fluid inclusions in the Seixo Bravo quartz masses are different in composition. No heating or freezing runs were performed on the small inclusions in the quartz masses.

Homogenization temperatures

The large size of the Panasqueira fluid inclusions is an advantage in freezing runs but a handicap in heating runs as inclusions with high CO₂ densities often explode before they homogenize. Only small type I

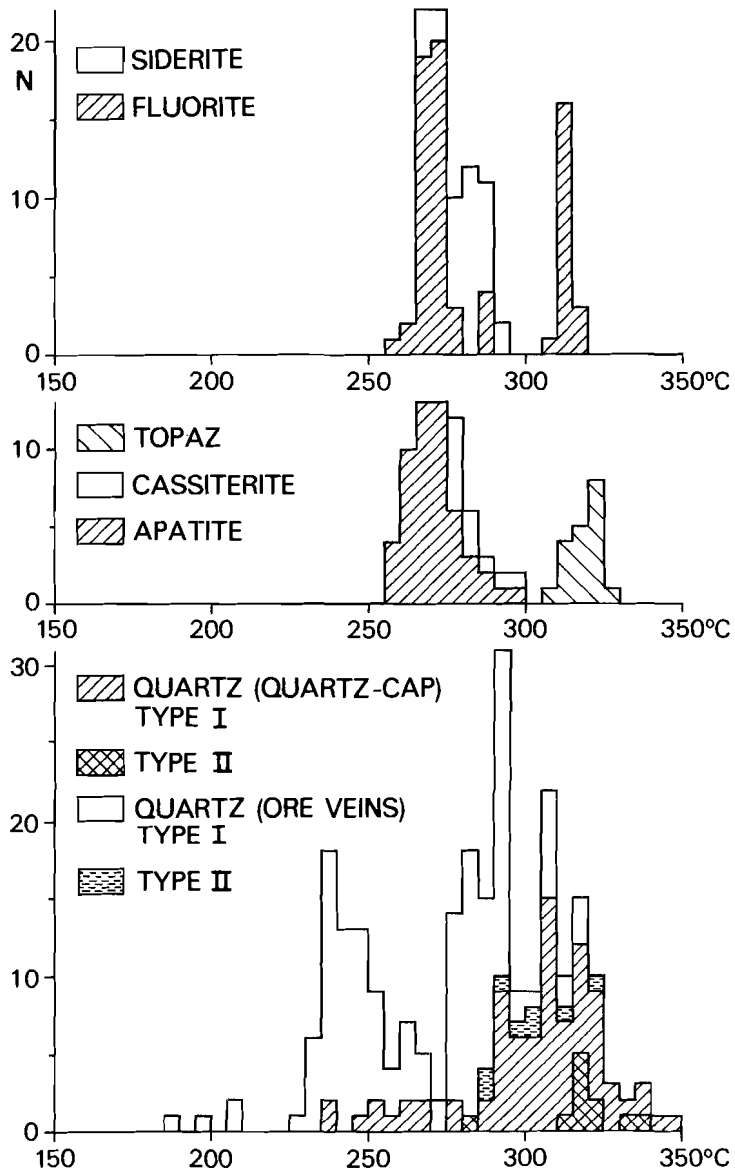


Fig. 3. Homogenization temperatures in quartz, topaz, fluorite, cassiterite, apatite and siderite.

and II inclusions with liquid CO₂ could be homogenized. Explosion of large inclusions often resulted in destruction of the sample plate. This fact points to a high internal pressure during heating runs in this type of fluid inclusion. Homogenization temperatures of type II inclusions are not accurate as the exact moment at which the vapour phase fills the entire inclusion is difficult to recognize.

Homogenization temperatures of fluid inclusions in various minerals are given in Fig. 3. Temperatures in the quartz-cap vary between 305 and 330°C. During the oxide-silicate stage temperatures ranged from 325°C in topaz to 280°C in quartz with wolframite. In the main sulphide and pyrrhotite alteration stages homogenization temperatures range from 250 to 285°C in apatite and siderite. Homogenization temperatures in the late carbonate stage range from 150°C in fluorite to 100°C in dolomite and perhaps calcite (Kelly & Rye, 1979).

Almost no minerals were deposited between the pyrrhotite alteration and late carbonate stage. Only some clear quartz, with very few fluid inclusions, is found between these stages with homogenization temperatures of 170 to 220°C.

Salinities

Salinities of the fluid inclusions are given in Fig. 4. If necessary, they were corrected for the presence of the CO₂-hydrate (Collins, 1979). Type I inclusions in the quartz-cap and ore veins have salinities of 6 to 8 wt% NaCl. During boiling in the oxide-silicate stage, salinities increase to about 10 wt% NaCl. Later fluids are more diluted, their salinities decrease to about 3 wt% NaCl for the low-salinity type III inclusions.

Salinities of type II inclusions can not be measured accurately as CO₂ reacts with water to form the CO₂-hydrate, increasing the salinity of the remaining water phase. However, melting points are close to zero and indicate very low salt contents.

LAMMA mass-spectrometer analyses (Gijbels, pers. comm., 1981) were done on some opened type I inclusions and confirm the analyses by Kelly & Rye (1979). The composition is mainly NaCl with some KCl; calcium and magnesium are below the limit of detection but rubidium and cesium

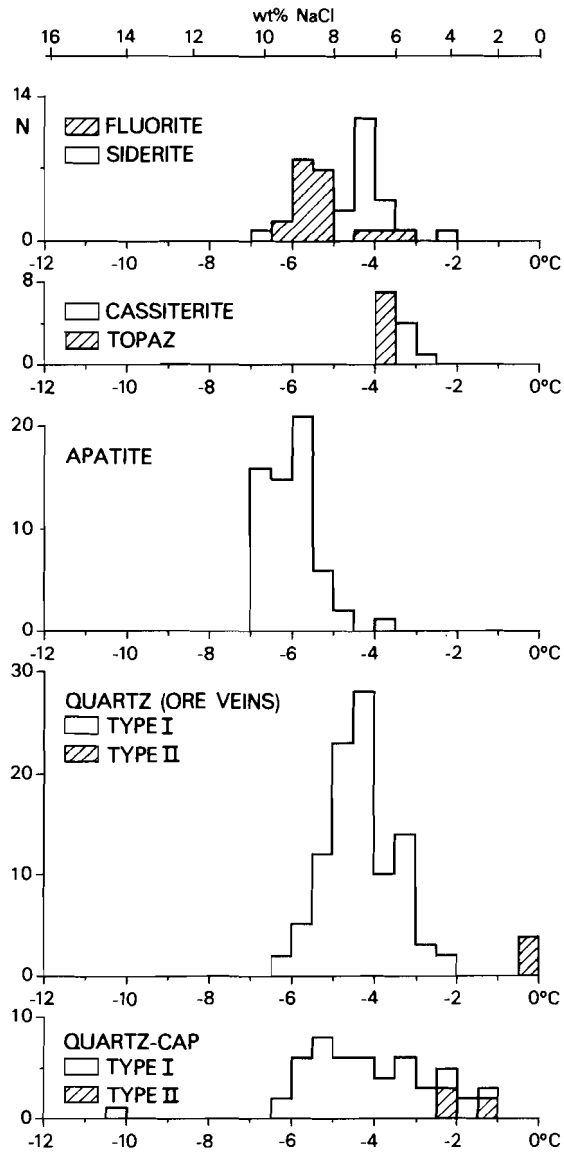


Fig. 4. Melting temperatures of ice in quartz, topaz, fluorite, cassiterite, apatite and siderite.

were detected. This interesting fact is corroborated by rubidium and cesium anomalies in the wall rock of the veins (see Chapter 3).

High salinity type III inclusions with homogenization temperatures between 80 and 160°C may contain a halite cube. First melting temperatures of the ice are between -60 and -30°C indicating Na-K-rich fluids with Ca and/or Mg (Roedder, 1963). Salinities vary between 15 and 45 wt% equivalent NaCl. These type III inclusions are probably not related to the tungsten-tin veins. They may belong to the late Alpine(?) vertical faults which cut through the tungsten-tin veins.

Carbondioxide content

The fluid inclusion studies indicate the presence of CH₄ and N₂, apart from CO₂. Melting points of CO₂ range from -57 to -62°C (Fig. 5) which indicates 7 to 30% CH₄ relative to CO₂ (Swanenberg, 1979; Heyen et al., 1982). Upon cooling to -150°C liquid methane was formed in some inclusions, especially in the CO₂-rich type II. The type I and II inclusions in the oxide-silicate stage contain more CH₄ than similar inclusions in the quartz-cap. In the later type I inclusions CO₂ and especially CH₄ are less conspicuous, solid CO₂ in these inclusions was difficult to detect and "evaporated" at temperatures between -60 and -57°C.

Temperatures of homogenization of CO₂ into the liquid or the gas phase, not given by Kelly & Rye (1979), were used to estimate CO₂ densities which were corrected for the presence of CH₄ (Swanenberg, 1979; Heyen et al., 1982). Densities of CO₂ in the ore veins range from 0.06 to 0.11 g/cm³. Type I inclusions contain 0.5 to 2 mol% CO₂ and type II inclusions 6 to 10 mol% CO₂.

Fluid inclusions in the quartz-cap are different in that they contain liquid CO₂ instead of gaseous CO₂, reflecting much higher densities. Densities of CO₂, corrected for CH₄, are mostly 0.2 to 0.9 g/cm³. CO₂ concentrations in the quartz-cap are 5 to 17 mol% CO₂ for type I and 33 to 68 mol% CO₂ for type II inclusions.

The presence of CO₂ is also confirmed by the formation of hydrate during freezing runs. Melting of hydrate (Fig. 6) is difficult to observe but if solid phases are present they start moving in the

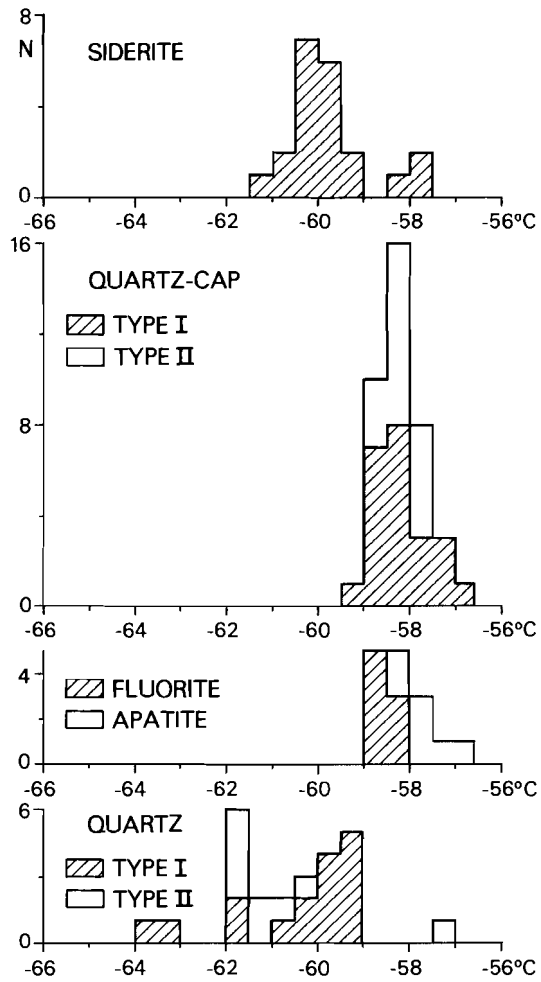


Fig. 5. Melting temperatures of CO₂ in quartz, apatite and siderite.

inclusions, probably during the last melting of the hydrate.

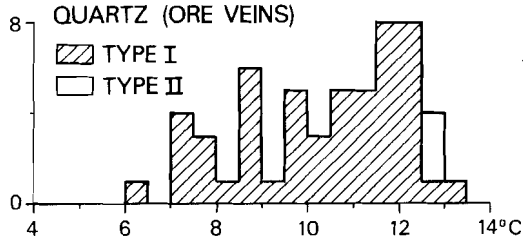
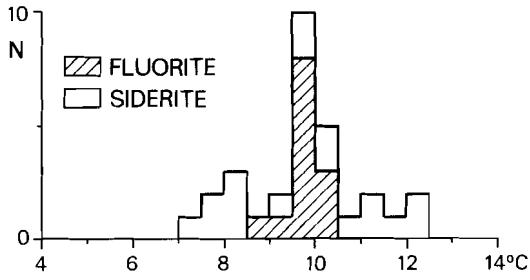
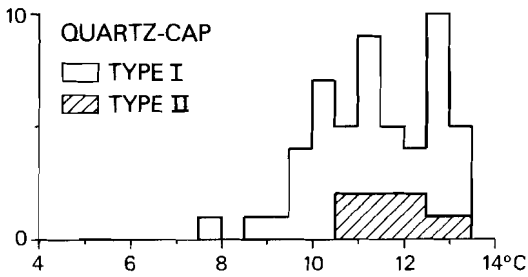


Fig. 6. Melting temperatures of CO₂-hydrate.



GAS COMPOSITIONS

Analyses by gaschromatography are given in Fig. 7 and Table I. The main constituents are CO₂, CH₄ and N₂. Water was not measured as earlier experiments indicated unreliable results caused by adsorption. Quartz, wolframite, siderite and topaz samples fall in restricted composition fields; the quartz samples are from the quartz-cap and ore veins. Total gas contents fluctuate strongly in these samples but their composition remains virtually constant. Later fluids in siderite have similar gas compositions as quartz, wolframite and topaz, but some samples have lower CH₄ contents.

Table I: Gas analyses and $\delta^{13}\text{C}$ values of CO_2 from fluid inclusions.

Sample nr.		% CO_2	% N_2	% CH_4	$\delta^{13}\text{C}$ of CO_2	Sample nr.		% CO_2	% N_2	% CH_4	$\delta^{13}\text{C}$ of CO_2
PQ 13	Seixo Bravo	48	20	32	-6.1	PQ 31	Quartz	50	17	33	-9.3
PQ 14	Seixo Bravo	56	20	24	-5.2	PQ 36	Quartz	77	12	11	-8.0
PQ 30	Seixo Bravo	56	19	25	-8.9	PQ 38	Quartz	24	42	34	
PQ 520	Greisen	49	17	34	-12.0	PQ 44	Quartz	60	19	21	-10.0
PQ 521	Greisen	9	17	74	-4.4	PQ 45	Quartz	82	10	8	-9.3
PQ 522	Greisen	49	12	39		PQ 47	Quartz	70	14	16	-7.2
PQ 523	Greisen	15	33	52		PQ 48	Quartz	80	12	8	
PQ 524	Greisen	45	13	42	-6.4	PQ 51	Quartz	81	12	7	-10.3
PQ 524	Greisen	54	13	33	-6.0	PQ 54	Quartz	82	8	10	-11.3
PQ 525	Greisen	23	19	58	-7.2	PQ 56	Quartz	81	11	8	-8.7
PQ 37b	Topaz	76	12	12	-9.0	PQ 60	Quartz	82	11	7	-10.3
PQ 76	Topaz	73	14	13	-10.5	PQ 61a	Quartz	82	11	7	-11.8
PQ 76	Topaz	74	15	11	-9.2	PQ 70	Quartz	74	15	11	-9.7
PQ 76-2	Topaz	70	16	14	-10.6	PQ 71	Quartz	76	12	12	-7.5
PQ 72	Arsenopyrite	39	15	46		PQ 71	Quartz	82	10	8	-9.6
PQ 72	Arsenopyrite	46	9	45	2.9	PQ 71	Quartz	83	10	7	-8.2
PQ 105	Arsenopyrite	30	26	44		PQ 73	Quartz	77	11	12	-8.3
PQ 204	Arsenopyrite	4	17	79		PQ 75	Quartz	88	8	4	-9.1
PQ 207	Arsenopyrite	15	15	70		PQ 79	Quartz	71	13	16	-10.8
PQ 211	Arsenopyrite	20	11	69	-10.9	PQ 83	Quartz	80	12	8	-9.0
PQ 227	Arsenopyrite	5	8	87		PQ 233	Quartz	54	25	21	-3.7
PQ 229	Arsenopyrite	10	13	77		Quartz Vale da Ermida	66	21	13	-7.5	
PQ 234	Arsenopyrite	21	7	72		PQ 27b	Chalcopyrite	7	23	70	
Wolframite 1		70	9	21	-4.4	PQ 206	Chalcopyrite	35	15	50	2.4
Wolframite 2		74	10	16	-4.7	PQ 209	Sphalerite	31	18	51	0.7
Wolframite 3		75	8	17	-4.6	PQ 209-2	Sphalerite	28	18	54	0.1
PQ 27c	Wolframite	72	12	16	-4.6	PQ 213	Sphalerite	21	10	69	2.2
PQ 199	Wolframite	69	15	16	-4.8	PQ 213-2	Sphalerite	11	12	77	-4.7
PQ 200	Wolframite	63	15	22	0.1	PQ 213-2	Sphalerite	19	13	68	-4.7
PQ 201	Wolframite	64	13	23	-1.3	PQ 96-3	Marcasite	86	8	6	-19.6 ++
PQ 202	Wolframite	64	13	23	-0.5	PQ 96-3-2	Marcasite	42	26	32	
PQ 214a	Wolframite	67	14	19	-3.7	PQ 96-3-3	Marcasite	40	31	29	
PQ 214b	Wolframite	69	15	16	-4.0	PQ 27c	Siderite	83	16	1	
PQ 214b-2	Wolframite	69	15	16	-4.1	PQ 38	Siderite	79	20	1	
PQ 12	Quartz	72	14	14	-10.6	PQ 205	Siderite	78	11	11	
PQ 21d	Quartz	73	15	12	-11.5	PQ 208	Siderite	79	14	7	
PQ 26	Quartz	53	23	24	-9.1	PQ 226	Siderite	65	21	14	
PQ 28	Quartz	78	13	10	-8.6						

++ Sample heated up to about 150°C.

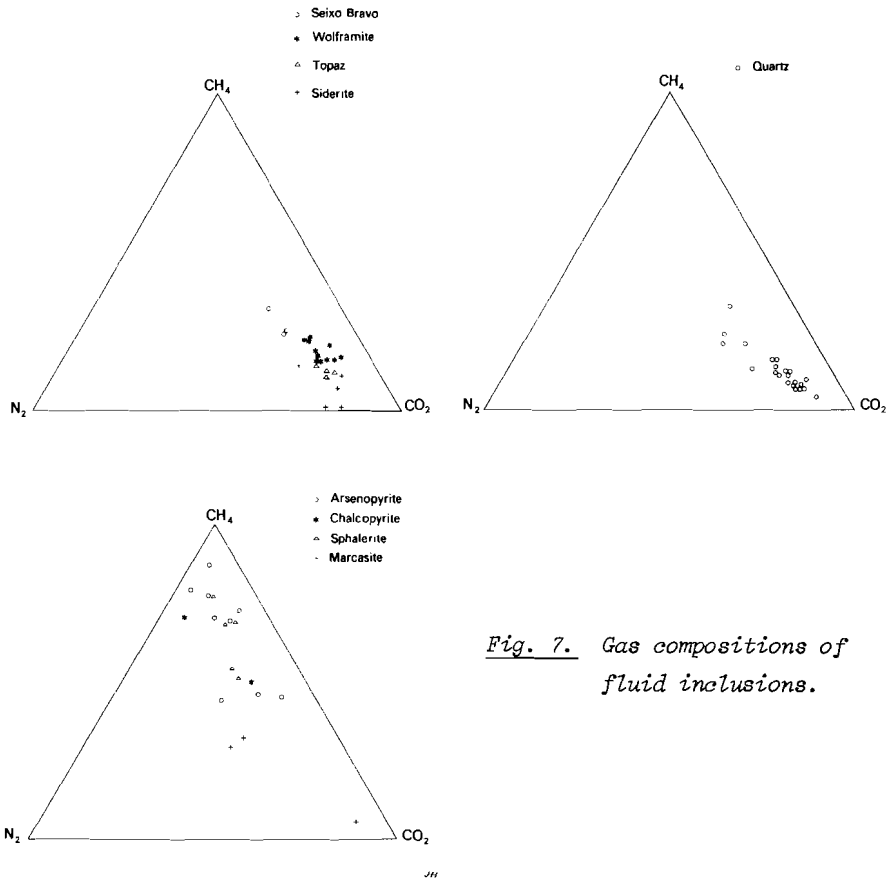


Fig. 7. Gas compositions of fluid inclusions.

Sulphides gave different results; they scatter towards a CH₄-rich fluid. No systematics could be found from the early arsenopyrite to the late marcasite. It is interesting to note that Kelly & Rye (1979) measured hydrogen isotopes of fluid inclusions in sulphides; their results are also not in agreement with the stable isotope measurements of the other minerals.

The introduced shift of the sulphides and greisens towards a more CH₄-rich fluid is probably due to adsorption effects of CO₂ (and some N₂?) on the newly created surfaces. This effect is often enhanced by the low gas contents obtained during crushing. Heating of sulphides to

about 150°C releases CO₂ and the gas composition plots in the field for simultaneously formed quartz and/or wolframite. However, the isotopic composition of the released CO₂ shifts to more negative values compared to quartz (see stable isotope section) which is an indication for adsorption of CO₂. Therefore, the gas analyses as well as the isotopic composition of the sulphides and greisens were rejected.

DISCUSSION OF FLUID INCLUSION DATA

Gas compositions

The analyses of gases from quartz, topaz, wolframite, siderite and "Seixo Bravo" indicate the presence of CO₂, CH₄ and N₂ (Fig. 7). Quartz, topaz, wolframite, Seixo Bravo and siderite occupy restricted composition fields. The main gas composition of fluid inclusions in quartz, topaz and wolframite is about 65-80% CO₂, 10-20% CH₄ and 10-17% N₂. Seixo Bravo quartz is more CH₄-rich than quartz of the mineralized veins. This Seixo Bravo probably represents the fluid composition during the regional metamorphism but with an additional influence of the ore veins. Some quartz samples of the ore veins fall in the field of Seixo Bravo quartz, probably caused by a strong influence of the host rock along the veins. The content of CH₄ in later fluids in siderite is about the same as in quartz although some siderite samples contain lower amounts of CH₄, down to 0.1%.

Gas analyses of wolframite show slightly more CH₄ than simultaneously formed quartz (Fig. 7). Although the increase in CH₄ is small, it may indicate a more CH₄-rich fluid during deposition. On the other hand, the $\delta^{13}\text{C}$ values of CO₂ from wolframite are lower than those of quartz and may suggest some adsorption effects of wolframite.

The origin of the CH₄ is probably found in the Beira schists. About 0.2% organic matter occurs in the shales and assimilation of the shales causes an addition of CH₄, CO₂ and possibly also N₂ to the CO₂ of the granite. The rather constant C/N ratio and composition of the fluids indicate that mixing occurred at much deeper levels. The fluctuations

of the CO_2/CH_4 ratio of the fluids may have been caused by local inhomogeneity in the veins, combined with reactions with the host rock or influx of airated water.

The presence of CH_4 in the fluid indicates a reducing environment during ore deposition. This is also reflected in the mineralogy; only in the pyrrhotite alteration stage hematite and magnetite occur which could indicate an increase of the CO_2/CH_4 ratio.

Boiling of the ore fluids

Immiscibility in fluid systems is a common phenomenon (e.g. Roedder & Coombs, 1967; Kelly & Turneaure, 1970; Landis & Rye, 1974; Rye & Sawkins, 1974; Ramboz, 1980; Pichevant et al., 1982; Ramboz et al., 1982). The association of two inclusion types, one homogenizing into the liquid phase and the other homogenizing into the gas phase, both at the same temperature, suggests immiscibility or "boiling". Trapping of these inclusion types occurred simultaneously in the same crystal, close to each other. Some inclusions trapped non-homogeneous fluids having gas/liquid ratios in between those of type I and II inclusions and homogenization temperatures above 400°C . Heterogeneous trapping is also a good evidence of fluid immiscibility (Ramboz et al., 1982).

The two immiscible fluid phases in the mineralized veins, trapped in inclusions of types I and II, have the following characteristics:

Type I	Type II
$T = 290 - 325^\circ\text{C}$	$T = 290 - 325^\circ\text{C}$
$D_{\text{fluid}} = 0.81 \text{ g/cm}^3$	$D_{\text{fluid}} = 0.26 \text{ g/cm}^3$
NaCl 8 - 10 wt%	NaCl < 0.5 wt%
$d_{\text{CO}_2} = 0.07 - 0.11 \text{ g/cm}^3$	$d_{\text{CO}_2} = 0.09 - 0.12 \text{ g/cm}^3$
$X_{\text{CH}_4} = 0.05 - 0.07$	$X_{\text{CH}_4} = 0.10 - 0.12$
$\text{CO}_2 = 0.5 - 2 \text{ mol\%}$	$\text{CO}_2 = 6 - 10 \text{ mol\%}$

The CO_2 densities were corrected for the presence of CH_4 and are equivalent CO_2 densities (Swanenberg, 1979). Both inclusion types are closely associated and homogenize between 290 and 320°C . Data by

Takenouchi & Kennedy (1965) and Gehrig (1980) indicate that our analytical data are consistent with a fluid immiscibility at about 305°C and 100 to 200 bars. During later stages no boiling occurred, therefore the pressures in these stages must at least be as large as those during boiling. Somewhat lower temperatures in these stages will give pressures of 80 to 150 bar.

The associated type I and II inclusions are also found in the quartz-cap and greisen. However, their CO₂ densities are much higher than those in the mineralized quartz veins. The occurrence of these inclusion types also suggests immiscibility. Applying data by Gehrig (1980) and Takenouchi & Kennedy (1965) indicates a fluid immiscibility at 300 to 320°C but with a very large pressure range of 350 to about 1500 bars. The largest obtained pressures occurred in primary inclusions, lower pressures were found in pseudo-secondary and secondary inclusions. The occurrence of lower pressures in (pseudo-) secondary inclusions indicates a pressure drop during formation of the quartz-cap. Boiling of the ore fluids was probably caused by opening of the sub-horizontal joint system and may be the cause of ore deposition.

Type I and II inclusions with high CO₂ contents, like those in the quartz-cap, are also found in the tungsten-tin veins. However, these inclusions are earlier than type I and II inclusions with low CO₂ contents and always occur along the border of the veins where they may be found in vein quartz. The occurrence of inclusions with high CO₂ contents in the tungsten-tin veins, reported by Kelly and Rye, can be ascribed to these early veinlets. They represent the first sign of vein development as the sub-horizontal joints were slowly opened and filled with quartz.

The depth of mineralization can be estimated, assuming that the ore veins were in open communication with the surface, in which case the pressure corresponds to the weight of the fluid column. The depth of mineralization was probably of the order of 1600 to 2000 m with a pressure of about 150 bar.

Fluid salinities

Salinities in the fluid inclusions show no evidence of saline brines apart from the late high-salinity type III inclusions. Salinities fluctuate between 5 and 10 wt% NaCl during the oxide-silicate, main sulphide and pyrrhotite alteration stage. The salts are mainly NaCl with some KCl. No Ca or Mg was found, instead Rb and Cs were detected. The salinity drops below 5 wt% during deposition of the late fluorite and calcite.

In the oxide-silicate stage both temperature and salinity show distinct fluctuations, possibly as a result of boiling but there is no correlation between the two (Kelly & Rye, 1979).

Depositional temperatures

Homogenization temperatures during boiling require no pressure correction. The obtained fluid pressures in the veins of 100 to 200 bars indicate that the pressure correction for the inclusions is negligible for non-boiling fluids (Potter, 1977).

Fluids during the oxide-silicate stage ranged in temperature from 280 to 325°C with a medium temperature around 300°C (Fig. 8). The fluids were boiling at several periods during this stage. Depositional temperatures during the main sulphide and pyrrhotite alteration stage range from 250 to 290°C with a medium temperature of about 275°C (Fig. 8). During these stages fluids were not boiling. Boiling ceased during the later stages, probably caused by somewhat lower temperatures, decreasing amounts of CO₂ in the fluids and/or a higher pressure in the veins. Subsequently, temperatures dropped to about 150°C during deposition of fluorite and to about 100°C during dolomite and calcite deposition.

Temperatures of ore formation are relatively low at Panasqueira. Tin-tungsten deposits formed at different temperatures of 200 to 600°C such as in Bolivia (Kelly & Turneure, 1970), in Peru (Landis & Rye, 1974), in France (Ramboz, 1980) and in the Erzgebirge (Durisova et al., 1979; Thomas & Baumann, 1980; Thomas, 1982). Earlier estimates of temperature and pressure for Panasqueira were based on unreliable

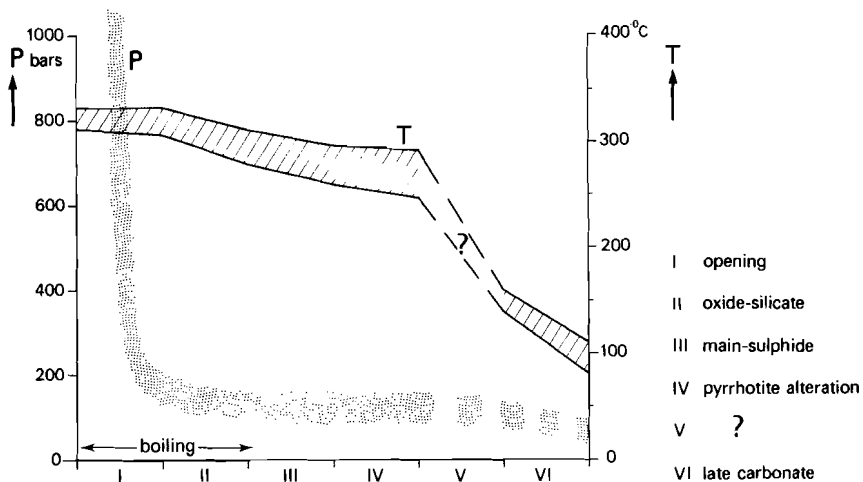


Fig. 8. Temperature and pressure variations during various stages of mineralization.

exsolution features (Orey, 1967) or later discredited sulphide thermometers (Clark, 1964).

Over-pressures

Occasionally higher pressures occur, especially in the quartz-cap and its related veins. Liquid CO₂ with densities up to 0.9 g/cm³ is found in the fluid inclusions. Pressure estimates for the associated type I and II inclusions in the quartz-cap range from 350 to about 1500 bars (Takenouchi & Kennedy, 1965; Gehrig, 1980). In the quartz-cap, inclusions with the highest CO₂ densities were found to be primary, lower densities occurred in secondary trails.

Boiling in the open vein system gives pressure estimates of 100 to 200 bars. In a closed system a lithostatic pressure of 250 to 550 bars may occur. The obtained pressure estimates of the opening stage, however, are much higher and must have another explanation. Fast erosion of the schist host rocks is not possible in a relatively short time because the inclusions in the quartz-cap point to a rather fast

pressure drop.

Another possibility is trapping of fluids against an impermeable granite-schist contact. The overpressure of about 1000 bars, in the opening stage, can be explained by trapping of CO₂-rich fluids against this barrier. The pressure drop in the quartz-cap occurred as the sub-horizontal vein system was slowly opened to permit access for the mineralizing fluids. This pressure drop caused boiling in the entire vein system as the horizontal joints were opened and filled with fluid. As the vein system reached the surface, boiling continued until the excess CO₂ was removed from the fluids.

The impermeable granite-schist contact prevented the escape of fluids from the granite. However, an influx of meteoric water through this barrier is also not possible. This might suggest that at least the early fluids had a magmatic origin.

STABLE ISOTOPES

The Panasqueira tungsten-tin veins are related to a granitic stock, probably with more granitic rocks at deeper levels. This is the "common" situation of tin-tungsten veins throughout the world (Taylor, 1979). The shallow setting of the mineralization implies that meteoric water could have been an important constituent of the fluids. Stable isotopes can give details about the origin of fluids (Rye & Ohmoto, 1974). The isotope values are reported as per mil deviations from a standard: $\delta^{18}\text{O}$, $\delta^{13}\text{C}$ and $\delta^{15}\text{N}$ values are given relative to SMOW, PDB and AIR respectively.

Carbon isotopes

The $\delta^{13}\text{C}$ values of CO₂ of the vein fluids at Panasqueira were estimated by two different methods.

Indirectly: Siderites of the pyrrhotite alteration stage give $\delta^{13}\text{C}$ values of -8.3 to -12.7 per mil (Table II). The dolomites and calcites of the late carbonate stage give similar $\delta^{13}\text{C}$ values of -8.8 to -13.4 per mil. The $\delta^{13}\text{C}$ of CO₂ in the fluids (Fig. 9) in equilibrium with

Table II: $\delta^{13}\text{C}$ values of siderite, dolomite and calcite.

		$\delta^{13}\text{C}$
PQ 21B	Siderite	-12.3
PQ 36-2	Siderite	-10.9
PQ 38S	Siderite	-9.8
PQ 80	Siderite	-8.3
PQ 82	Siderite	-10.8
PQ 82S	Siderite	-10.6
PQ 100-1	Siderite	-9.2
PQ 103	Siderite	-11.6
PQ 128	Siderite	-9.6
PQ 129	Siderite	-12.7
PQ 132	Siderite	-8.7
PQ 27A	Dolomite	-10.2
PQ 80	Dolomite	-9.2
PQ 102-1	Dolomite	-12.6
PQ 102-2	Dolomite	-11.3
PQ 120	Dolomite	-9.8
PQ 122	Dolomite	-10.1
PQ 27A-2	Dolomite	-10.6
PQ 27A-5	Dolomite	-10.6
PQ 94-3	Dolomite	-10.8
PQ 103	Calcite	-10.9

$\delta^{13}\text{C}$ relative to PDB.

the carbonates was calculated according to fractionation curves of O'Neil et al. (1969).

Directly: Measurements of CO_2 from fluid inclusions give $\delta^{13}\text{C}$ values of -4 to -12 per mil with some higher values up to 2 per mil (Fig. 10 and Table I). While the crushing method gave reproducible results for quartz, the amounts of CO_2 released from sulphides were very small and increased upon heating to 150°C . This is an indication of CO_2 adsorption on newly formed surfaces and explains the large difference in isotopic composition obtained by crushing sulphides formed simultaneously with quartz. The sulphides show a shift toward several

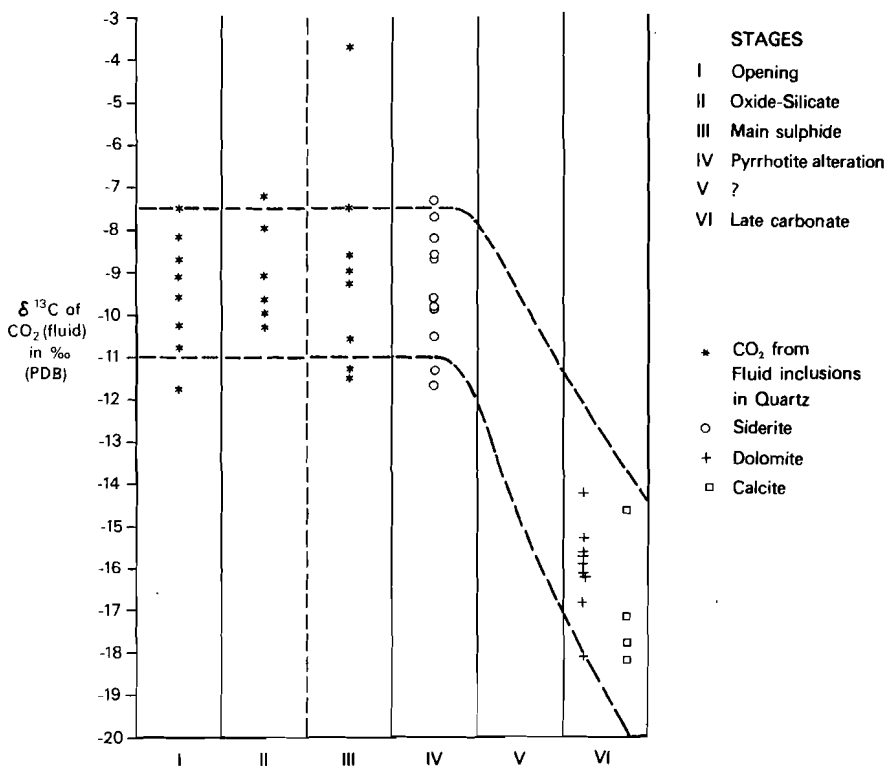


Fig. 9. $\delta^{13}\text{C}$ (PDB) of carbonates and CO_2 from fluid inclusions in quartz. Classification in zone II and III is in some cases arbitrary.

per mil higher values. Wolframite showed only a small isotopic shift. Also, the $\delta^{13}\text{C}$ values of total carbon in the fluids (the sum of oxidized CH_4 and CO_2) were measured and range from -10 to -14 per mil (Fig. 11 and Table III).

Oxygen isotopes

The $\delta^{18}\text{O}$ values of granite and greisen samples range from 11.4 to 13.0 per mil (Kelly & Rye, 1979) but the larger granitic bodies of Belmonte and Covilha, with which Panasqueira is probably related, have

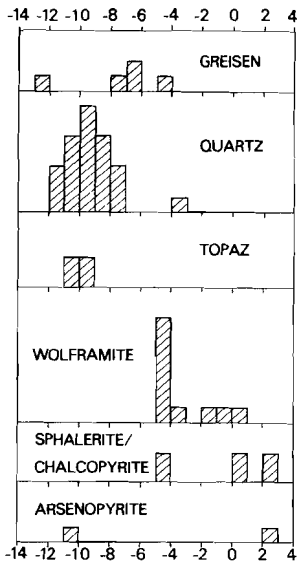


Fig. 10. $\delta^{13}\text{C}$ (PDB) of CO_2 from fluid inclusions.

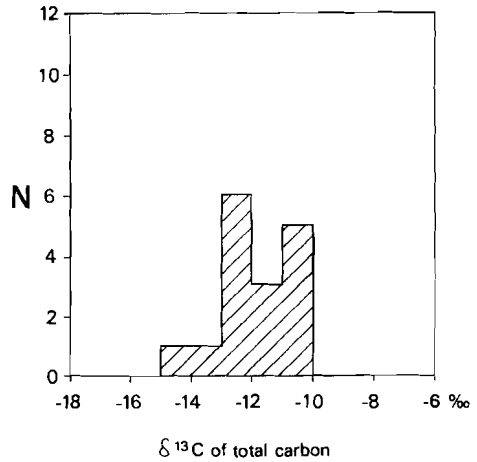


Fig. 11. $\delta^{13}\text{C}$ (PDB) of total carbon in fluid inclusions.

$\delta^{18}\text{O}$ values of 10.5 per mil (Table IV).

In contrast with $\delta^{13}\text{C}$, the $\delta^{18}\text{O}$ composition of the vein fluids in the different stages can only indirectly be determined from oxygen isotope ratios in minerals. Zoning in quartz crystals, outlined by muscovite flakes, permitted to give a rather accurate range of depositional temperatures for each zone. The calculated $\delta^{18}\text{O}$ values of the fluids from which these quartz zones and other minerals were deposited, are given in Fig. 12 and range from about 6.5 per mil during the opening stage to about 3 per mil in the pyrrhotite alteration stage. The fractionation curve of Clayton et al. (1972) was used for quartz. For wolframite and cassiterite the fractionation curves of Landis & Rye (1974) and Burshevskiy et al. (1979) were used.

Calculated $\delta^{18}\text{O}$ values for fluids of the late carbonate stage are lower and range from -4 to +3 per mil, indicating a dominant meteoric water component in the fluid.

Table III: $\delta^{15}\text{N}$ and $\delta^{13}\text{C}$ values of total carbon in fluid inclusions.

		$\delta^{15}\text{N}$	$\delta^{13}\text{C}$ (total carbon)
PQ 13	Seixo Bravo	2.8	-11.5
PQ 14	Seixo Bravo	3.4	-10.2
PQ 10	Quartz	4.5	-10.0
PQ 12	Quartz	0.3	-14.1
PQ 21D	Quartz	4.2	-13.9
PQ 23	Quartz	4.8	-12.2
PQ 31	Quartz	3.1	-10.5
PQ 32A	Quartz	4.0	-12.9
PQ 44	Quartz	4.4	-12.0
PQ 45	Quartz	4.1	-11.2
PQ 51	Quartz	4.4	-12.2
PQ 53	Quartz	5.1	-12.9
PQ 71	Quartz	4.4	-11.5
PQ 79	Quartz	4.2	-10.9
PQ 81	Quartz	3.6	-12.4
PQ 202	Wolframite	3.7	-10.5

$\delta^{15}\text{N}$ and $\delta^{13}\text{C}$ relative to AIR and PDB respectively.

Instead of using homogenization temperatures of individual minerals, which can give erroneous results in the case of (pseudo-)secondary inclusions, the $\delta^{18}\text{O}$ values of the fluid of data by Kelly & Rye (1979) were recalculated, using temperature ranges for each stage (Fig. 12). A siderite sample formed in the pyrrhotite alteration stage gives a $\delta^{18}\text{O}$ fluid value of +3 per mil, using the dolomite-water fractionation curve (Northrop & Clayton, 1966).

Nitrogen isotopes

Nitrogen isotopes were measured directly on gases in fluid inclusions in vein quartz, Seixo Bravo quartz and wolframite (Table III). Because the yield of gases from the late stage minerals was minor, $\delta^{15}\text{N}$ analyses could only be made on the earlier stages. Most values are between +3 and +5 per mil (Fig. 13), indicating a rather homogeneous source for nitrogen. The N_2 probably originated

Table IV: $\delta^{18}\text{O}$ values of quartz, cassiterite, wolframite, Beira shales and the porphyritic biotite granites.

		$\delta^{18}\text{O}$	T ^o C	Stage
PQ 61A	Quartz	15.0	280 - 320 ^o	Opening
PQ 71-3	Quartz	12.4	300 - 330 ^o	Opening
PQ 72	Quartz	15.0	280 - 320 ^o	Opening
PQ 72-5	Quartz	13.9	300 - 320 ^o	Opening
PQ 74-4	Quartz	12.9	300 - 320 ^o	Opening
PQ 49	Cassiterite	4.2	280 - 310 ^o	Oxide-silicate
PQ 94	Cassiterite	4.6	280 - 310 ^o	Oxide-silicate
PQ 103	Cassiterite	4.2	280 - 310 ^o	Oxide-silicate
PQ 21D	Wolframite	5.2	280 - 310 ^o	Oxide-silicate
PQ 38	Wolframite	5.6	280 - 310 ^o	Oxide-silicate
PQ 27D	Quartz	12.8	280 - 310 ^o	Oxide-silicate
PQ 42	Quartz	13.2	280 - 310 ^o	Oxide-silicate
PQ 27F	(1) Quartz	14.4	280 - 310 ^o	Oxide-silicate
	(2) Quartz	13.1	270 - 290 ^o	Main sulphide
	(3) Quartz	14.1	250 - 280 ^o	Pyrrhotite alteration
PQ 27F-8	(1) Quartz	13.7	280 - 310 ^o	Oxide-silicate
	(2) Quartz	13.2	280 - 310 ^o	Oxide-silicate
	(3) Quartz	14.4	250 - 270 ^o	Pyrrhotite alteration
	(4) Quartz	16.6	180 - 200 ^o	??
PQ 101A	(1) Quartz	13.4	250 - 280 ^o	Pyrrhotite alteration
	(2) Quartz	14.6	210 - 240 ^o	??
PQ 101C	Quartz	13.7	260 - 280 ^o	Main sulphide
PQ 21D	Siderite	12.9	250 - 280 ^o	Pyrrhotite alteration
X.02	Whole rock	13.5	Beira shale	
0.101	Whole rock	11.3	Beira shale	
0.138	Whole rock	12.8	Beira shale	
Fun 67	Whole rock	10.5	Porphyritic (muscovite)-biotite	
Fun 76	Whole rock	10.6	granite of Covilha.	

$\delta^{18}\text{O}$ relative to SMOW.

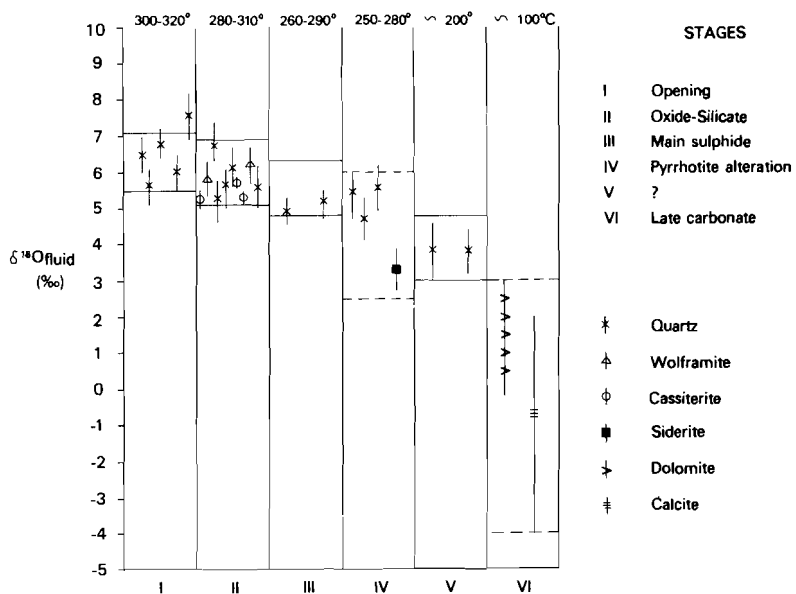


Fig. 12. The calculated $\delta^{18}O_{fluid}$ (SMOW) for different stages. Blocks indicate our recalculated $\delta^{18}O$ ranges from data by Kelly & Rye (1979).

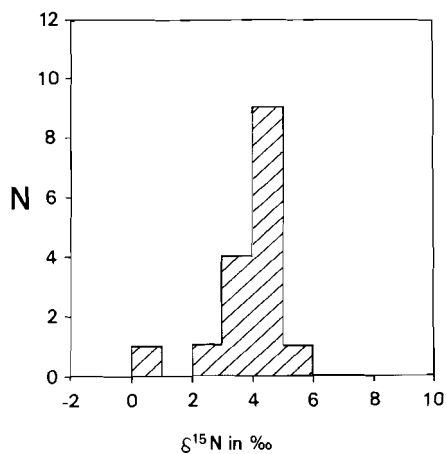


Fig. 13. $\delta^{15}N$ (AIR) of fluid inclusions in quartz and wolframite.

from organic matter in assimilated Beira shales at deeper levels as circulation through the schist is not possible (impermeable granite-schist contact). The rather constant C/N ratio and homogeneous $\delta^{15}\text{N}$ values indicate that melting and mixing occurred already at deeper levels in the granite. The interpretation of the $\delta^{15}\text{N}$ values is difficult as little information is available about nitrogen isotopes in hydrothermal fluids.

DISCUSSION OF STABLE ISOTOPE DATA

Throughout the mineralization, much of the carbon was derived from a homogeneous source as indicated by the $\delta^{13}\text{C}$ of total carbon. The low $\delta^{13}\text{C}$ values of CO_2 and total carbon indicate a contribution of organic matter in the fluids (Fig. 9). Until the end of the pyrrhotite alteration stage, the presence of methane suggests a reducing environment. The CH_4 and N_2 probably originated from organic matter present in the Beira shales. The low $\delta^{13}\text{C}$ values of CO_2 in the late stages (Fig. 9) indicates that carbon of the late carbonate stage contains a larger contribution of oxidized organic matter than in the earlier stages. Oxidation may have been caused by influx of airated meteoric water in the vein system (see also oxygen isotopes).

The large overpressure of 1 kbar in the earliest stage requires an impermeable granite-schist contact. This barrier also prevented the influx of meteoric water and indicates that circulation of heated meteoric water through the Beira shales into the still warm granite is not possible. In that case, the rather low $\delta^{13}\text{C}$ values of CO_2 from the veins indicate mixed sources, e.g. "magmatic" CO_2 and CO_2 derived from organic matter.

Most of the calculated $\delta^{18}\text{O}$ values for water from the oxide-silicate stage are greater than 5 per mil (Fig. 12). Fluids in isotopic equilibrium with the Panasqueira granite should have $\delta^{18}\text{O}$ values between 5 and 7 per mil at temperatures between 270 and 330°C. Values higher than 5 per mil are no proof of a magmatic origin of the fluid because meteoric waters can attain magmatic values due to

isotopic exchange with high-temperature rocks (Taylor, 1974; Kelly & Rye, 1979), provided that water/rock ratios are low. Any fluid with a $\delta^{18}\text{O}$ value lower than 5 per mil probably contains some meteoric water. According to the low $\delta^{18}\text{O}$ values of fluids in the late carbonate stage, meteoric water dominated in this stage (Fig. 12).

The $\delta^{18}\text{O}$ values of the altered Panasqueira granite and greisen cupola are about 2 per mil higher than observed in the unaltered granitic rocks and are within the range of the Beira schist (Kelly & Rye, 1979). The high $\delta^{18}\text{O}$ values of the greisen were probably obtained by exchange with post-magmatic fluids. The high $\delta^{18}\text{O}$ values of the granite were inherited by anatexis of Beira schist at much deeper levels. Panasqueira represents an example of an S-type granite (Chappell & White, 1974), originating from anatexis of sedimentary rocks. The granite has high $\delta^{18}\text{O}$ values (10 to 12 per mil) and a high initial $^{87}\text{Sr}/^{86}\text{Sr}$ ratio of 0.713. It is also one of the Younger Hercynian granites for which an anatectic origin has been documented elsewhere (Albuquerque, 1971, 1978).

Hydrogen isotope data by Kelly & Rye (1979) suggests that two fluids were involved during the early stages of vein development. It is, however, not clear how these two different fluids coexisted in the vein system without changes in fluid salinity or temperature. Our own experiments indicate strong adsorption effects on crushed sulphides and suggest that the deuterium-poor fluids might represent a sample preparation effect.

Origin of fluids

Fluid inclusions indicate an overpressure of 1 kbar in the opening stage. This is explained by trapping of CO_2 against an impermeable granite-schist contact, which at the same time prevented an influx of meteoric water into the granite.

Carbon, oxygen, nitrogen and sulphur isotopes indicate a homogeneous source for the early stage fluids until the end of the pyrrhotite alteration stage. The combination of high overpressures in the opening stage with relatively constant oxygen, carbon, sulphur and nitrogen isotopes strongly suggests a vein fluid derived from, or in equilibrium

with, the granites. Although the carbon values of -7 to -11 per mil in the early stages are more negative than "normal magmatic" values, they can be explained by melting of organic-rich sediments and assimilation of the Beira shales. Until the pyrrhotite alteration stage, the isotopic composition does not deviate much from the earliest stage.

In the late carbonate stage, however, carbon and oxygen isotopes show distinct changes:

- i) oxygen isotope values decrease more rapidly and approach meteoric water values,
- ii) carbon isotope values are more negative, corresponding to increasing amounts of oxidized organic matter or methane.

Kelly & Rye (1979) found that sulphur isotopes show very large $\delta^{34}\text{S}$ variations at this stage. The isotopic values all favour an influx of surface water into the vein system at this stage.

CONCLUSIONS

This section will summarize all the obtained data of fluid inclusions and stable isotopes. A comparison with other tin-tungsten deposits is possible but the Panasqueira features are unique compared to the other deposits.

The Panasqueira cupola

The Panasqueira tungsten-tin veins are spatially associated with one or more greisenized granite cupolas. This is the common association for tin-tungsten deposits although exceptions do occur (Taylor, 1979). Clark's (1964) proposal, that there is a continuity between cupola consolidation and hydrothermal mineralization, is not confirmed. Instead a large gap occurs between consolidation and mineralization because the ore veins cut across the crystallized and jointed granite (Kelly & Rye, 1979). The earliest temperatures in vein and greisen samples are around 330°C and are far below the lowest magmatic range. This gap in time and temperature is also found in other tin-tungsten deposits.

The cupola(s) provided an emanative centre for the ore fluids which evolved from deeper parts in the granite and concentrated in the apical parts. The fluids were also responsible for the greisenization of the cupola and simultaneous filling of the hydrothermal ore veins. Other cupolas are supposed to be present below Corga Seca and Vale da Ermida. Strong contact-metamorphism and greisen veins point to another greisen cupola below the Zèzere river at Rio (Fig. 1, Chapter 4).

Clark (1964) studied the mineral sequence in the greisenized granite and compared it with the vein mineralization. The hydrothermal greisenization and vein deposition bear a striking resemblance, thus the late hydrothermal alteration of the cupola and filling of the tungsten-tin veins were essentially contemporaneous (Kelly & Rye, 1979). This requires a permeable cupola which is confirmed by the strong alteration and many small sub-vertical greisen veins in the deeper granite.

Unaltered granite is not available at Panasqueira but the least altered samples indicate a correlation of this granite with the Younger porphyritic biotite-(muscovite) granites in Portugal. Stable isotope studies give high $\delta^{18}\text{O}$ contents for the Panasqueira granite but also for the unaltered porphyritic granites north of Panasqueira. This indicates an S-type granite for the Panasqueira and porphyritic Younger granites. The strontium isotope ratio of 0.713 (Priem & den Tex, 1982) confirms this. Albuquerque (1971, 1978) proposed an anatexitic origin for the Younger Hercynian granites, according to petrochemical studies. The S-type granite bears fundamental relations with tin and tungsten mineralizations and is derived by partial melting of meta-sedimentary rocks.

The quartz-cap

Fluid inclusions indicate a hydrothermal filling of this cap, formed at the apex of the granite. The earliest quartz-forming fluids were extremely rich in CO_2 at temperatures between 300 and 325°C, well below the magmatic range. In the early boiling period, which is found in the quartz-cap and in small quartz veinlets along the ore veins, CO_2 contents are up to 17 mol% in type I inclusions. These early pressures

reached values of more than 1500 bars, introducing an overpressure of about 1000 bar or more. High fluid pressures during formation of the quartz-cap may have lifted the schist cover off the granite. The high overpressures in the early stage are explained by trapping of CO₂-rich fluids against an impermeable granite-schist contact. At the same time this barrier prevented an influx of meteoric water into the granite. The quartz-cap was formed by a relatively fast pressure release through opening of the flat joint-system with a simultaneous quartz filling.

All stable isotopes of minerals from the quartz-cap are indistinguishable from those of the hydrothermal ore veins. The high internal pressures in the quartz-cap are difficult to explain with a convection system of meteoric water. The early fluids are probably "magmatic" and the high pressures can be explained by CO₂ evolving from a slowly crystallizing granite at depth.

The hydrothermal tungsten-tin veins

Characteristic of the Panasqueira tungsten-tin veins is their horizontal nature. Kelly & Rye (1979) explained the hydraulic dilation and support of the vein openings which were stabilized by the fluid pressure. Fluid inclusion studies indicate a mineralization depth of about 1800 m and adequate pressures for lifting the existing rock load along the sub-horizontal joints.

The horizontal joints are clearly post tectonic and of late Hercynian age. The joints postdate the regional metamorphism (Kelly, 1977), and continued during the vein filling (Marignac, 1982). Opening of the joints occurred over a limited depth range of about 75 m but this increases to about 300 m above the greisen cupola. The lateral extent of the vein system is much larger and may amount to 2000 m or even more. It seems that the vein system is parallel to the granite-schist contact of the underlying main batholith.

The similarity in paragenesis for all the veins, apart from Vale da Ermida, indicates that most ore veins remained open from the oxide-silicate stage to the late carbonate stage. According to the hydrothermal alteration along the veins, it appears that the Beira schists were of low permeability, apart from the opened vein channels

(Kelly & Rye, 1979).

The filling of the tungsten-tin veins is rather coarse, crystal sizes are larger than normally observed in this type of deposits, especially for wolframite and apatite. Wolframite, arsenopyrite, apatite and siderite may attain a large size and perfection. The unusual coarse crystal size in the ore veins was attributed by Kelly & Rye (1979) to extremely slow rates of crystal nucleation and growth, in combination with a low degree of supersaturation and slow velocities in vein fluids. Flow directions in the ore veins are visible by preferred orientation of crystals and shadowing with later precipitates or mineral debris.

Although several mineralization stages can be recognized in the Panasqueira veins, no large pressure or temperature ranges were encountered. For the oxide-silicate, main sulphide and pyrrhotite alteration stage, temperatures were slowly declining from about 320 to 260°C with salinities of about 10 to 6 wt% NaCl. Major changes only occurred during the late carbonate stage; temperatures dropped to about 100°C and salinities below 4 wt% NaCl.

At Panasqueira temperatures above 400°C did not occur as in some other tin-tungsten deposits. Fluid inclusions with high salinities (NaCl cubes) were found but these fluids probably do not belong to the Panasqueira vein system. The high-salinity fluids are secondary in all the minerals at Panasqueira, even in the late fluorite. Homogenization temperatures are between 80 and 160°C and salinities between 15 and 45 wt% NaCl.

CO₂ contents show fluctuations but it is generally decreasing throughout time. In the opening and oxide-silicate stage CO₂ contents were above the saturation levels, causing an intense boiling in the veins. The high pressures, recorded for the early vein fluids of the quartz-cap, were not found in the ore veins. During the oxide-silicate stage CO₂ contents dropped to about 2 mol% with pressures between 100 and 200 bars. In the later stages CO₂ contents remained between 0.2 and 2 mol% and boiling did no longer occur, probably caused by lower CO₂ contents in the vein system.

Gas analyses indicate the presence of N₂ and CH₄ during the early

stages. During the main mineralization the presence of CH₄ suggests a reducing environment.

Origin of the ore fluids

The association of the hydrothermal ore veins with a greisenized granite cupola of approximately the same age, indicates that magmatic water may have been an important constituent in the fluids. A crystallizing granite at depth below the vein system would provide a source for the high overpressures, encountered in the quartz-cap. These high pressures were capable of opening the sub-horizontal vein system.

To characterize these fluid sources, stable isotopes were measured. As well carbon, nitrogen, oxygen as sulphur isotopes are relatively constant in the early periods, indicating a homogeneous source for the fluids. In the late carbonate stage meteoric water appears to be the major fluid source.

The hydrogen isotope data of Panasqueira are contradicting, they indicate the presence of two different water types in the oxide-silicate stage and possibly also in the opening stage. These two fluids occur in different minerals which are contemporaneous. Gas analyses of fluid inclusions in sulphides indicate strong adsorption effects on newly created surfaces which are probably responsible for the strange gas and isotopic compositions. From the hydrogen isotope data no source can be specified because the magmatic and meteoric water values overlap.

The high initial pressures, combined with stable isotope data shows that the mineralizing fluids had a magmatic origin. The presence of meteoric water becomes apparent in the late carbonate stage.

REFERENCES

- Albuquerque, C.A.R. de (1971): Petrochemistry of a series of granitic rocks from Northern Portugal. *Bull. Geol. Soc. Amer.*, 82, 2783-2798.
- Albuquerque, C.A.R. de (1978): Rare earth elements in "Younger" granites, Northern Portugal. *Lithos*, 11, 219-229.
- Bloot, C. & de Wolf, L.C.M. (1953): Geologic features of the Panasqueira tin-tungsten ore occurrence (Portugal). *Bol. Soc. Geol. Portugal*, 11, 1-58.
- Borschhevskiy, Yu.A. & Borisova, S.L. & Pavlovskiy, A.B. & Marshukova, N.K. (1979): Oxygen-isotope features of cassiterites from deposits of Central Asia. *Intern. Geol. Rev.*, 21, 937-944.
- Chappell, B.W. & White, A.J.R. (1974): Two contrasting granite types. *Pacific Geology*, 8, 173-174.
- Clark, A.H. (1964): Preliminary study of the temperatures and confining pressures of granite emplacement and mineralization, Panasqueira, Portugal. *Trans. Inst. Min. Metall.*, 73, section B, 813-824.
- Clark, A.H. (1965a): Discussions and author's reply to paper of Clark (1964). *Trans. Inst. Min. Metall.*, 74, section B, 217-223, 296, 663-672.
- Clark, A.H. (1965b): Notes on the mineralogy of the Panasqueira tin-tungsten deposit, Portugal: The occurrence of magnetite, stibnite, bertrandite, scheelite, tungstite, hydrotungstite and scorodite. *Com. Serv. Geol. Portugal*, 48, 201-212.
- Clayton, R.N. & Mayeda, T.K. (1963): The use of bromine pentafluoride in the extraction of oxygen from oxides and silicates for isotopic analysis. *Geoch. Cosmo. Acta*, 27, 43-52.
- Clayton, R.N. & O'Neil, J.R. & Mayeda, T.K. (1972): Oxygen isotope exchange between quartz and water. *Journ. Geophys. Research*, 77, no. 17, 3057-3067.
- Collins, P.L.F. (1979): Gas hydrates in CO₂-bearing fluid inclusions and the use of freezing data for estimation of salinity. *Econ. Geol.*, 74, 1435-1444.
- Durisova, J. & Charoy, B. & Weisbrod, A. (1979): Fluid inclusion studies in minerals from tin and tungsten deposits in the Krusné Hory Mountains (Czechoslovakia). *Bull. Minéral.*, 102, 665-675.
- Gaines, R.V. & Thadeu, D.C. (1971): The minerals of Panasqueira. *Mineral Rec.*, 2, 73-78.

- Gehrig, M. (1980): Phasengleichgewichte und pVT-Daten ternärer Mischungen aus Wasser, Kohlendioxid und Natriumchlorid bis 3 kbar und 550°C. Dissertation Universitaet Karlsruhe.
- Heyen, G. & Ramboz, C. & Dubessy, J. (1982): Simulation des équilibres de phases dans le système CO₂-CH₄ en dessous de 50°C et de 100 bar. Application aux inclusions fluides. C.R. Acad. Sci. Paris, 294, 203-206.
- Hosking, K.F.G. (1973): The search for tungsten deposits. Geol. Soc. of Malaysia, Bull. No. 5.
- Isaacs, A.M. & Peacor, D.R. & Kelly, W.C. (1979): Thadeuite, Mg(Ca,Mn)(Mg,Fe,Mn)₂(PO₄)₂(OH,F)₂, a new mineral from Panasqueira, Portugal. Amer. Mineral., 64, 359-361.
- Isaacs, A.M. & Peacor, D.R. (1981): Panasqueiraite, a new mineral: the OH-equivalent of isokite. Can. Mineral., 19, 389-392.
- Ito, E. & Clayton, R.N. (1983): Submarine matamorphism of gabbros from the Mio-Cayman Rise: an oxygen isotope study. Geoch. Cosmo. Acta, 47, 535-546.
- Kelly, W.C. (1977): The relative timing of metamorphism, granite emplacement and hydrothermal ore deposition in the Panasqueira district (Beira Baixa, Portugal). Com. Serv. Geol. Portugal, 61, 239-244.
- Kelly, W.C. & Rye, R.O. (1979): Geologic, fluid inclusions and stable isotope studies of the tin-tungsten deposits of Panasqueira, Portugal. Econ. Geol., 74, 1721-1822.
- Kelly, W.C. & Turneure, F.S. (1970): Mineralogy, paragenesis and geothermometry of the tin and tungsten deposits of the eastern Andes. Econ. Geol., 65, 609-680.
- Kelly, W.C. & Wagner, G.A. (1977): Paleothermometry by combined application of fluid inclusion and fission track methods. N. Jahrb. Min. Monatsh., 1, 1-15.
- Kreulen, R. & Schuiling, R.D. (1982): N₂-CH₄-CO₂ fluids during formation of the Dôme de l'Agout, France. Geoch. Cosmo. Acta, 46, 193-203.
- Landis, G.P. & Rye, R.O. (1974): Geologic, fluid inclusion and stable isotope studies of the Pasto Bueno tungsten-base metal ore deposit. Econ. Geol., 69, 1025-1059.
- Marignac, Chr. (1982): Geologic, fluid inclusions, and stable isotope studies of the tin-tungsten deposits of Panasqueira, Portugal. A discussion. Econ. Geol., 77, 1263-1266.
- McCrea, J.M. (1950): On the isotopic chemistry of carbonates and a paleotemperature scale. Journ. Chem. Phys., 18, 849-857.
- Northrop, D.A. & Clayton, R.N. (1966): Oxygen isotope fractionation in

- systems containing dolomite. *Journ. Geology*, 74, 174-196.
- Ohmoto, H. & Rye, R.O. (1979): Isotopes of sulphur and carbon. In: Barnes, H.L.: *Geochemistry of hydrothermal ore deposits*. 2nd edition. John Wiley, New York. 509-567.
- O'Neil, J.R. & Clayton, R.N. & Mayeda, T.K. (1969): Oxygen isotope fractionation in divalent metal carbonates. *Journ. Chem. Physics*, 51, 5547-5558.
- Orey, F.C de (1967): Tungsten-tin mineralization and paragenesis in the Panasqueira and Vale da Ermida mining districts, Portugal. *Com. Serv. Geol. Portugal*, 52, 117-167.
- Pichavant, M. & Ramboz, C. & Weisbrod, A. (1982): Fluid immiscibility in natural processes: use and misuse of fluid inclusion data. I. Phase equilibria analysis - A theoretical and geometrical approach. In: R. Kreulen and J. Touret (Guest-editors), *Current research on fluid inclusions*. *Chem. Geol.*, 37, 1-27.
- Potter, R.W. (1977): Pressure corrections for fluid inclusion homogenization temperatures based on the volumetric properties of the system NaCl-H₂O. *Journ. Research U.S. Geol. Survey*, 5, 603-607.
- Poty, B. & Leroy, J. & Jachimowicz, L. (1976): Un nouvel appareil pour la mesure des températures sous le microscope: l'installation de microthermométrie Chaixmeca. *Bull. Soc. Fr. Minéral. Cristallog.*, 99, 182-186.
- Priem, H.N.A. & den Tex, E. (1982): Tracing crustal evolution in the NW Iberian Peninsula through Rb-Sr and U-Pb systematics of Paleozoic granitoids: a review. *International Colloquim "Géochimie et Petrologie de granitoids"*, Clermont-Ferrand, May 1982, Volume of Abstracts.
- Ramboz, C. (1980): *Géochimie et étude des phases fluides de gisements et indices d'étain-tungstène du sud du massif central (France)*. Thèse 3e cycle. Université Nancy.
- Ramboz, C. & Pichavant, M. & Weisbrod, A. (1982): Fluid immiscibility in natural processes: use and misuse of fluid inclusion data. II. Interpretation of fluid inclusion data in terms of immiscibility. In: R. Kreulen and J. Touret (Guest-editors), *Current research on fluid inclusions*. *Chem. Geol.*, 37, 29-48.
- Roedder, E. (1963): Studies on fluid inclusions II: Freezing data and their interpretation. *Econ. Geol.*, 58, 167-211.
- Roedder, E. (1979): Fluid inclusions as samples of ore fluids. In: Barnes, H.L.: *Geochemistry of hydrothermal ore deposits*. 2nd edition. John Wiley, New York. 684-737.

- Roedder, E. & Coombs, D.S. (1967): Immiscibility in granitic melts, indicated by fluid inclusions in ejected granitic blocks from Ascension Island. *Journ. Petrol.*, 8, 417-451.
- Rye, R.O. & Ohmoto, H. (1974): Sulphur and carbon isotopes and ore genesis: a review. *Econ. Geol.*, 69, 826-842.
- Rye, R.O. & Sawkins, F.J. (1974): Fluid inclusion and stable isotope studies on the Casapalca Ag-Pb-Zn-Cu deposit, Central Andes, Peru. *Econ. Geol.*, 69, 181-205.
- Saraiva, M. (1971): A composico e distribuico das wolframites no jazigo das Minas da Panasqueira (Portugal central) Congresso Hispano-Luso-Americano. *Geol. Econ. Secc. 4 Invest. Mineira, Madrid* 11, 917-932.
- Swanenberg, H.E.C. (1979): Phase equilibria in carbonic systems, and their application to freezing studies of fluid inclusions. *Contr. Min. Petrol.*, 68, 303-306.
- Takenouchi, S. & Kennedy, G.C. (1965): The solubility of carbon dioxide in NaCl solutions at high temperatures and pressures. *Am. Journ. Science*, 263, 445-454.
- Taylor, H.P. jr. (1974): The application of oxygen and hydrogen isotope studies to problems of hydrothermal alteration and ore deposition. *Econ. Geol.*, 69, 843-883.
- Taylor, R.G. (1979): *Geology of tin deposits. Developments in economic geology no. 11.* Elsevier Scientific Publishing Company - Amsterdam.
- Thadeu, D. (1951): *Geologia do couto minero da Panasqueira. Com. Serv. Geol. Portugal*, 32, 1-64.
- Thomas, R. & Baumann, L. (1980): Ergebnisse von thermometrischen und kryometrischen Untersuchungen an Kassiteriten des Erzgebirges. *Z. Geol. Wiss.*, 10, 1281-1299.
- Thomas, R. (1982): Ergebnisse der thermobarogeochemischen Untersuchungen an Fluessigkeitseinschlussen in Mineralen der postmagmatischen Zinn-Wolfram Mineralisation des Erzgebirges. *Freiberg. Forschungsh.*, C 370, pp. 85.

APPENDIX

Major element analyses

GRAN-1	N=47	Major element analyses		GN-02	N=90
		mean	st.dev.		
SiO ₂	71.42	.25	70.32	.13	
TiO ₂	.29	.03	.33	.03	
Al ₂ O ₃	14.18	.10	14.58	.03	
Fe ₂ O ₃	1.03	.17	1.22	.12	
FeO	1.15	.14	1.13	.08	
MnO	.07	.01	.09	.01	
HgO	.48	.03	.85	.03	
CaO	1.47	.08	2.14	.06	
Na ₂ O	3.42	.08	3.47	.10	
K ₂ O	5.34	.08	4.25	.09	
P ₂ O ₅	.09	.01	.13	.01	
H ₂ O	.47	.10	1.02	.12	
CO ₂	.0		.0		
Tot.	99.48	.35	99.53	.26	

concentrations in percentages

Gran-1 N=14 INAA analyses

	mean	st.dev.
Rb	323	9
La	123	7
Ce	222	7
Zn	68	6
Th	42	2
Hf	8.6	.5
U	6.1	1.0
Sc	5.3	.1
Yb	4.4	.2
Cs	4.2	.2
Ta	2.1	.1
Eu	1.32	.10
Tb	1.22	.05
Lu	.81	.06

concentrations in ppm

INAA analyses

STt-1	N=8	INAA analyses			RGM-1	N=4
		mean	st.dev.	literature		
Zn	243	11	235	35	3	34
Rb	120	7	120	145	11	155
La	170	9	160	24	5	24
Ce	270	8	260	46	2	50
Th	31	1	32	14	1	15
Cs	1.7	.2	1.5	11	1	10
Hf	30	1	27	6.4	.1	6.0
Ta	17	2	18	.8	.1	.9
U	7.7	.8	9	5.8	.4	5.8
Sc	.57	.03	.69	4.6	.2	4.8
As	4.8	1.3	4	3.5	1.4	2.9
Eu	4.25	.84	3.6	.79	.12	.7
Tb	1.36	.09	1.6	.57	.03	.74
Yb	4.55	.45	4.3	2.5	.4	2.5
Lu	.71	.07	.66	.48	.06	.42

concentrations in ppm

INAA analyses

BHVO	N=30	INAA analyses			Mag-1	N=12
		mean	st.dev.	literature		
Zn	120	10	103	138	7	130
Sc	32	1	30			
Rb	27	1	10	147	5	147
Cs				10	5	8
La	18	1	17	47	3	42
Ce	39	2	41	86	3	88
As	1.1	.3	1.5	10	1	8
Eu	2.34	.22	2.0	1.47	.07	1.51
Tb	1.17	.19	1.0	.87	.15	.99
Yb	2.0	.2	2.0	2.5	.1	2.7
Lu	.35	.05	.32	.45	.05	.39
Hf	4.6	.3	4.2	3.6	.1	3.5
Ta	1.3	.3	1.1	.9	.1	1.0
Th	1.2	.1	1.0	11	.4	12
U				2.2	.3	2.7

concentrations in ppm

XRF and AAS analyses						XRF analyses									
RGM-1	N=7			SDC	N=10			ACV-1	N=6			G-2	N=6		
	mean	st.dev.	literature	mean	st.dev.	literature		mean	st.dev.	literature	mean	st.dev.	literature		
Rb	157	5	170	130	4	128	Rb	67	5	67	158	4	170		
Sr	109	3	105	186	5	180	Sr	667	36	660	455	9	480		
Zr	226	8	210	291	13	300	Zr	226	24	230	300	16	300		
Nb	6	1	9	16	2	18	Nb	11	3	16	10	1	13		
U	6	3	6	3	1	3	U				2	1	2		
Ba	790	65	750	635	15	590	Ba	1165	55	1200	1650	75	1850		
Ta	2	1	1				Ta	5	2	1					
Sn	2	1	4	1	1	3	Sn	3	1	4	2	2	2		
Cs	4	2	10	4	2	4	Cs	< 2		1	2	1	1		
P	135	25	220	675	30	740	P	1950	100	2180	555	60	600		
Ti	1525	30	1620	5440	130	6115	Ti	5840	100	6300	2460	50	3000		
W	< 4			2	1		W				< 1		< 1		
Cu	10	2	11	29	9	30									
Li	55	3	51	33	2	34									

concentrations in ppm

concentrations in ppm

XRF and AAS analyses						XRF analyses									
Granite HST.2	N=13			Schist HST.	N=8			SCO-1	N=6			STM-1	N=7		
	mean	st.dev.		mean	st.dev.			mean	st.dev.	literature	mean	st.dev.	literature		
Rb	535	6	538 INAA	385	10	384 INAA	Rb	117	4	118	126	6	120		
Sr	30	1	32 ICP	49	3	48 ICP	Sr	169	9	175	750	28	710		
Zr	40	2		208	6		Zr	165	16	165	1345	36	1200		
Nb	22	2		10	1		Nb	10		9	250	35	270		
U	8	2	8 INAA	4	1	4 INAA	U	< 1		2					
Ba	100	11	123 ICP	555	23	560 ICP	Ba	606	28	550	555	40	550		
Sn	54	2		25	2		Sn	3	2	4	3	1	7		
Cs	50	2	62 INAA	72	3	71 INAA	Cs	2	2	8	2		2		
P	1935	85	1870 ICP	755	20	800 ICP	P	815	70	1000	580	100	700		
Ti	490	10	550 ICP	5120	70	4730 ICP	Ti	3940	65	3840	685	20	780		
W	9	1	9 INAA	31	4	23 INAA	W	< 2			4	1			
Ta	10	3	9 INAA												
Cu	9	2	15 ICP	50	7	56 ICP									
Zn	51	6	59 ICP	160	15	185 ICP									
Li	522	13	555 ICP												
F	2400	100													

concentrations in ppm

analyses in ppm

Fundão (granó)-diorites.

	CW 04	CW 091	Fu 81	FU 91	* 21	* 60
	j-2	j-2	j-2	j-2	j-2	j-2
SiO ₂	67.79	67.95	64.13	68.63	68.38	68.35
TiO ₂	.61	.59	.66	.39	.86	.66
Al ₂ O ₃	15.28	15.07	16.79	15.59	15.02	15.06
Fe ₂ O ₃	.60	3.51	.74	.21	.85	.75
FeO	2.80	d.l.	3.55	2.82	2.80	2.85
MnO	.05	.04	.14	.11	.03	.02
MgO	1.44	1.18	2.16	1.30	.97	2.00
CaO	3.00	3.06	4.48	3.10	3.34	3.46
Na ₂ O	3.51	3.98	4.01	3.80	3.86	3.84
K ₂ O	2.73	2.27	2.46	2.47	2.67	2.36
P ₂ O ₅	.29	.29	.26	.19	.19	.24
H ₂ O	1.10	1.23	1.10	1.43	.87	.44
CO ₂			d.l.	d.l.	d.l.	
F	.06	.06				
	99.26	99.23	100.48	100.04	99.84	100.03

(d.l. means below detection limit).

CIPW - norm

Q	27.8	28.9	16.9	26.9	26.3	25.6
C	1.9	1.3	.0	1.5	.2	.5
Or	16.3	13.5	14.5	14.6	15.8	13.9
Ab	29.9	33.9	33.8	32.1	32.7	32.4
An	12.8	13.1	20.4	14.1	15.4	15.6
En	3.6	3.0	5.4	3.2	2.4	5.0
Fs	3.8	.0	5.1	4.6	3.1	3.6
Mt	.9	.0	1.1	.3	1.2	1.1
Hm	.0	3.5	.0	.0	.0	.0
Il	1.2	.1	1.2	.7	1.6	1.3
Ru	.0	.5	.0	.0	.0	.0
Ap	.7	.7	.6	.5	.5	.6
Pr	.1	.1	.0	.0	.0	.0
	99.0	98.6	99.0	98.5	99.2	99.6

Albite-muscovite granite and 'greisen' of Quinteiros.

	FUN 5	FUN 19	FUN 20
	j-5	j-5	j-5
SiO ₂	75.16	76.37	76.45
TiO ₂	.07	.04	.06
Al ₂ O ₃	14.13	13.80	13.32
Fe ₂ O ₃	.48	1.24	1.57
FeO	.54	.84	.86
MnO	.01	.00	.01
MgO	.26	.28	.37
CaO	.23	.02	.04
Na ₂ O	3.13	.20	1.27
K ₂ O	4.84	4.36	4.41
P ₂ O ₅	.20	.13	.11
H ₂ O	1.12	2.25	1.89
CO ₂	d.l.	.17	d.l.
F	.01	.03	.01
	100.18	99.73	100.17

(d.l. means below detection limit).

CIPW - norm

Q	37.7	58.3	51.4
C	3.7	8.8	6.4
Or	28.5	25.8	26.0
Ab	26.4	1.7	10.7
En	.6	.3	.9
Fs	.5	.5	.2
Mt	.7	1.8	2.3
Il	.1	.1	.1
Ap	.4	.0	.1
Mg	.0	.3	.0
	98.6	97.6	98.1

* Data by Costa et al. (1971)

Fundão (grano)-diorites.

	BB 01	CW 01	FU 101	* 51/52	BB 02	CW 02	FU 100	* 57
	j-0	j-0	j-0	j-0	j-1	j-1	j-1	j-1
SiO ₂	68.18	67.05	69.12	66.34	67.53	67.53	68.24	66.36
TiO ₂	.62	.66	.39	.82	.63	.63	.47	1.02
Al ₂ O ₃	15.59	15.80	15.63	15.03	15.67	15.59	15.72	15.12
Fe ₂ O ₃	1.16	.99	.23	1.61	.60	.61	.46	1.23
FeO	2.20	2.76	2.56	2.48	2.78	2.94	2.68	2.98
MnO	.10	.13	.08	.04	.10	.14	.10	.01
MgO	1.36	1.62	1.07	1.63	1.45	1.63	1.50	1.85
CaO	3.05	3.40	2.88	3.48	3.12	3.18	3.20	3.84
Na ₂ O	4.18	4.74	4.58	4.43	3.84	4.29	3.70	4.00
K ₂ O	2.31	2.38	1.83	2.34	2.75	2.78	2.92	2.57
P ₂ O ₅	.22	.25	.17	.27	.26	.26	.20	.25
H ₂ O	.69	.77	1.16	1.04	.62	.84	1.21	.95
CO ₂	d.l.	d.l.	d.l.		d.l.	d.l.	d.l.	
F	.06	.06			.06	.07		
	99.72	100.61	99.70	99.51	99.41	100.49	100.40	100.18

(d.l. means below detection limit).

CIPW - norm

Q	26.3	19.9	26.4	22.0	25.1	21.6	25.1	22.0
C	1.3	.0	1.3	.0	1.4	.5	1.1	.0
Or	13.7	13.9	10.8	13.9	16.3	16.3	17.2	15.2
Ab	35.5	39.9	38.9	37.7	32.7	36.1	31.2	33.8
An	13.4	14.7	13.2	14.3	13.6	13.7	14.5	15.7
Wo	.0	.1	.0	.5	.0	.0	.0	.7
En	3.4	4.0	2.7	4.1	3.6	4.0	3.7	4.6
Fs	2.3	3.4	4.0	2.0	3.8	4.1	3.9	2.8
Ms	1.7	1.4	.3	2.3	.9	.9	.7	1.8
Il	1.2	1.2	.7	1.6	1.2	1.2	.9	1.9
Ap	.5	.6	.4	.6	.6	.6	.5	.6
Fr	.1	.1	.0	.0	.1	.1	.0	.0
Df	.0	.1	.0	1.0	.0	.0	.0	1.4
	99.4	99.2	98.7	100.0	99.3	99.1	98.8	100.5

Fundão (grano)-diorites.

	FU 341	* 59	* 61	* 62
	j-3	j-3	j-3	j-3
SiO ₂	70.07	69.21	71.98	76.65
TiO ₂	.29	.60	.39	.16
Al ₂ O ₃	15.43	15.41	15.18	15.55
Fe ₂ O ₃	.51	.65	.55	.43
FeO	1.58	1.77	1.65	.60
MnO	.05	.08	.01	.01
MgO	.75	1.53	.32	.05
CaO	1.18	1.41	1.52	.76
Na ₂ O	3.23	3.66	3.52	3.55
K ₂ O	3.62	3.78	3.84	3.95
P ₂ O ₅	.17	.21	.23	.28
H ₂ O	2.72	1.67	.81	1.16
CO ₂	d.l.			
F	.06			
	99.66	99.98	100.00	103.15

(d.l. below detection limit).

CIPW - norm

Q	33.6	27.9	32.8	38.5
C	4.6	3.2	3.0	4.6
Or	21.5	22.3	22.7	22.6
Ab	27.4	31.0	29.8	29.1
An	4.4	5.6	6.0	1.9
En	1.9	3.8	.8	.1
Fs	2.1	1.9	2.0	.5
Ms	.7	.9	.8	.6
Il	.6	1.1	.7	.3
Ap	.4	.5	.5	.6
	97.3	98.2	99.1	98.8

* Data by Coata et al. (1971)

Porphyritic biotite granites of Covilha, Belmonte,
Caria and Alpedrinha.

	CWJB	CA 344	CA 345	FUN 32	FUN 67	FUN 70	FUN 71	FUN 75
SiO ₂	70.95	72.38	73.76	69.95	72.98	72.84	73.49	71.05
TiO ₂	.49	.13	.21	.33	.25	.34	.31	.48
Al ₂ O ₃	14.53	14.55	13.94	15.28	14.03	14.28	15.44	14.63
Fe ₂ O ₃	.44	d.l.	.20	.57	.27	.38	.22	.50
FeO	2.36	1.60	1.69	1.67	1.42	2.22	1.87	2.34
MnO	.15	.05	.07	.03	.01	.04	.03	.01
MgO	.73	.22	.27	.60	.33	.47	.45	.66
CaO	1.12	.59	.64	.56	.70	.70	.65	.80
Na ₂ O	3.48	3.47	3.20	4.19	2.85	2.98	2.96	2.82
K ₂ O	5.12	4.91	4.73	4.84	5.47	4.89	4.84	5.14
P ₂ O ₅	.32	.33	.29	.36	.21	.28	.25	.28
H ₂ O	.79	1.48	1.48	1.43	.79	.96	.95	1.09
CO ₂	d.l.	d.l.	d.l.	d.l.	d.l.	d.l.	d.l.	d.l.
F				.07	.13	.18	.16	.20
	100.48	99.71	100.48	99.88	99.44	100.56	101.62	100.00

(d.l. means below detection limit).

CIPW - norm

Q	26.8	31.6	34.7	25.2	33.7	34.2	35.0	32.2
C	2.0	3.3	3.1	3.1	3.0	3.9	5.0	4.1
Or	30.1	29.1	27.8	28.6	32.5	28.7	28.1	30.4
Ab	29.3	29.4	26.9	35.5	24.3	25.1	24.6	23.9
An	3.4	.8	1.3	.1	1.3	.5	.6	.9
En	1.8	.6	.7	1.5	.8	1.2	1.1	1.6
Fs	3.4	2.8	2.7	2.1	2.0	3.3	2.8	3.1
Mt	.6	.0	.3	.8	.4	.5	.3	.7
Il	.9	.2	.4	.6	.5	.6	.6	.9
Ap	.8	.8	.7	.9	.5	.7	.6	.7
Fr	.0	.0	.0	.1	.2	.3	.3	.4
	99.1	98.6	98.6	98.5	99.2	99.0	99.0	98.9

Fine-grained two-mica granite of Capinha.

	CA 114	CA 120
SiO ₂	71.42	74.40
TiO ₂	.23	.05
Al ₂ O ₃	14.79	14.30
Fe ₂ O ₃	.20	d.l.
FeO	1.86	1.18
MnO	.10	.12
MgO	.57	.08
CaO	.66	.49
Na ₂ O	3.25	3.60
K ₂ O	4.21	4.29
P ₂ O ₅	.39	.31
H ₂ O	1.76	1.30
CO ₂	d.l.	d.l.
	99.44	100.12

(d.l. means below detection limit).

CIPW - norm

Q	34.0	35.7
C	4.6	3.6
Or	25.0	25.3
Ab	27.7	30.4
An	.7	.4
En	1.4	.2
Fs	3.1	2.3
Mt	.3	.0
Il	.4	.1
Ap	.9	.7
	98.1	98.7

Argemela quartz-albite.

	ARG 1	ARG 4	ARG 5	ARG 6	ARG 18	PQ XIV
SiO ₂	67.39	67.37	68.46	67.39	68.67	68.30
TiO ₂	.00	.00	.00	.00	.01	.00
Al ₂ O ₃	18.09	18.20	17.36	18.01	17.66	18.03
Fe ₂ O ₃	.03	.15	.04	.06	d.l.	.07
FeO	.35	.40	.28	.32	.29	.25
MnO	.05	.06	.08	.05	.07	.07
MgO	.01	.04	.04	.01	.03	.04
CaO	.05	.23	.18	.21	.11	.15
Na ₂ O	6.35	4.45	5.38	5.37	5.65	4.96
K ₂ O	2.67	3.43	2.62	2.91	2.55	2.80
P ₂ O ₅	1.64	1.62	1.72	1.47	1.54	1.42
H ₂ O	1.81	2.31	1.35	1.86	.90	1.92
CO ₂	.75	d.l.	d.l.	d.l.	d.l.	d.l.
F	1.04	.77	.86	1.07	.99	1.11
Li ₂ O	.88	.56	.82	.95	.90	.95
	101.11	99.59	99.19	99.68	99.37	100.07

(d.l. means below detection limit).

GIPW - norm

Q	19.9	28.2	27.2	25.0	26.1	28.7
C	4.7	7.2	5.8	6.1	5.7	6.9
Or	15.7	20.5	15.7	17.4	15.3	16.7
Ab	53.6	38.0	46.3	46.0	48.6	42.3
En	.0	.1	.1	.0	.1	.1
Fs	.7	.7	.6	.6	.7	.5
Mt	.0	.2	.1	.1	.0	.1
Ap	.1	.4	.3	.4	.2	.3
	94.7	95.3	96.1	95.6	96.7	95.6

Atalaia granite (j-8).

	FUN 10	FUN 14	FUN 17	FUN 25	FUN 28	FQ V	* 37
SiO ₂	74.80	72.65	74.00	72.49	72.53	72.70	74.27
TiO ₂	.02	.10	.13	.12	.16	.07	.05
Al ₂ O ₃	14.47	15.03	15.10	14.90	14.97	15.17	15.18
Fe ₂ O ₃	.35	.25	d.l.	.58	.52	.73	.01
FeO	.52	1.07	.94	1.02	1.12	.71	.67
MnO	.04	.04	.04	.05	.01	.03	.03
MgO	.16	.35	.05	.42	.36	.32	.05
CaO	.18	.24	.28	.29	.32	.18	.51
Na ₂ O	3.50	3.69	4.21	3.74	3.32	3.65	4.20
K ₂ O	4.10	4.40	4.11	4.31	4.57	4.48	4.12
P ₂ O ₅	.38	.54	.51	.47	.53	.46	.38
H ₂ O	1.38	1.01	1.37	1.32	1.29	1.56	.66
CO ₂	d.l.	d.l.	d.l.	d.l.	d.l.	.32	
F	.21	.47	.27	.28	.26	.24	
	100.11	99.84	101.01	99.99	99.96	100.62	100.13

(d.l. means below detection limit).

* Data by Costa et al. (1971)

CIPW - norm

Q	38.1	33.1	32.7	33.0	34.6	33.8	33.4
C	4.3	4.2	3.7	4.1	4.6	4.3	3.8
Or	24.2	26.0	24.0	25.5	27.0	26.3	24.3
Ab	29.6	31.3	35.3	31.7	28.1	30.7	35.5
En	.4	.9	.1	1.0	.9	.1	.1
Fs	.7	1.7	1.6	1.3	1.4	.6	1.2
Mt	.5	.4	.0	.8	.8	1.1	.0
Il	.0	.2	.2	.2	.3	.1	.1
Ap	.3	.4	.5	.5	.6	.3	.9
Hg	.0	.0	.0	.0	.0	.6	.0
	98.1	98.2	98.1	98.1	98.3	97.9	99.3

Albite granite of Panasqueira (Group A).

	PQ B11	PQ B12	PQ 491	PQ 548	PQ 574	PQ 576
SiO ₂	74.16	72.62	74.97	72.53	72.37	73.02
TiO ₂	.12	.22	.23	.21	.29	.23
Al ₂ O ₃	14.13	14.73	13.54	14.68	14.51	14.68
Fe ₂ O ₃	.86	.43	.12	.27	.00	.03
FeO	.67	1.17	1.47	1.49	1.66	1.71
MnO	.04	.06	.05	.06	.02	.04
MgO	.27	.36	.31	.40	.74	.37
CaO	.55	.67	.63	.48	.39	.34
Na ₂ O	2.96	2.12	2.98	3.32	2.65	3.33
K ₂ O	4.26	5.74	4.42	4.87	4.84	4.50
P ₂ O ₅	.42	.47	.34	.40	.57	.48
H ₂ O	1.18	1.43	1.39	.93	1.24	1.09
CO ₂	d.l.	.10	d.l.	d.l.	.51	d.l.
F	.45	.39	.36	.45	.39	.50
	100.07	100.51	100.81	100.09	100.18	100.32

(d.l. means below detection limit).

CIPW - norm

Q	40.0	37.0	38.9	32.9	36.8	34.5
C	4.6	5.0	3.8	3.9	4.9	4.3
Or	25.2	33.7	25.9	28.8	28.5	26.5
Ab	25.0	17.8	25.0	28.1	22.4	28.1
En	.7	.7	.8	1.0	.7	.9
Fs	.4	1.5	2.3	2.3	2.6	2.8
Mt	1.2	.6	.2	.4	.0	.0
Il	.2	.4	.4	.4	.6	.4
Ap	1.0	1.1	.8	.9	.7	.6
Fr	.0	.1	.3	.0	.0	.0
Hg	.0	.2	.0	.0	1.0	.0
	98.3	98.1	98.4	98.7	98.2	98.1

Albite granite of Panasqueira (Group B).

	PQ 492	PQ 498	PQ 545
SiO ₂	71.19	71.59	71.55
TiO ₂	.20	.23	.21
Al ₂ O ₃	14.55	14.48	14.68
Fe ₂ O ₃	.39	d.l.	.31
FeO	1.83	2.38	1.85
MnO	.06	.07	.07
MgO	.40	.41	.41
CaO	.90	.78	.71
Na ₂ O	2.45	2.61	2.45
K ₂ O	4.83	4.58	5.08
P ₂ O ₅	.70	.56	.68
H ₂ O	1.62	.47	1.18
CO ₂	.32	d.l.	d.l.
F	.58	.86	.66
	100.02	99.02	99.84

(d.l. means below detection limit).

CIPW - norm

Q	37.0	36.8	36.0
C	5.3	5.3	5.2
Or	28.5	27.3	30.1
Ab	20.7	22.3	20.8
En	.3	1.0	1.0
Fs	2.8	4.2	2.9
Mt	.6	.0	.5
Il	.4	.4	.4
Ap	1.6	1.3	1.3
Fr	.0	.1	.0
Hg	.6	.0	.0
	97.8	98.7	98.2

Albite granite of Panasqueira (Group C).

	PQ 493	PQ 550	PQ 570	PQ 571
SiO ₂	72.55	72.52	69.93	71.72
TiO ₂	.23	.20	.26	.28
Al ₂ O ₃	13.67	13.54	15.50	13.80
Fe ₂ O ₃	.67	.47	.41	.51
FeO	2.54	2.50	2.39	2.78
MnO	.09	.09	.07	.08
MgO	.43	.45	.78	1.10
CaO	.88	.63	.87	.64
Na ₂ O	1.11	1.04	2.33	1.65
K ₂ O	4.04	4.62	4.14	4.01
P ₂ O ₅	.64	.62	.89	.64
H ₂ O	1.24	1.50	1.71	1.63
CO ₂	d.l.	.78	.16	d.l.
F	.72	.85	1.02	1.01
	98.81	99.81	100.46	99.85

(d.l. means below detection limit).

CIPW - norm

Q	48.8	47.0	37.7	43.2
C	7.6	6.8	7.2	6.8
Or	24.2	27.4	24.4	23.7
Ab	9.5	8.8	19.6	14.0
En	1.1	.0	1.6	2.7
Fs	3.9	4.0	3.7	4.4
Ht	1.0	.7	.6	.7
Il	.4	.4	.6	.5
Ap	1.5	1.1	1.6	1.2
Fr	.1	.0	.0	.0
Mg	.0	.9	.3	.0
	98.1	97.1	97.3	97.2

Greisenized granite of Panasqueira (Group D).

	PQ 494	PQ 495	PQ 551	PQ 560	PQ 562
SiO ₂	73.95	76.54	73.99	73.34	73.65
TiO ₂	.03	.04	.01	.01	.00
Al ₂ O ₃	14.22	13.04	14.58	14.33	14.77
Fe ₂ O ₃	.48	.61	.50	.54	.40
FeO	1.29	1.10	1.21	1.41	1.14
MnO	.05	.05	.04	.05	.03
MgO	.26	.15	.28	.49	.20
CaO	.49	.43	.34	.32	.38
Na ₂ O	2.50	2.25	2.56	1.40	3.04
K ₂ O	3.99	3.26	4.16	4.71	3.94
P ₂ O ₅	.33	.39	.34	.33	.34
H ₂ O	1.74	.47	1.66	1.61	1.73
CO ₂	d.l.	.24	.14	.42	d.l.
F	.31	.53	.33	.37	.44
	99.64	99.10	100.14	99.33	100.06

(d.l. means below detection limit).

CIPW - norm

Q	43.0	50.7	42.0	46.3	39.7
C	5.8	5.9	5.9	7.0	5.5
Or	23.7	19.4	24.5	28.0	23.3
Ab	21.2	19.2	21.6	11.9	25.7
En	.7	.0	.4	.3	.5
Fs	2.0	1.6	1.9	2.2	1.8
Ht	.7	.9	.7	.8	.6
Il	.1	.1	.0	.0	.0
Ap	.8	.8	.6	.6	.7
Fr	.1	.0	.0	.0	.0
Mg	.0	.3	.3	.8	.0
	98.1	98.9	97.9	97.9	97.8

Level 2 greisen samples (Group E).

	PQ 224	PQ 225	PQ 226	PQ 227b	PQ 313	PQ 315	PQ 514
SiO ₂	76.90	75.29	76.90	75.03	74.48	75.77	75.36
TiO ₂	.06	.04	.04	.02	.03	.03	.02
Al ₂ O ₃	13.35	13.43	12.70	13.63	14.31	13.14	13.25
Fe ₂ O ₃	.28	.86	.56	.95	.62	1.19	1.50
FeO	1.24	1.63	1.57	1.44	.96	1.25	1.02
MnO	.04	.05	.06	.05	.04	.05	.04
MgO	.20	.18	.09	.16	.19	.19	.09
CaO	.43	.42	.41	.30	.45	.32	.29
Na ₂ O	2.36	1.48	1.74	1.40	2.45	1.78	1.86
K ₂ O	3.04	3.46	3.21	3.61	4.56	3.31	3.63
P ₂ O ₅	.33	.37	.37	.34	.33	.26	.32
H ₂ O	1.31	1.76	1.24	1.92	1.38	1.76	1.55
CO ₂	d.l.	d.l.	d.l.	d.l.	.13	.16	d.l.
F	.40	.45	.42	.43	.22	.35	.38
	99.94	99.42	99.31	99.28	100.15	99.56	99.31

(d.l. means below detection limit).

CIPW - norm

Q	50.4	52.4	53.6	52.3	42.0	52.3	50.6
C	6.2	7.3	6.4	7.5	5.3	6.7	6.3
Or	18.0	20.6	19.1	21.5	26.9	19.6	21.6
Ab	20.0	12.6	14.8	11.9	20.7	15.1	15.8
En	.5	.5	.2	.4	.2	.1	.2
Fs	2.0	2.3	2.5	1.9	1.3	1.4	.7
Mt	.4	1.3	.8	1.4	.9	1.7	2.2
Il	.1	.1	.1	.0	.1	.1	.0
Ap	.8	.8	.7	.5	.8	.6	.5
Mg	.0	.0	.0	.0	.2	.3	.0
	98.4	97.9	98.2	97.4	98.4	97.9	97.9

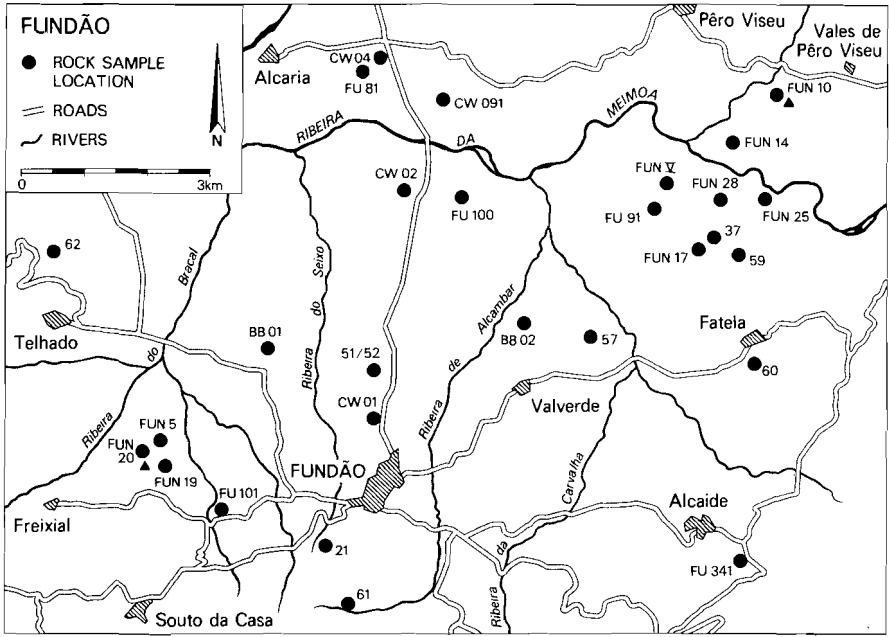
Level 1 greisen samples (Group F).

	PQ 02	PQ 04	PQ 202	PQ 204	PQ 205	PQ 215	PQ 216
SiO ₂	73.75	70.87	73.33	72.87	73.79	71.75	71.74
TiO ₂	.02	.02	.02	.02	.02	.02	.02
Al ₂ O ₃	12.36	13.76	14.35	13.86	14.01	14.72	15.18
Fe ₂ O ₃	1.96	2.47	1.01	2.28	1.90	2.29	1.08
FeO	1.90	1.91	1.83	1.84	1.57	1.59	2.14
MnO	.05	.06	.08	.05	.05	.05	.06
MgO	.13	.16	.13	.09	.13	.08	.09
CaO	.48	.42	.34	.32	.28	.25	.26
Na ₂ O	.20	.16	.54	.30	.20	.29	.24
K ₂ O	3.94	4.52	4.51	4.13	4.30	4.38	4.92
P ₂ O ₅	.38	.34	.30	.30	.27	.27	.27
H ₂ O	.76	.84	1.82	3.50	1.84	2.31	1.72
CO ₂	.18	.21	d.l.	d.l.	.23	d.l.	d.l.
F	.47	.55	.48	.43	.45	.56	.48
	96.58	96.29	98.74	99.99	99.04	98.56	98.20

(d.l. means below detection limit).

CIPW - norm

Q	58.6	53.9	52.2	54.5	56.1	53.5	50.9
C	8.0	8.9	8.7	8.9	9.1	9.6	9.6
Or	24.1	27.7	27.0	24.4	25.7	26.3	29.6
Ab	1.8	1.4	4.6	2.5	1.7	2.5	2.1
En	.0	.0	.3	.2	.0	.2	.2
Fs	2.0	1.6	2.7	1.6	1.4	1.1	3.2
Mt	2.9	3.7	1.5	3.3	2.8	3.4	1.6
Ap	.9	.8	.6	.6	.5	.5	.5
Mg	.3	.3	.0	.0	.3	.0	.0
	98.6	98.3	97.6	96.0	97.6	97.1	97.7



Sample location of the Fundao pluton.

Curriculum Vitae

Toegevoegd op verzoek van het College van Decanen van de Rijksuniversiteit te Utrecht.

De schrijver van dit proefschrift behaalde in 1971 het diploma HBS-b aan het Rhedens Lyceum te Velp. In datzelfde jaar werd begonnen met de studie Geochemie aan de Rijksuniversiteit te Utrecht. In mei 1975 werd het kandidaats examen G 5 afgelegd, in april 1979 volgde het doctoraal examen, met hoofdvak Geochemie en bijvakken Structurele en Toegepaste Geologie en Economische Geologie. In de jaren 1976 tot 1979 werden assistenschappen vervuld bij het Vening Meinesz Laboratorium (afdeling Geochemie). Van april 1979 tot en met maart 1982 was de schrijver werkzaam bij de afdeling Geochemie, als wetenschappelijk assistent in dienst zijnde bij de Nederlandse Organisatie voor Zuiver-Wetenschappelijk Onderzoek (Z.W.O.).